

Master Thesis, Department of Geosciences

**Geomorphological studies of a karst
system in a permafrost environment at
Linnédalen, western Spitsbergen**

Sara Mollie Cohen



UNIVERSITY OF OSLO

FACULTY OF MATHEMATICS AND NATURAL SCIENCES

S. M. Cohen

Geomorphological studies of a karst system in a permafrost environment at Linnédalen, western Spitsbergen

Sara Mollie Cohen



Master Thesis in Physical Geography

Department of Arctic Geology

University Centre in Svalbard

Longyearbyen

July 2013

Geomorphological studies of a karst system in a permafrost environment at Linnédalen, western Spitsbergen

Sara Mollie Cohen



Master Thesis in Geosciences

Discipline: Physical Geography

Department of Geosciences

Faculty of Mathematics and Natural Sciences

University of Oslo

July 2013

© Sara Mollie Cohen, 2013

Supervisor: Professor Hanne H. Christiansen

This work is published digitally through DUO – Digitale Utgivelser ved UiO

<http://www.duo.uio.no>

It is also catalogued in BIBSYS (<http://www.bibsys.no/english>)

All rights reserved. No part of this publication may be reproduced or transmitted, in any form or by any means, without permission.

ABSTRACT

The following thesis is the culmination of a two year study on Svalbard, an archipelago located in the high Arctic. The main purpose of this thesis is to investigate the presence of a karst lake system and its implications for the surrounding periglacial environment at Linnédalen, located in western Spitsbergen. Spitsbergen is the largest island comprising the Svalbard archipelago. The resulting thesis combined data collection in the field, analysis of archived data and consideration of other literature. The objective of the thesis was reached by considering three research questions focusing on the geomorphology, thermal regime, and landscape development of the field site.

Principle data collection methods in the field included geomorphological mapping, bathymetric mapping, temperature logger deployment and instillation, photography, pit excavations, surveying, and water column profiling with data loggers. The primary field period took place over July and August 2012, but other campaigns to the field site occurred between the entire time span of summer 2010 to spring 2013.

The initial results from the study determine that the karst system has an integral role in influencing the geomorphology, ground thermal regime and landscape development at the study site. Geomorphological mapping reveals the importance of both periglacial and karst processes in shaping the study site. The map also gives an insight into how the system has developed throughout the Holocene. Air, water and ground temperature data analysis points to the influence of the karst system on the ground thermal regime, revealing that an active karst system has effect on proximal ground temperatures, possibly altering the state of permafrost in the area. A schematic figure displaying the landscape development details the emergence of the karst lake system and surrounding periglacial environment, beginning with deposition in the late Carboniferous and early Permian and concluding with the current system observed today.

ACKNOWLEDGEMENTS

First I need to thank the person who made this entire project possible, my supervisor, Professor Hanne H. Christiansen. Thank you for giving me this incredible opportunity. You introduced me to the fascinating world of permafrost and periglacial geomorphology, and gave me the chance to work at the most beautiful field site in the world. You gave me the means to design my own project, where anything I wanted to do was possible. I must also thank you for the opportunity to teach the AG-212 course which was an integral learning and growing experience.

I also would like to thank Professors Mike Retelle, Al Werner and Steve Roof for their scientific expertise and plethora of knowledge concerning the Linnédalen area. Mike, oh man we have had some good adventures out there!

Thank you to Svalbard Science Forum for the financial support which was needed to make this project possible.

This thesis would not be possible without the help of my students and field assistants from the AG-212 course. Lauren, Lukas, Elin, Hanna, Dagmar and Louise: I had so much fun with you all out there and I hope you learned as much from the experience as I did! This thesis is dedicated to you guys!

I thank Jordan Mertes and Max Eckertorfer for being two mentors who I looked up to during my entire academic career at UNIS. Jordan, thanks for the first summer out at Linné, and for the encouragement to apply for this master's degree. Max, thanks for the all of the help and good times over the years.

This project would not be possible, or at least not nearly as enjoyable without the great people from Basecamp Spitsbergen. I am positive that no other graduate student has ever experienced luxury like I did while staying out at Isfjord Radio. Thank you for accommodating all of my needs throughout my thesis.

I must thank all those who have helped me in the field and at UNIS during the past three and a half years. This includes Graham Gilbert, Samuel Faucherre, Kamilla Buran, Maren

Garsjø, Harald Andreassen, Nils Arne Walberg, Tom Anders Bakken, Knut Ola Lund, Sten Andreas Grundvåg, Mikkel Arne Kristiansen and Helge Kollsete Gjelberg among others. I also need to thank all the good people at the Radisson for the mental support needed during the thesis.

Wesley Farnsworth, there is no way I would have done any of this if not for your constant source of support. Words cannot describe what your friendship means to me.

Finally, thank you to my family and friends who have sent me love and support from the other side of the world over the past three and a half years. Your love means the world to me.

PERSONAL MOTIVATION

Growing up in Alaska, I learned to love the mountains, ocean and cold temperatures. I never imagined I would find another place which exhibited the same natural beauty and ease of living. On a whim I came to Svalbard in January 2010 to study abroad for one semester. There is something magical about moving to a new place in the complete darkness, only to have another small piece of the puzzle revealed each day as the light returns. I quickly fell under the Svalbard spell, and have found a reason to stay ever since. The opportunities presented by UNIS to study and live in this unparalleled natural laboratory is something I cherish deeply. This master's thesis gave me the opportunity to study and form a deeper understanding for the nature and environment I grew up enthralled with. There is no greater pleasure for me than walking along, alone in nature, and being able to conceptualize the environmental dynamics surrounding me.

TABLE OF CONTENTS

LIST OF FIGURES.....	vii
LIST OF TABLES.....	xi
CHAPTER 1. INTRODUCTION.....	1
1.1. Research Questions.....	2
1.2. Research Objectives and Scope.....	3
1.3. Thesis Structure.....	3
CHAPTER 2. LITERATURE AND THEORY.....	5
2.1. Permafrost.....	5
2.1.1. Permafrost Distribution.....	6
2.1.2. Thermal Characteristics of Permafrost.....	9
2.1.3. Permafrost Hydrology.....	11
2.2 Thermokarst.....	13
2.3 Periglacial Geomorphology.....	14
2.4 Karst.....	17
2.5 Permafrost & Karst in the Arctic.....	20
2.6 Literature.....	22
CHAPTER 3. STUDY AREA.....	25
3.1. Location- SVALBARD.....	25
3.2. Climate & Meteorology of Svalbard.....	26
3.3. Geology of Svalbard.....	27
3.4. Geography and Geomorphology of Svalbard.....	32
3.5. Linnédalen.....	34
3.5.1. Linnédalen Climate & Meteorology.....	36
3.5.2. Linnédalen Geology.....	37
3.5.3. Linnédalen Geography & Geomorphology.....	38
3.5.4. Linnédalen Measurement Sites.....	43
CHAPTER 4. METHODS.....	47
4.1. Geomorphological Mapping.....	47
4.2. Bathymetric Mapping.....	48
4.3. Temperature Profiles.....	49
4.3.1. Temperature Loggers.....	49

4.3.2. Pit Profiles.....	51
4.4. Automatic Digital Camera.....	52
4.5. Surveying with TOPCON Total Station.....	52
4.6. Conductivity Temperature Depth (CTD) Profiles.....	53
4.7. Additional Data Loggers.....	53
CHAPTER 5. RESULTS: GEOMORPHOLOGICAL MAP.....	54
CHAPTER 6. RESULTS: LAKE STATISTICS AND SURVEYING RESULTS.....	58
CHAPTER 7. RESULTS: BATHYMETRIC PROFILES.....	60
CHAPTER 8. RESULTS: TEMPERATURE AND LAKE LEVEL PROFILES.....	62
CHAPTER 9. DISCUSSION.....	70
9.1. Geomorphological Map Discussion.....	70
9.1.1. Lakes 1, 2, 3, 4 and Relict Fluvial Channel.....	70
9.1.2. Lake 5 and Relict Channel Connecting Lake 4 and 5.....	77
9.1.3. Lakes 6, 7, 8, 9 and Relict Channel.....	79
9.1.4. Åkerman Map Comparison.....	84
9.2. Temperature, Thermal Regime Discussion, and Lake Level Discussion.....	85
9.2.1. Thermal Regime and Temperature Data Lakes 1, 2, 3 and 4.....	86
9.2.2. Thermal Regime and Temperature Data Lakes 6, 7 and 8.....	92
9.2.3. Thermal Regime and Temperature Tunsjøen and Strand flat Area.....	94
9.3. Karst System Development Discussion.....	96
9.4. Potential Error.....	102
Chapter 10. CONCLUSION.....	103
10.1. Summary and Conclusions.....	103
10.2. Study Implications.....	105
10.3. Future Prospects.....	105
REFERENCES.....	107
APPENDIX.....	116

LIST OF FIGURES

CHAPTER 2

Figure 2.1: Map showing mean annual ground temperature (MAGT) of the Arctic. Points are boreholes where temperature is taken at depth of zero annual amplitude. (Figure from Romanovsky et al, 2010).....	8
Figure 2.2: Schematic model showing relationship between air temperature and ground temperature with the influence of surface cover, snow cover, and geology. (Figure from Smith and Riseborough, 2002).....	9
Figure 2.3: Typical ground thermal regime for permafrost, trumpet curve in blue. (Modified from French, 2007; ACGR, 1988).....	11
Figure 2.4: Schematic model of a water pathway through taliks in a permafrost zone, surfacing in an aufeis (icing). (Figure from Clark and Lauriol, 1997).....	12
Figure 2.5: Ice wedge formation and classification. (Figure from Mackay, 2000).....	15
Figure 2.6: Typical features and layout of a karst system: landforms, features & dynamics. (Figure from Ford and Williams, 2007)	20
Figure 2.7: How a karst system functions in various permafrost environments. (Figure from Ford and Williams, 2007).....	21
Figure 2.8: Schematic diagrams interpreting the karst groundwater system at Vardeborsletta, Linnédalen. The first figure shows drainage of water through a talik under Lake 1 into a warm groundwater system underneath. The second figure shows Lakes 2-3-4 and 5 with two sinkholes where water is actively draining into the subsurface. (Figure from Salvigsen and Elgersma, 1985).....	24

CHAPTER 3

Figure 3.1: Svalbard, located in the Barents Sea. (Figure from http://www.ngdc.noaa.gov/mgg/bathymetry/arctic/arctic.html).....	25
Figure 3.2: Precipitation and Mean Annual Air Temperature (MAAT) beginning in 1911, recorded from Longyearbyen Airport. (Figure from Humlum et al, 2003).....	27
Figure 3.3: Geological map of Svalbard. (Figure from Norsk Polar Institutt).....	28
Figure 3.4: Svalbard at palaeolatitudes, showing characteristic lithologies and facies from each time period as Svalbard traveled from the equator to its present location. (Figure from Worsley & Aga, 1986).....	29
Figure 3.5: Kapp Ekholm stratigraphy reflecting glaciation (till) and deglaciation (marine-to-littoral sediments). (Figure from Ingólfsson, 2011, modified from Mangerud & Svendsen, 1992).....	32
Figure 3.6: Distribution of glaciers and permafrost on Svalbard. Glaciers are indicated by white, permafrost by grey. (Figure from Humlum et al. 2003).....	33
Figure 3.7: Linnédalen, west central Spitsbergen & inset map of Svalbard showing Linnédalen. 1) Linnédalen 2) Linnébreen extent 1936. The glacier front had retreated almost 1.5km from 1936-2008. 3) Little Ice Age Moraine 4) Kongressvatnet 5) Linnéelva inflow from Linnébreen 6) Linnévatnet 7) Outflow from Linnévatnet to Isfjord 8) Vardeborgsletta (beach terraces with karst Lake system). 9) Tunsjøen Lake, located on the strand flat. Background photo from Norsk Polar Institutt, 1936. Inset map from Norsk Polar Institutt. (Cohen, 2013).....	36
Figure 3.8: Geological Map of Linnédalen and simplified bedrock map. Scale is 1:100,000 (Modified from Norsk Polar Institute & Mangerud et al, 1990).....	38
Figure 3.9: Active layer depths from Linnédalen, collected from 1972-2005. (Figure from Åkerman, 2005).....	39

Figure 3.10: Borehole data from three boreholes at Kapp Linné. (Figure from Christiansen et al, 2010).....	41
Figure 3.11: Slope movement rates for various geomorphological features at Kapp Linné. (From Åkerman, 2005).....	42
Figure 3.12: Locations map showing all monitoring sites where data was obtained at Vardeborsletta, Lakes 1, 2, 3 and 4. Basemap is from Åkerman, 1980. Inset map is from Norsk Polarinstitut. (Cohen, 2013).....	44
Figure 3.13: Locations map showing all monitoring sites where data was obtained at Vardeborsletta, Lakes 5, 6, 7, 8 and 9. Basemap is from Åkerman, 1980. Inset map is from Norsk Polarinstitut. (Cohen, 2013).....	45
Figure 3.14: Locations map showing all monitoring sites where data was obtained near Tunsjøen Lake, Linnédalen. Temperature profiles created from data at the tiny temp logger locations are located in the appendix. Basemap is from Åkerman, 1980. Inset map is from Norsk Polarinstitut. (Cohen, 2013).....	46
CHAPTER 4	
Figure 4.1: Mapping in the field at Vardeborgsletta, summer 2010. (Mertes, 2010).....	47
Figure 4.2: Using a zodiac to make bathymetric profiles. (Cohen, 2012).....	48
Figure 4.3: Tiny tag loggers at Vardeborgsletta. (Cohen, 2012).....	49
Figure 4.4: Lake 3 & 4 drained during the winter 2012, observed April 1 st , 2012. (Cohen, 2012).....	50
Figure 4.5: Tiny tag thermistor string ready to go into Lake 7, spring 2012. (Cohen, 2012).....	51
Figure 4.6: Taking temperature in an excavated pit, summer 2012. (Cohen, 2012).....	52
CHAPTER 5	
Figure 5.1: Geomorphological map displaying geomorphological processes, periglacial landforms and Quaternary surface cover of the study area at the Vardeborgsletta plain, Linnédalen, Spitsbergen. The inset map is modified from Humlum et al, 2003. (Cohen, 2013).....	54
Figure 5.2: Legend and inset map for figure 6.1, the geomorphological map. Inset map is from Humlum et al, 2003. (Cohen, 2013).....	55
CHAPTER 7	
Figure 7.1: Bathymetric map of the karst lakes at Vardeborgsletta. The bathymetric figures are overlaid on a 1990 aerial photograph from Norsk Polarinstitut. (Cohen, 2013).....	60
Figure 7.2: Vertical profiles showing the bathymetry of the karst lakes at Linnédalen. (Cohen, 2013).....	61
CHAPTER 8	
Figure 8.1: Temperature profiles from Lakes 4, 7 and Tunsjøen. Temperature is taken at three different depths in each lake, according to lake depth. Air temperature is from weather station at Isfjord Radio, located approximately 3km west of Vardeborgsletta and 1km north of Tunsjøen. Air temperature from this weather station was available until 05.08.2012. After this date, air temperature is taken from Longyearbyen Airport, located approximately 60km east of the study site, which is the closest weather station available. (Cohen, 2013).....	62
Figure 8.2: Pit profiles from various locations around Lake 4, Lake 7 and Tunsjøen. Excavations were made by students from AG-212 course over summer, 2012. (Cohen, 2013).....	64
Figure 8.3: Temperature profiles from thermistor strings at locations around the Kapp Linné area. Data available from the TSP (thermal state of permafrost) project from http://www.tspnorway.com . (Cohen, 2013).....	66

Figure 8.4: Temperature profiles from thermistor strings at locations around the Kapp Linné area. Data available from the TSP (thermal state of permafrost) project from <http://www.tspnorway.com>. (Cohen, 2013).....68

Figure 8.5: Precipitation, level change, temperature, conductivity data for Lake 4, summer 2012. (Figure from Farnsworth & Glaw, 2012).....69

CHAPTER 9

Figure 9.1: Lakes 2, 3, 4 and Isfjord to the North. Photo taken 04.08.2010. (Cohen, 2010).....71

Figure 9.2: Slopes and features at Lakes 3 and 4. 1) Southeastern slope behind Lake 4. This is the escarpment face, showing the marine deposit sequence and the newly exposed face as the top beach cobble falls down slope. 2) The northern shorelines of Lake 3, showing steep slopes composed of marine deposits on the eastern side and shallow slopes covered with organic mat on the western side. 3) Southern slope behind the sinkhole and Lake 4, showing active slope processes. 4) Active layer detachment on the eastern side of Lake 4, occurred 25.07.2012. (Cohen, 2013).....72

Figure 9.3: Lake 1 basin, base aerial photograph is from Norsk Polar Institutt, 2010. (Cohen, 2013).....74

Figure 9.4: Photographs of Lake 1 and surrounding features. 1) The Lake 1 basin. 2) Solifluction lobes at the Lake 1 basin. 3) Debris flows traveling down slope at the Lake 1 basin. 4) Relict sinkhole (circled in black) above the eastern shore of Lake 1. (Cohen, 2013).....75

Figure 9.5: The relict fluvial channel which runs between the highest relict shorelines of Lake 3 and the highest relict shorelines of Lake 1 (figure 9.1). The southern side of the channel is heavily vegetated, indicating no recent activity, while the northern side of the channel contains deposits of rounded boulders. (Cohen, 2013).....77

Figure 9.6: Lake 5, Isfjord is seen to the north. (Cohen, 2013).....78

Figure 9.7: Relict fluvial channel connecting Lakes 5 and 4. 1) Closer to Lake 4, the channel contains boulders of differing sizes, lots of vegetation, and some water appears from small springs. 2) Closer to Lake 5 the channel exhibits almost no vegetation. A large pond with its own set of fresh shorelines from the current season is observed, possibly another sinkhole. (Cohen, 2013).....79

Figure 9.8: Lakes 8 and 7 facing south. Lake 8 is the proximal lake and Lake 7 is distal. (Cohen, 2013).....80

Figure 9.9: Examples of frozen ground features from the Lake 7 and 8 area. 1) Sorted stripes exhibiting many different clast sizes which are sorted. 2) Large non sorted polygons are frequent in the area. 3) Sorted circles near Lake 7 and 8, sorted stones are carbonate bedrock. Figure 4) Sorted netting near Lake 7, sorted limestones. (Cohen, 2013).....81

Figure 9.10: Lake 6, Isfjord to the north. The relict sinkholes are filled with snow at the time of this picture. (Cohen, 2013).....82

Figure 9.11: Relict sinkhole on the northeastern shoreline of Lake 6, located below relict shorelines. (Cohen, 2013).....82

Figure 9.12: Relict fluvial channel between Lake 6 and 7. Large rounded boulders and cobbles are deposited in the middle of the channel. (Cohen, 2013).....83

Figure 9.13: Vardeborgsletta portion of Åkerman's 1980 geomorphological map, with legend below. (Figure from Åkerman, 1980).....85

Figure 9.14: Perennial snow and ice patch at the eastern side of Lake 4, 07.09.2012. (Cohen, 2013).....87

Figure 9.15: Photographs taken at Lake 4. 1) The sinkhole area at Lake 4 shown dry on 21.07.2012. 2) The sinkhole area filled up with water on 25.07.2012. 3) The sinkhole with water draining through

on 25.07.2012. 4) Photograph of the sinkhole area dry and drained on 01.08.2012. Area was completely drained by 29.07.2012. (Cohen, 2013).....	88
Figure 9.16 Lake 3 and Lake 4 drained during winter 2012. (Retelle, 2012).....	89
Figure 9.17: Lake 4, 3, 2 from automatic digital camera, 19.03.2013 (top) and 18.04,2013 (bottom). No drainage or movement during winter/spring 2013 at Lakes 3 and 4. There is also significantly more snow cover. (Cohen, 2013).....	90
Figure 9.18: Pits dug at Vardeborgsletta by Salvigsen and Elgersma, 1985. Pit A is located at the northeast shore of Lake 1. Pit B is located at Lake 5. Pit C & D are located by the eastern shores of Lake 1. (Figure from Salvigsen and Elgersma, 1985).....	92
Figure 9.19: Development of the karst system at Vardeborgsletta, Linnédalen. 1) Stage 1 Carboniferous and Permian Development. Inset shows location of Vardeborgsletta in Nordenskiöldland, western Spitsbergen. 2) Stage 2 is karstification phase during Permian. 3) Stage 3 is tectonic phase from beginning of the Tertiary. 4) Stage 4 is the glacial stage from the Quaternary. 5) Stage 5 is the current development phase from the mid to late Holocene. 6) Stage 6 is the current stage; geomorphological map from figure 6.1 is used to portray current processes. (Cohen, 2013)..	100
Figure 9.20: Schematic figure showing possible karst groundwater system at Lakes 2-3-4, Vardeborgsletta, Linnédalen, Spitsbergen. (Cohen, 2013).....	102
Appendix A: Temperature profiles created from the data from figure 8.3, showing maximum, minimum and average temperatures at depth for each temperature logger. (Cohen, 2013.).....	116
Appendix B: Temperature profiles created from the data from figure 8.4, showing maximum, minimum and average temperatures at depth for each temperature logger. (Cohen, 2013).....	118
Appendix C: Trumpet curves from borehole data at three boreholes at Kapp Linné, data from the TSP (thermal state of permafrost) project. http://www.tspnorway.com (Cohen, 2013).....	121
Appendix E: Conductivity at depth for Lakes 1-9. (Figure from Axén and Roalkvam, 2012).....	122
Appendix F: Formatted geomorphological map.....	123

LIST OF TABLES

CHAPTER 3

Table 1: Modified table of permafrost conditions at Kapp Linné.....	40
--	----

CHAPTER 5

Table 2: Lake Statistics.....	58
--------------------------------------	----

Table 3: Surveying Altitudes and Locations.....	59
--	----

APPENDIX

Table A: Summary of maximum, minimum and average temperatures for the temperature profiles proximal to Lake 4.....	117
---	-----

Table B: Summary of maximum, minimum and average temperatures for the temperature profiles from figure 8.4.....	119
--	-----

CHAPTER 1. INTRODUCTION

In the past few decades, interest and studies which focus on the science of the High Arctic have increased substantially. Within this immense spectrum a peak in the interest of permafrost science is apparent. The purpose of this thesis is to address the dynamics and interactions of a karst groundwater system within a continuous permafrost and periglacial landscape. This study aims to look at a very specific situation from a multitude of techniques and methods, in order to gain a more complete understanding as to how this unique system operates.

Large areas of the ice-free, terrestrial earth are underlain by carbonate rock which has undergone karst processes (Ford and Williams, 2007). Karst groundwater systems are considered a vital asset to the human race as a freshwater resource, and are thoroughly studied in mid-latitude locations. 20-25% of drinking water originates from karst groundwater systems (Ford and Williams, 2007). The study of karst groundwater systems in High Arctic permafrost zones are limited, predominantly to older studies dating to the past century. With much uncertainty concerning future climate scenarios, particularly at high latitudes, an up-to-date perspective on a karst groundwater system in a permafrost zone acts as added perspective to a growing permafrost database.

Permafrost underlies over 20% of the earth's terrestrial area. Permafrost is predominately found at northern latitudes, and can be divided by extent to continuous, discontinuous, sporadic and isolated, depending on what percent of an area has ground temperatures at 0°C or below for two consecutive years. A conservative estimate of five to eight million people, live in periglacial environments (French, 2007). Permafrost hydrology, an important sub-discipline in permafrost science still has vast gaps in understanding, especially concerning studies which include real field data. The first review for permafrost hydrology on Svalbard is currently in the process of being written.

Svalbard is an ideal location for this study, as a karst system in a continuous permafrost environment is found at Linnédalen. Linnédalen is an ideal area to study this system due to the long history of scientific studies from the area. Jonas Åkerman began geomorphological studies at Linnédalen in the 1970's and continues research there to this day, publishing many papers (Åkerman 1980; 1984; 1992; 2005). Many studies concerning Quaternary and

Holocene climates of Svalbard include Linnédalen (Ingólfsson, 2011; Ingólfsson and Landvik, 2013; Landvik et al, 1987; Lønne and Mangerud, 1991; Mangerud and Svendsen, 1990; 1992). Due to Linnédalen's proximity to the Tertiary fold and thrust belt, studies by Braathen and Bergh (1995a; 1995b) give a geological history of the area. Permafrost studies from Linnédalen also exist including Christiansen et al, 2010 and Wanatabe et al, 2013. These studies are only a portion of the publications which include Linnédalen. The easy accessibility of Linnédalen from Longyearbyen, and the infrastructure available by the Isfjord Radio Station also makes it a preferable location.

Motivation for this project originate with the two studies which introduce the karst lakes in Linnédalen (Åkerman, 1980; Salvigsen and Elgersma, 1985) but which leave the question as to how the system originated and how it operates. Further, temperature data has been collected throughout the area beginning in 2004, and the area is currently used as a “natural laboratory” for undergraduate courses from both the United States Research Experience for Undergraduates (US REU) and the University Centre in Svalbard (UNIS). This gives a research objective, as well as a plentitude of data and accessibility to the field site. It should be mentioned that the students from the 2012 summer field course: AG-212 (Holocene and Modern Climate Change in the High Arctic Svalbard Landscape) acted as field assistants for this thesis and spent a month in the field during July and August 2012 collecting data which is used in this study. The students also turned in reports at the end of the course. Some of the figures from the reports are included in this study.

This study takes place at Linnédalen, western Spitsbergen; part of the High Arctic archipelago, Svalbard, comprised of several islands located in the Barents Sea, a few hundred kilometers north of Norway. The study utilizes almost a decade of temperature data, geomorphological mapping, water column data, bathymetric data, surveying data and past studies to accomplish several goals: a geomorphological map detailing current processes; bathymetric profiles; air, ground and water temperature analysis; and conceptual models showing how the system has developed overtime, concerning both surface and subsurface processes.

1.1. Research Questions

- What does geomorphological mapping reveal about the landscape development and current processes at the study site?
- How do the karst lakes affect the thermal and hydrological regime of the study site?
- What geological and geomorphological processes have occurred to form the current karst lake system?

1.2. Research Objectives and Scope

When this project was proposed to study the karst lake system located in the continuous permafrost environment at Linnédalen, dozens of ideas formed for methods which could be utilized in order to investigate this system. This thesis topic is unique in that there was no one study which existed that could be replicated in order to investigate the system. The scientific objective of this project is to understand how a karst lake system originated, operates, and affects the surrounding landscape in a continuous permafrost environment. Three topics were chosen to grasp this understanding: geomorphological mapping; temperature profiling and analysis; and long-term landscape development and current system processes.

Geomorphological mapping is an important tool for understanding landscape dynamics and current processes. Creating a geomorphological map is not only critical for understanding the karst lake system, but can be useful to anyone who wishes to study geography and geology in the Linnédalen area. The geomorphological map allows for a visualization of how the study area is influenced by the presence of the karst lakes and the permafrost, and the subsequent reactions.

Temperature data and profiles give a quantifiable result to add to the interpretation of how the karst lake system currently operates and affects the surrounding landscape and thermal regime. The availability of air, ground and water temperatures allows for understanding the origins of thermal influences to the system.

Finally the long-term landscape development and current system processes puts the entire system into perspective in terms of how each part of the geologic and geomorphologic history came together to result in such a system.

1.3. Thesis Structure

This thesis consists of ten chapters. Chapter two reviews the theory and literature of permafrost, periglacial environments, and karst in the Arctic. Sections include theory on permafrost, thermokarst, periglacial geomorphology and karst. Chapter three gives a general site description of Svalbard, and then focuses in on the study site at Linnédalen. Three maps are in this chapter, which display the exact locations where data was acquired from. Chapter four describes the methods used for this study. The results are presented in chapters five, six, seven and eight. Chapter five presents the geomorphological map. Chapter six presents lake statistics and survey data. Chapter seven presents the bathymetric profile results. Chapter eight includes all of the temperature profiles. Chapter nine gives the discussion of the results, as well as potential sources of error. Chapter ten wraps up the thesis with the summary, conclusions, implications and future prospects. The references and appendix follow Chapter 10.

CHAPTER 2. LITERATURE AND THEORY

2.1. Permafrost

In the disciplines of geosciences and engineering, permafrost is a well-studied topic, with portions of several textbooks dedicated to the subject (French, 2007; Harris, 1986; Hinzman et al, 2006; Muller 2008). The term “permafrost” was first coined by S.W. Muller, a Professor of Geology from Stanford University during the Second World War (French, 2007). Permafrost is defined by temperature: it is ground which holds a temperature of 0°C or less for at least two consecutive years. Permafrost is not necessarily frozen, due to the possibility that the freezing point of water is depressed (French, 2007).

Permafrost forms either during or after the host sediment is deposited. If the permafrost forms after deposition it is defined as epigenetic. The lag time between deposition and permafrost formation can take millions of years to occur. Permafrost can also form during deposition, defined as syngenetic. If sedimentation is occurring in a cold-climate then the base of the active layer may aggrade towards the surface (French and Shur, 2010).

Permafrost is often associated with the presence of moisture (liquid or solid) although any material which is frozen for two or more years is considered permafrost (French, 2007). The freezing process which allows for the presence of ice is highly dependent upon the host material. The varying properties of soil, including but not limited to: heat conductivity, moisture content, grain size, and adsorption properties of mineral particle surfaces all affect the freezing process. The properties of the water, mostly concerning salt content, also play a factor (French, 2007).

If moisture is present within soil it can form segregation ice by moving towards the freezing plane during the freezing process (French, 2007). Two processes can occur when the ground begins to freeze; either the freezing plane will remain above the soil particles, or the ice will creep into the pores (French, 2007). If the freezing plane keeps stationary above the soil particles the water will move upwards and ice crystals can develop. As long as there is a supply of moisture the process can continue to form lenses of segregated ice (French, 2007). The main factor determining if segregated ice will form is cryosuction. Cryosuction is expressed in terms of P_i (pressure of ice), and P_w (pressure of water). This is because tension

controls the water reaching the freezing plane. High tension is needed to keep the freezing plane stationary. This situation is common in fine-grained materials, termed “frost-susceptible” (French, 2007).

In situations where the freezing plane does not hold stationary, and ice descends through the pores, pore ice forms in-situ (French, 2007). Pore ice will form when tension of cryosuction is not great enough and cannot hold the freezing plane. This occurs in coarser grained materials which are not as “frost-susceptible” as fine-grained materials (French, 2007). Other types of ice include: intrusive ice which is formed by water intrusion under some kind of pressure, and vein ice which is formed by water penetration into a crack at the ground surface.

Global and regional maps and distribution analysis originates mostly from small-scale studies, as well as interpolated mean annual air temperatures, boreholes, and regional monitoring programs such as the Permafrost Observatory Project: A Contribution to the Thermal State of Permafrost (TSP) (Christiansen et al, 2010). During the International Polar Year (IPY), a special effort in permafrost studies was made in the Polar Northern Hemisphere, culminating in several papers examining the state of permafrost (Christiansen et al, 2010; Romanovsky et al, 2010; Smith et al, 2010). The IPY project identified 575 boreholes which are currently being monitored in North America, Russia, and the Nordic Region (Romanovsky et al, 2010). The synthesis of the various studies contributing to this IPY project summarized that within continuous permafrost zones the mean annual ground temperature (MAGT) varies from above -1°C to -15°C . Permafrost warming began approximately two to three decades ago and has continued to the present (Romanovsky et al, 2010). It was discovered however, that when ground temperature is close to 0°C , it warms much slower than colder permafrost (Romanovsky, et al, 2010).

2.1.1. Permafrost Distribution

Permafrost underlies at least 20% of the world’s land area (French 2007). Figure 2.1 shows an approximate thermal distribution of permafrost in the circum-Arctic region (Romanovsky et al, 2010). Permafrost distribution is generally classified into three zones: continuous permafrost zones underlay >90% of the ground surface; discontinuous permafrost zones

underlay 10-90% of the ground surface; and sporadic permafrost zones underlay <10% of the ground surface for a given region (Burn, 2011). Permafrost distribution in the northern hemisphere is heavily influenced by the presence of land and sea, where ocean currents influence both the energy distribution and meteorological patterns (Romanovsky, et al, 2010). Most of the regions in the northern hemisphere where permafrost is encountered have continental climates, such as Canada, Russia and parts of Alaska. In these regions vast areas of continuous permafrost are common. In other regions, such as Scandinavia, and southern Alaska, the climate is maritime, and the discontinuous permafrost is encountered (Romanovsky, et al, 2010).

It is challenging to determine the extensiveness and state of permafrost because perennially frozen ground is found in especially rugged and unexplored terrain, and is continuously changing due to changes in climate (Christiansen et al. 2010; Smith and Riseborough, 2002). Because permafrost is a thermal phenomenon, climate is considered the most important control on permafrost distribution. Other spatial controls include the thermal conductivity and diffusivity of ground material, vegetation and snow cover, topography, aspect, fire, and water bodies (French, 2007). Several models exist for the purpose of estimating the extent of permafrost. One of the most widely used is the TTOP model, which works by linking the temperature at the top of the permafrost (TTOP) to the atmospheric climate through both seasonal surface transfer functions and subsurface thermal properties (Smith and Riseborough, 2002). The TTOP ultimately results from the combination of air temperature, nival offset, and thermal offset (Smith and Riseborough, 2002). As expected, the TTOP generally increases as the latitude decreases, as a function of increasing mean annual air temperature (MAAT) (Smith and Riseborough, 2002). Some critical factors exist which help determine the geographical limits of permafrost. To the north, in the continual permafrost zone, snow cover (nival offset) influences permafrost limits. To the south, in the discontinuous permafrost zone, the ground thermal conductivity (thermal offset) influences permafrost limits.

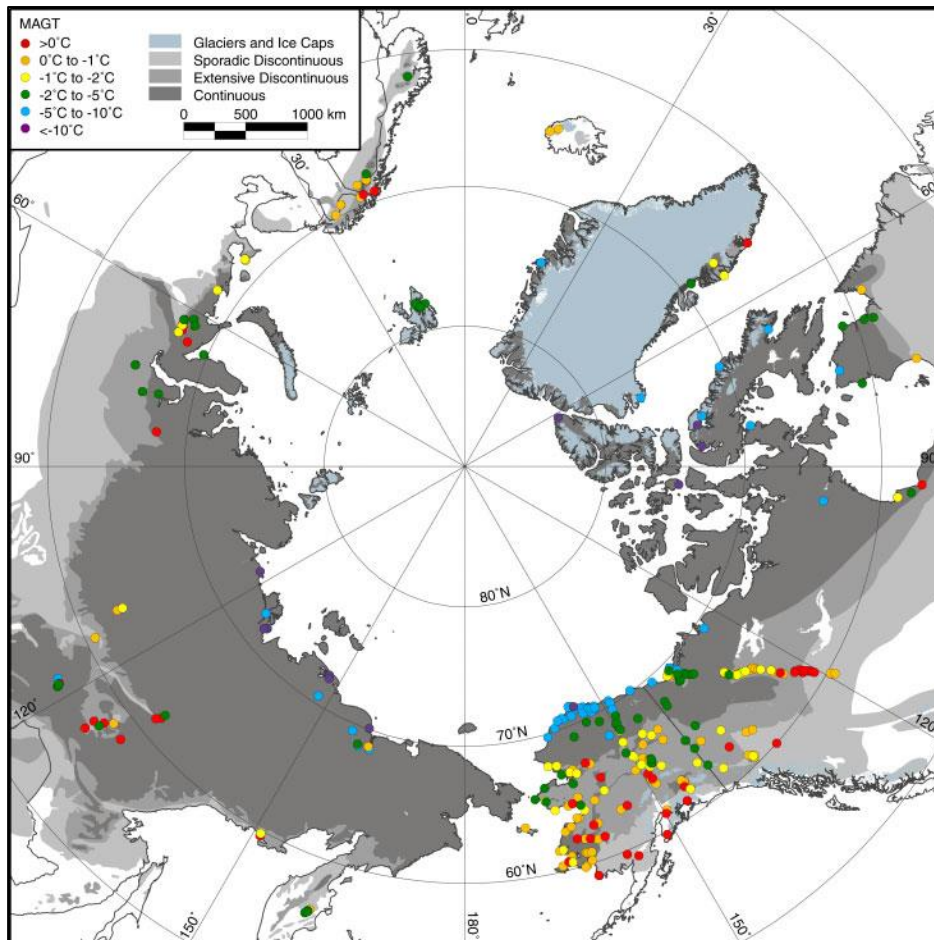


Figure 2.3: Map showing mean annual ground temperature (MAGT) of the Arctic. Points are boreholes where temperature is taken at depth of zero annual amplitude. (Figure from Romanovsky et al, 2010)

It is difficult to quantitatively define the permafrost-climate relationship. A schematic relationship (figure 2.2) between permafrost and climate has been developed which defines the presence of permafrost as a function of MAAT at different levels (Smith and Riseborough, 2002; Lachenbruch et al, 1988). The levels follow:

1. The air temperature, measured at standard height above the seasonal snow cover (MAAT)
2. The temperature at the ground surface (MAGST)
3. The temperature at the top of the permafrost (TTOP)

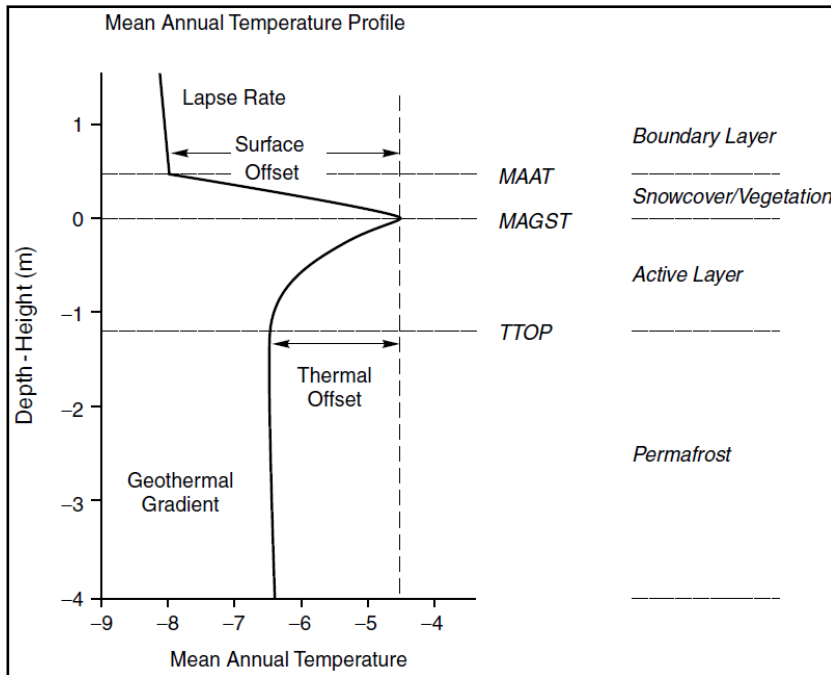


Figure 4.2: Schematic model showing relationship between air temperature and ground temperature with the influence of surface cover, snow cover, and geology. (Figure from Smith and Riseborough, 2002)

The diagram (figure 2.2) shows the depth to temperature relationship. Above the boundary layer the temperature is often a function of elevation due to the vertical lapse rate. The MAAT is measured at a standard height above the ground. Between the measured MAAT and the ground surface, where the MAGST is measured, there is often a surface offset. This may be due to either snow or vegetation cover which can act as a ground insulator, causing greater surface temperatures than air temperature. (Smith and Riseborough, 2002). The temperature typically decreases from the MAGST to a value where the TTOP is measured, at the frost table. The in-between is considered the active layer, which thaws seasonally. The temperature difference between the MAGST and the TTOP, through the active layer, is called the thermal offset. This value changes seasonally, as the ground thaws and freezes. It is especially pronounced because the thermal conductivity of ice is four times greater than water (Smith and Riseborough, 2002). Below the TTOP is permafrost, where temperatures slightly increase with depth due to a geothermal gradient, until the base of the permafrost is reached.

2.1.2. Thermal Characteristics of Permafrost

Figure 3 depicts a typical ground thermal regime for a permafrost zone. At the top is the ground surface, overlying the active layer. The active layer is a seasonal phenomenon, which freezes every winter and thaws over the duration of the melt season to the depth of the frost table (Burn, 2011). The thawing of the active layer is what accounts for surface movement and displacement during the melt season in permafrost environment. This includes slope instability, mass movements, and solifluction (French, 2007). Below the active layer is the transient layer. The transient layer is not rigid, and can reflect trends in climate on a decadal and century scale (Shur et al, 2005). It is often ice-rich and therefore acts as a buffer between the active layer and the permafrost. The excess ice increases the latent heat needed to thaw the permafrost below (Shur et al, 2005). Below this the ground is frozen to a certain depth, depending on the geothermal heat gradient (French, 2007). Total permafrost thickness can extend from meters to over a kilometer in depth (French, 2007). This permafrost reflects the climate on a scale of centuries to millennia (French, 2007).

There are several terrain factors which affect the ground thermal regime in permafrost environments. The relief and aspect on a given slope is important, particularly zones of discontinuous permafrost. Both relief and aspect will determine the amount of incoming solar radiation the ground and snow receive (French, 2007). Lithology is another important factor, due to both differing albedo and thermal conductivity values depending on rock type. This is a big factor in continuous permafrost zones, where the ground is already frozen, regardless of the terrain. The lithology will affect both the temperature of the permafrost, and the depth of the active layer reached during the melt season (French, 2007). Vegetation is one of the most complex factors, which heavily affects the thermal regime, regardless of the permafrost zone. Vegetation shields the ground from solar radiation, and acts as an insulator. The amount and type of vegetation is a key factor in determining the thermal offset and the active layer (French, 2007). Snow is another factor which acts as an insulator for the underlying permafrost. The roll of snow as an insulator is complicated because the effect it has on the underlying permafrost depends on thickness, duration and type (French, 2007).

The seasonal spectrum of temperature for permafrost in one location, usually at a borehole, is often represented by a trumpet curve (Figure 2.3). The tops of the two stems represent the maximum and minimum temperatures attained during a period of one year. The two stems

meet at the depth of zero annual amplitude, which is the depth where meteorological factors no longer affect the permafrost temperature. From there the ground eventually reaches temperatures above 0°C , depending on the geothermal gradient (Burn, 2011).

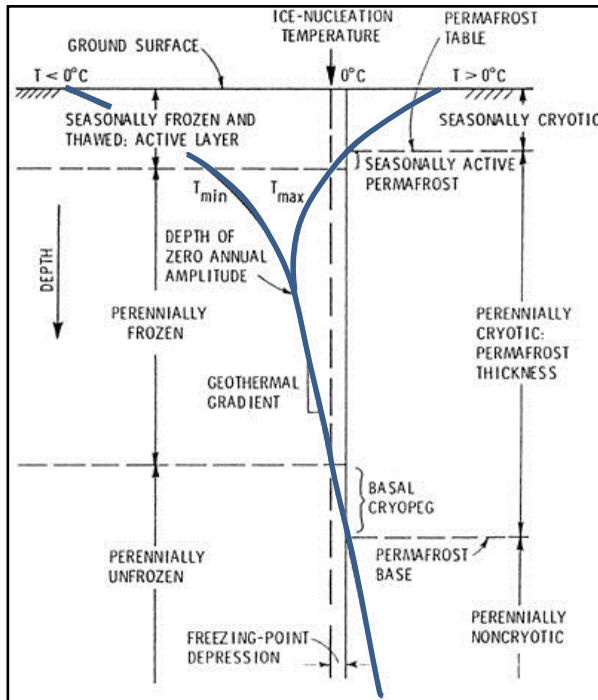


Figure 2.3: Typical ground thermal regime for permafrost, trumpet curve in blue. (Modified from French, 2007; ACGR, 1988)

2.1.3. Permafrost Hydrology

By definition permafrost is ground which is $<0^{\circ}\text{C}$ for a period of at least two years, which would then inhibit hydrologic systems to the surface and the seasonal active layer. In reality this is not the case, perennial unfrozen zones, called taliks, exist within permafrost which allow for active groundwater systems (Michel and van Everdingen, 1994; French, 2007). There has been a general increase in the amount of studies and understanding of subsurface permafrost hydrology, which contributes to the already established studies of surface hydrology in permafrost environments (Woo et al, 2008). In continuous permafrost zones the mean annual air temperature will be $<0^{\circ}\text{C}$, with negative degree days outnumbering positive degree days. Therefore the water input to the hydrological system is frozen for the majority of the year. Water can remain unfrozen year-long in permafrost environments, dependent on

multiple factors including chemistry, landforms and the presence of taliks. This is documented in various cases where factors such as the salinity of water, or water from glaciers end up surfacing in springs or an aufeis (icing) (Woo et al, 2008).

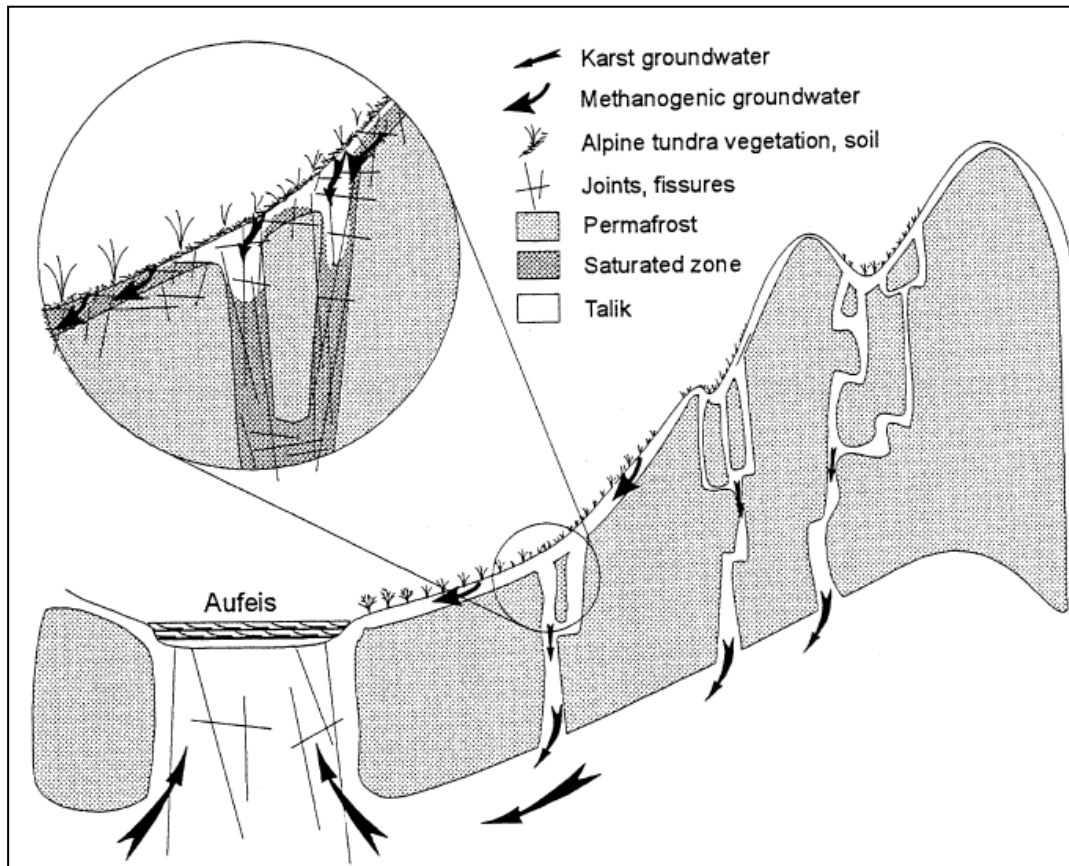


Figure 2.4: Schematic model of a water pathway through taliks in a permafrost zone, surfacing in an aufeis (icing). (Figure from Clark and Lauriol, 1997)

Hydrology in the Arctic is a factor of physical elements including snow, ice, permafrost, soil, surface energy balance, and the phase change of snow and ice to water (Kane et al, 1991). In the arctic, the period of the year when the phase change of snow and ice to water occurs is the major hydrological event (Kane et al, 1991). Due to a combination of little precipitation and a majority of precipitation falling in a solid state, snow and glaciers are the most important inputs for water into the hydrological system in Svalbard (Liestøl, 1975). Precipitation in central Svalbard is low, estimated at an annual value of 435mm water equivalence (w.e.) for Linnédalen (Humlum, 2002). The water which is released during this initial pulse of water from snowmelt follows water tracks to larger streams and rivers, or

pools up on the ground surface (Kane et al, 199). As the active layer thaws, water stored from previous years also contributes to summer runoff (Woo et al, 2008).

Groundwater systems in permafrost zones are confined to taliks. If a talik is significantly developed, the available water may be enough sustain groundwater flow year round (Clark and Lauriol, 1997). Localities with carbonate bedrock are most favorable for perennial groundwater flow, due to the development of fractures and fissures in the rock (figure 2.4). Additionally, the solubility of CO₂ and calcite at cold temperatures favor higher levels of dissolution (Clark and Lauriol, 1997). Taliks can be defined by the process which led to their occurrence (French, 2007). Taliks existing below water bodies are referred to as closed taliks, which remain unfrozen due to the heat storage capacity of water. Hydrothermal taliks exist due to the heat supply from groundwater. Open taliks penetrate through the permafrost to the unfrozen zone beneath (French, 2007).

2.2 Thermokarst

Thermokarst is a broad term including the entire range of geomorphic effects which result from the interaction of subsurface water and landforms in permafrost environments (French, 2007). The development of thermokarst features is reliant on ice-rich permafrost thawing (Yoshikawa and Hinzman, 2003). Thermokarst terrain can develop over years to centuries, dependent upon the disturbances which include both natural and anthropogenic. These encompass changes to climate such as an increase in air temperature or snow depth, and changes which alter hydrological processes to change the surface heat balance. Extreme events such as flooding, fires, and human activities such as construction also disturb the permafrost leading to thermokarst development (Burn and Smith, 1990; Osterkamp et al, 2000). There is a common misconception that thermokarst is related to karst, though the two are not directly related. Physical processes are dominant in thermokarst development, while chemical processes are dominant in karst development (French, 2007).

A characteristic feature of thermokarst is a thermokarst lake, which signifies disturbances to the permafrost (Burn and Smith, 1990; Yoshikawa and Hinzman, 2003). Thermokarst lakes range from newly developed features, resulting from the thaw of an ice wedge polygon (Osterkamp et al, 2000), to old features, developing from warmer periods in the early

Holocene (Burn, 1997; Schwamborn, 2002). Following a disturbance, ice-rich permafrost can differentially thaw due to heterogeneous topography. Surface depressions may form which begin to pond which in turn accelerates the subsurface thaw due to lower albedo and heat advection through runoff (Yoshikawa and Hinzman, 2003). If the depression holds a significant amount of water, a talik may form underneath due to the depth of water being too great to freeze during the winter. These taliks have the potential to penetrate completely through the permafrost (Yoshikawa and Hinzman, 2003). Thermokarst lakes are characterized by their irregularities in circumference and depth. Because thermokarst lakes form in ice-rich areas of the permafrost, they normally enlarge over a long period of time. As the lakes enlarge, shorelines often collapse (Burn and Smith, 1990).

2.3 Periglacial Geomorphology

A periglacial landscape refers to an environment which is shaped by cold, but non-glacial processes (French, 2007). Permafrost is an important component of most periglacial landscapes, but is not defining. Periglacial geomorphology is a scientific discipline which concentrates on the presence of ice in the ground and the associated landforms and processes which shape the landscape (French, 2007). Approximately 25% of the Earth's land surface is considered periglacial, predominately encountered at high-latitude, glacier-free areas (French, 2007). It is important to consider that periglacial environments are not static and can be thought as a function of time owing to climate fluctuation (French, 2007). It is possible to encounter an environment which appears to be periglacial, but is either proglacial or paraglacial. Proglacial environments are those which are affected by ice-marginal conditions (French, 2007). Paraglacial environments are those which are affected by former glaciations and deglaciation (Ballantyne, 2002).

It is impossible to delineate the exact boundaries of periglacial zones. Common indicators, such as the extent of discontinuous permafrost, or tree-line, are not static and therefore cannot be used as a concrete boundary (French, 2007). Instead a thermal definition, similar to permafrost, is given. The periglacial domain is defined to include areas with an MAAT of $< 3^{\circ}\text{C}$. Frost action is the dominant geomorphological driver (French, 2007). Several characteristic periglacial landforms and processes are often observed, including: tundra

polygons, ice wedge polygons, pingos, thermokarst features, patterned ground, rock glaciers, palsas, block fields, frost shattering, and solifluction, among others (French, 2007).

Ice wedge polygons are the most widespread and characteristic feature in periglacial landscapes (French, 2007; Christiansen, 2005). Ice wedge polygons form when thermal contraction occurs in frozen ground, usually during the coldest parts of the winter (Sørbel and Tolgensbakk, 2002). During thaw, when the seasonally-induced active layer forms, water fills the cracks and then freeze below the thaw table. This process forms ice veins, which will grow if thermal contraction leading to cracking continues during future winters (Sørbel and Tolgensbakk, 2002). The ice wedges typically form to make polygonal patterns with diameters ranging from 10 to 70m (Sørbel and Tolgensbakk, 2002). Ice wedge polygons are classified as epigenetic, syngenetic and anti-syngenetic (figure 2.5) (Mackay, 1990; 1995; 2000). Epigenetic polygons grow in relatively stable ground, with little added or lost material at the ground surface. Syngenetic ice wedges grow in areas with aggrading permafrost. Anti-syngenetic polygons grow on slopes and degrade from the top as the material is moved downslope, often due to slow mass wasting processes (Mackay, 2000).

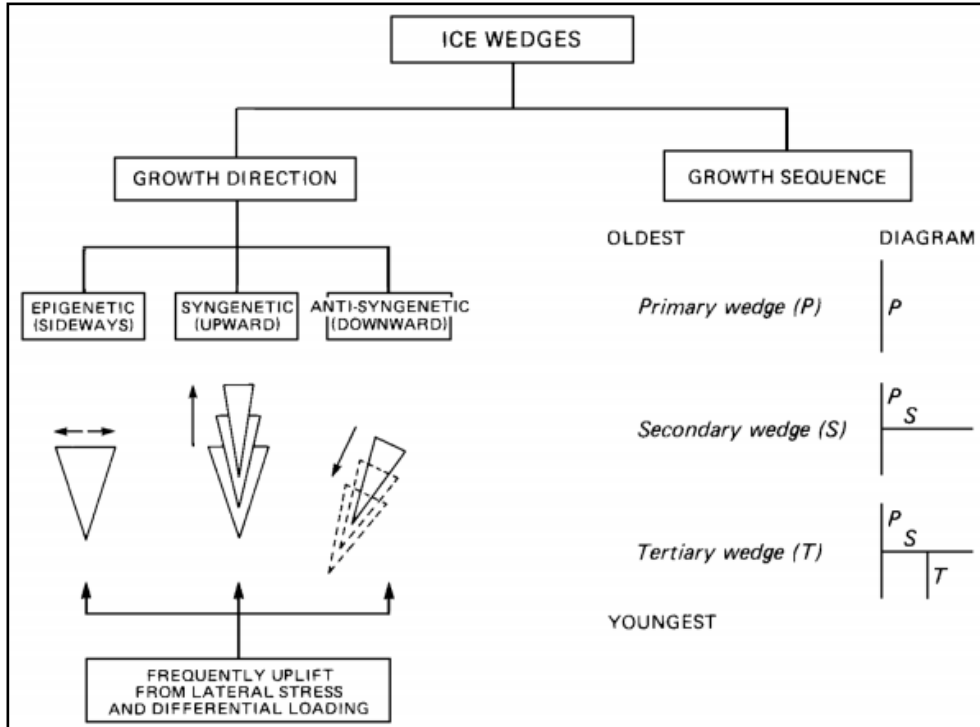


Figure 2.5: Ice wedge formation and classification. (Figure from Mackay, 2000)

Patterned ground is a predominately active layer phenomenon (French, 2007) which includes circles, nets, polygons, steps, stripes (Washburn, 1956), earth hummocks, and mud boils, among others (French, 2007). Washburn's 1956 paper gives over 19 possible hypotheses for the dominant processes which create these landforms. Recent studies suggest that patterned ground in periglacial environments forms due to a combination of frost-heave, thaw settlement, and movement due to the growth and melting of ice lenses in the active layer (Humlum et al, 2003). Patterned ground which is delineated by stone and fine-grained soil is defined as sorted patterned ground. Sorted patterned ground forms due to feedback mechanisms forced by freeze-thaw cycles, characteristic of arctic environments, and slope gradient (Kessler and Werner, 2003). Ice lenses which form in frozen soil sort the stones and soil by displacing the soil towards soil-rich domains, and the stones towards stone-rich domains. Following, the stones move along stone domains in an elongated pattern, due to the soil expanding as it freezes (Kessler and Werner, 2003). The various geometric shapes are attributed to differences in particle sorting, freezing and thawing, deformation of frozen soil and soil creep (Kessler and Werner, 2003).

Rock glaciers are considered a characteristic periglacial landform, typically tongue or lobe-shaped, encountered in areas of high relief (Humlum 1998; Humlum et al, 2003; French, 2007). Active rock glaciers are accumulations of sediments and ice, which deform under their own weight and move downslope (Humlum, 1998; Haeberli et al, 2006; French, 2007). Rock glaciers can give some indication of climate and palaeoclimate, and are generally found in drier, continental climates, with annual precipitation values not exceeding 1700mm w.e. (Humlum, 1998), although rock glaciers have been described in maritime climates (Humlum, 1998; Humlum et al, 2003; Haeberli et al, 2006) . Rock glaciers also indicate the divide between glacial and periglacial environments (Humlum, 1998), as well as the altitudinal limit of discontinuous permafrost (French, 2007). There is some scientific debate as whether the origin of rock glaciers is glacial, periglacial, or a combination of the two (Humlum 1998; 2000; 2007; Haeberli et al, 2006; French, 2007). Regardless of the ice origin, rock glaciers need a large sediment input, thus are predominately found either at the base of slopes which experience active slope processes culminating in high talus supply (Humlum et al, 2003; Haeberli et al, 2006; French, 2007), or below terminal moraines (Barsch, 1992; French, 2007).

The mechanical breakdown of bedrock in periglacial environments by rock shattering is a commonly encountered phenomenon (French, 2007). The result of bedrock shattering can be seen in large autochthonous blockfields of regolith covering the terrain in periglacial environments (Ballantyne, 2010). Large debris accumulations below vertical rock faces are another feature originating from rock shattering processes (French, 2007). Rock shattering has been mainly attributed to frost action which acts with in situ moisture and ice segregation. However, it is now considered that thermal stress may also be a factor which (French, 2007).

Solifluction is a slow mass wasting process driven by freeze-thaw action, occurring in fine grained soils (Matsuoka, 2001). Solifluction is wide-spread in the permafrost realm, and is observed in almost any environment where permafrost is encountered (Matsuoka, 2001; French, 2007). Solifluction is a slow process, with rates topping out at approximately 1 m $year^{-1}$ (Matsuoka, 2001). Therefore solifluction itself does not often lead to rapid and dramatic geomorphic transitions in the landscape, although because it is so widespread, the contribution to landscape evolution in periglacial environments is great (Matsuoka, 2001). Solifluction can also lead to ground instability which initiates slope failures, such as active-layer detachments (Matsuoka, 2001; Ballantyne and Harris, 1994). For solifluction to occur there must be three components at work: the potential for frost creep; the horizontal component of solifluction movement; and retrograde movement (French, 2007).

2.4 Karst

Karst is a well-studied discipline of geology. Entire textbooks are dedicated to the subject, such as Ford and Williams, 2007 and White 1988. Approximately 20-25% of the world population relies on groundwater aquifers for drinking water, developed through karst processes. With possibilities of future population growth and climate change, fresh water supply is an ever-growing concern (Ford and Williams, 2007).

Karst is a naturally occurring phenomenon encountered throughout the world. Lithologies which contain karst cover over 20% of Earth's ice-free terrestrial surface. Karst features are found at a wide range of latitudes and longitudes, though predominately in the northern hemisphere (Ford and Williams, 2007).

The term karst describes the processes and landforms which result from the dissolution of soluble rocks by water. When water comes into contact with the rock, the minerals dissolve into individual ions and molecules which diffuse into a solution (Ford and Williams, 2007). The amount of available water to input into the system controls the amount of rock denudation (Ford and Williams, 2007). The potential for karstification of landscapes exists wherever there is highly soluble rock, but other factors must occur for actual karstification to take place (Ford and Williams, 2007). In combination with soluble rock, well developed secondary, or fracture porosity is required (Ford and Williams, 2007). Rock structure also plays an important role in how efficient the karst process will be. Rocks which are dense, massive, homogenous, with coarse fractures will develop extensive karst. Rocks which are soluble, but have high primary porosity will rarely develop large karst systems (Ford and Williams, 2007). The most common type of rocks which produce karst terrains are carbonates and evaporates (Ford and Williams, 2007).

At a basic level, karst groundwater systems are similar to groundwater systems which develop in other rock types. As in other groundwater systems, a karst aquifer must be able to store, transmit and yield significant amounts of water (Ford and Williams, 2007). When carbonate rocks are formed they usually range from 25-80% in porosity from the interstitial spaces. Following, chemical processes such as dissolution and re-precipitation, and further fracturing due to tectonics will result in changes to the original porosity (Ford and Williams, 2007). The voids which form in the carbonate rocks come from varying origins, and are commonly classified into three different categories: granular (or matrix), fracture, and conduit (Ford and Williams, 2007).

When a system of interconnected conduits forms a well-developed karst aquifer solution caves may form. The development of the cave and shape it takes are dependent on many environmental, chemical and lithological factors, making these cave systems extremely complex (Ford and Williams, 2007). In cold, arctic regions frost shattering can act as an important means of cave development in limestone and dolomite lithologies (Ford and Williams, 2007).

Common indicators of karstified landscapes are sinking streams, caves, karrens, and dolines (sinkholes), among others (Figure 2.6). Landforms shaped by karst processes form from

hydrological and geochemical systems working together (Ford and Williams, 2007). Several important factors exist which essentially determine the location and type of karst landform that will form in a given environment. The hydrological processes at work are usually the most important control on where in the lithology the karst landform will begin, due to the control on erosion. The geology is also exhibits influence over the landform development. The geology will control the pathways which the solution erodes, the rock strength, and the possibilities of corrosion and corrasion. Differing amounts of runoff and temperature variation are also significant factors which control karst landform development (Ford and Williams, 2007).

One of the most common features found in karst landscapes are karrens (Figure 2.6). A karren is any small-scale dissolution pit, or groove and channel that form at the surface and underground in a karst environment. Karrens can range anywhere from 1cm to 10m in dimension (Ford and Williams, 2007). Another common landform found in karst environments are dolines, or sinkholes. This feature is perhaps one of the most recognized and associated feature with karst landscapes. The term doline can be used for any small to medium enclosed depression in karst lithology. Dolines are exclusively found in karst, and are considered index karst landforms (Ford and Williams, 2007). Dolines range in size from a meter to a kilometer in diameter and usually form a circular shape (Ford and Williams, 2007). The sides of dolines can be gently sloping to vertical, with depths ranging from a few meters to hundreds of meters deep (Ford and Williams, 2007). Dolines are often formed through dissolution, collapse and subsidence (Ford and Williams, 2007). There are six main types of dolines: solution, collapse, dropout, buried, caprock, and suffosion (Ford and Williams, 2007).

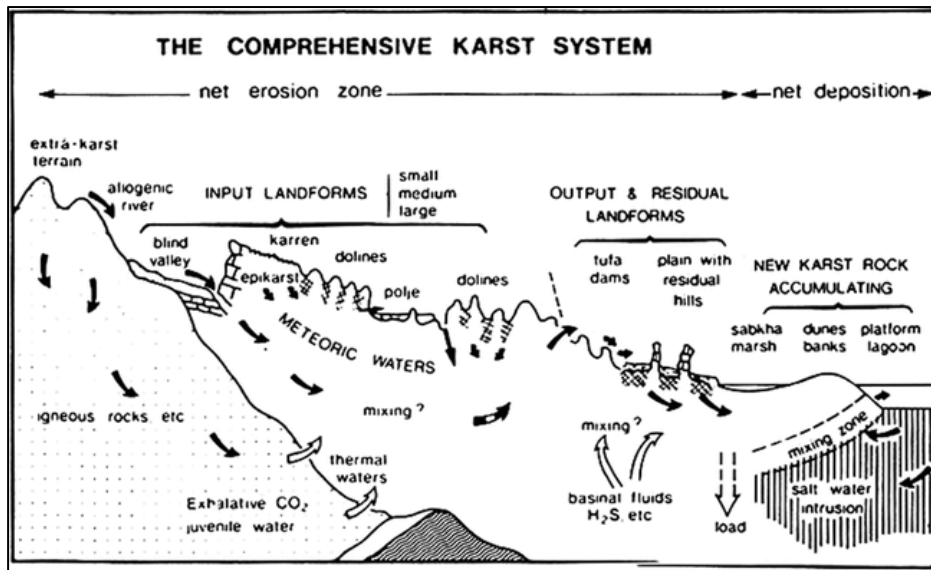


Figure 2.6: Typical features and layout of a karst system: landforms, features & dynamics.
(Figure from Ford and Williams, 2007)

2.5 Permafrost & Karst in the Arctic

The study of karst formations and processes in Arctic and High-Arctic permafrost environments is limited to relatively few studies. Ford and Williams (2007) developed a model (Figure 2.7) for karst development in permafrost areas based on studies in the Canadian Arctic. This model is general and limits the karst systems to either the seasonal active layer or to shallow taliks, unfrozen zones within permafrost (French 2007), directly beneath the lakes. Ford and Williams remark that the formation of intra-permafrost karst systems found in various parts of the Canadian arctic, were likely formed when conditions were favorable for karst formation (warmer and wetter). These conditions existed before the last glacial maximum or in areas which were left untouched by glaciers.

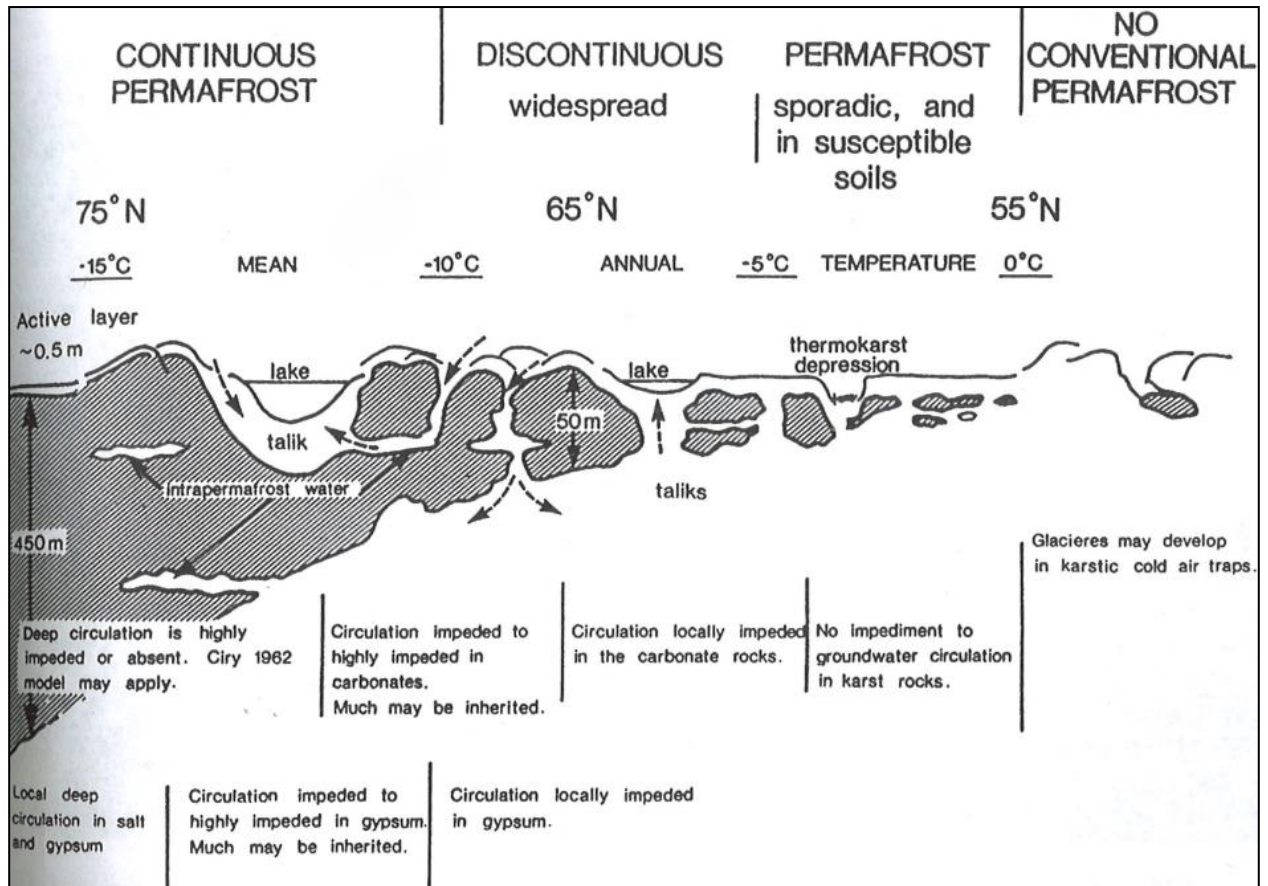


Figure 2.7: How a karst system functions in various permafrost environments. (Figure from Ford and Williams, 2007)

Other studies coming out of the Canadian Arctic include works by (Clark and Lauriol, 1997; Michel and van Everdingen, 1988; Michel and van Everdingen, 1994). In the Clark and Lauriol 1997 study, a large aufeis is the target of investigation in order to build an understanding on the subsurface hydrology in a permafrost zone. Geochemistry methods are utilized to trace water from the source, and shows that water is traveling through fissured taliks in carbonate bedrock. The Michel and Everdingen 1988 study is focused permafrost effects on karstic development in northern Canada. The study discusses the development of karst caves in high relief areas of the permafrost zone where extensive carbonate bedrock exists. Collapse leads to depressions and seasonal lakes forming in the area. Permafrost has both positive and negative effects on chemical weathering due to the transition from liquid water to ice (Michel & Everdingen, 1988). The study by Michel, 1994, discusses possible effects of karst systems in permafrost with regard to climate change. The paper suggests that

if climate warms, permafrost will degrade. With an increase in depth of the permafrost table, areas with karstic activity could develop into large near-surface unfrozen aquifers.

Implications of this include an increase in water-related discharge features, loss of lakes and wetlands due to better drainage, and slope instability and frost heave which could have geotechnical implications (Michel, 1994).

Salvigsen et al. (1983) identified several karst features from Mathiesondalen in Central Spitsbergen. Dolines, which are any small to intermediate enclosed karst depression (Ford and Williams 2007) occur in gypsiferous beds. Salvigsen and Elgersma (1985) determined that previously identified (Åkerman 1980) thermokarst features at Linnédalen in Western Spitsbergen as true karst features. Thermokarst includes the entire range of geomorphic effects resulting from subsurface water on features in permafrost zones (French 2007). These studies are some of the only available studies which mention karst in permafrost areas on Svalbard.

2.6 Literature

There are three main studies regarding karst systems in permafrost environments on Svalbard: Åkerman 1980, Salvigsen and Elgersma 1985, and Salvigsen et al. 1983.

Studies on periglacial geomorphology in West Spitsbergen

The works of Jonas Åkerman span three decades and include many studies regarding both permafrost and geomorphological processes at Linnédalen. The most extensive work is his 1980 PhD thesis, *Studies on Periglacial Geomorphology in West Spitsbergen*. This study spans seven years and includes sections regarding the climate, geology, geomorphology, icings, wind action, and maps of the Linnédalen area. Åkerman's purpose was to take an inventory of all of the geomorphological processes occurring in the Linnédalen area and attempt to correlate the geomorphological processes with climate data. The study goes into great detail taking into account all of the geomorphological processes and associated landforms in the Linnédalen area, and demonstrates what an exemplary place it is for the study of periglacial geomorphology. Åkerman makes reference to the karst lakes in his study, but attributes the lakes to thermokarst activity, instead of true karst. Åkerman

observes drainage of the lakes during the study period, and explains the subsurface drainage through intrapermafrost taliks.

All of Åkerman's field work and interpretation was conducted during the 1970's. It should not be surprising then, that there have been significant improvements and innovations in monitoring techniques. The terminology Åkerman uses to describe some of the periglacial features encountered in the area are also outdated. Åkerman bases much of his study upon previous studies and personal observations. He also utilizes aerial photography from the Norwegian Polar Institute. He conducted his own cartographic work using a flat-table Tachymeter (Wild RK 1) and various leveling methods.

Large-scale karst features and open taliks at Vardeborgsletta, outer Isfjorden, Svalbard

Salvigsen and Elgersma's 1985 work focuses on the same karst lakes included in Åkerman's 1980 thesis. This study goes on to assert that the lakes are not thermokarst features, but in fact true karst features. The author's make the argument that unconsolidated sediments are not so thick on Svalbard to allow for the lake's formation only from ice melt, so some interaction with the bedrock must be involved. Because the area is on top of calcareous bedrock, karst processes seemed a more likely explanation. They also conclude that the subsurface drainage system must be extensive enough to include the underlying bedrock. During the study the authors encountered high groundwater temperature measurements, which were surprising and offered no obvious explanation, except for an unknown geothermal heat source. Obtained measurements showed water temperatures up to 11°C, at over three meters depth. The authors created schematic models to interpret the groundwater system (figure 2.8). The first figure shows Lake 1, with water draining into the subsurface into a talik at the bottom of the lake and into a warm groundwater system. The second figure shows water draining through sinkholes at Lake 4 (the sinkhole in this study) and Lake 5.

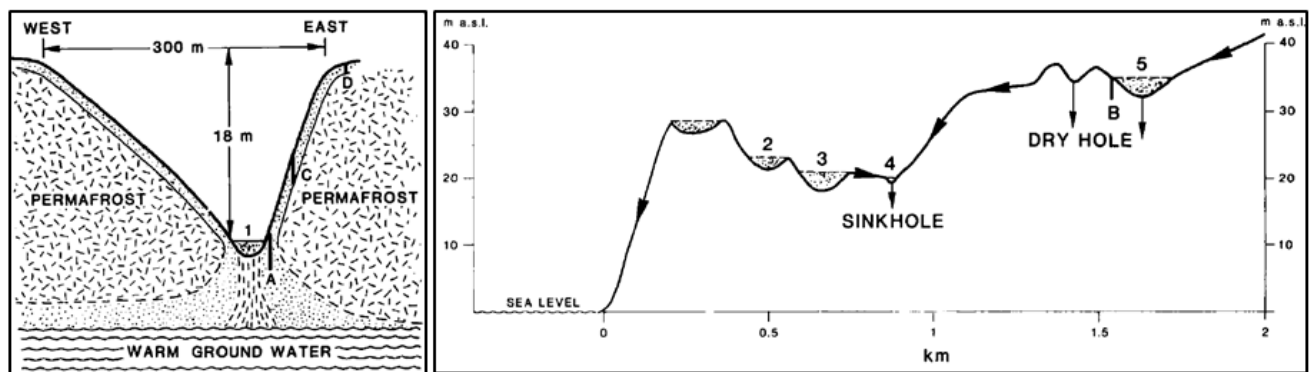


Figure 2.8: Schematic diagrams interpreting the karst groundwater system at Vardeborsletta, Linnédalen. The first figure shows drainage of water through a talik under Lake 1 into a warm groundwater system underneath. The second figure shows Lakes 2-3-4 and 5 with two sinkholes where water is actively draining into the subsurface. (Figure from Salvigsen and Elgersma, 1985)

Data from this study is obtained from the analysis of aerial photography, as well as observations through time spent at the field site. Digging by hand and thermometers were used to obtain ground and ground water temperatures. The rest of the data is from observations and previous studies. Dye tracing was also used in an attempt to trace water through the system, and find an outlet, but this brought no success. 1kg Rodamin B powder was dissolved with 6l technical alcohol.

Karst and karstification in gypsiferous beds in Mathiesondalen, Central Spitsbergen, Svalbard

This study was conducted north east of Linnédalen, in central Spitsbergen. During a field period the authors observed several closed depressions and other various karst features in the raised beaches at Mathiesondalen. Although on the surface the depressions appear to be thermokarst features, the authors determined that the water is flowing into underlying gypsiferous beds, and can be considered karst features. The authors conclude that water is flowing through sinkholes formed by the collapse of subsurface caves. The authors are left with the question of how it is possible for drainage to occur through the bottom of the active layer, which usually acts as an impermeable barrier. Methods for this study are simply observation during a field period and taking into account past geological studies of the area in order to understand the bedrock formation and deformation and how this lead to the karst features in the area.

CHAPTER 3. STUDY AREA

3.1. Location- SVALBARD

Svalbard is an archipelago located between 74° - 81° North and 10° - 35° East in the Barents Sea (Figure 3.1). Svalbard is classified as a High Arctic climate, and lies on the edge of the extreme arctic zone (Åkerman, 1992). The main islands comprising the archipelago are Spitsbergen, Nordaustlandet, Barentsøya, Edgøya, Kong Karls Land, Prins Karls Forland and Bjørnøya (Bear Island). The total land area of Svalbard is 62,160 km², 60% of which is covered by glaciers (Hagen et al., 1993, 2003). The remaining 40% is considered continuous permafrost (Humlum et al., 2003). Permafrost thickness ranges from approximately 100m in valleys to 400-500m in mountainous areas (Christiansen et al, 2010; Humlum et al, 2003; Liestøl, 1976). The landscape of Svalbard is generally mountainous, with extensive glacially-cut fjords extending towards the coast, to the Barents Sea. The altitude of Svalbard ranges from sea level to the highest peak of 1700m asl, in north-eastern Spitsbergen (Ingólfsson, 2011).

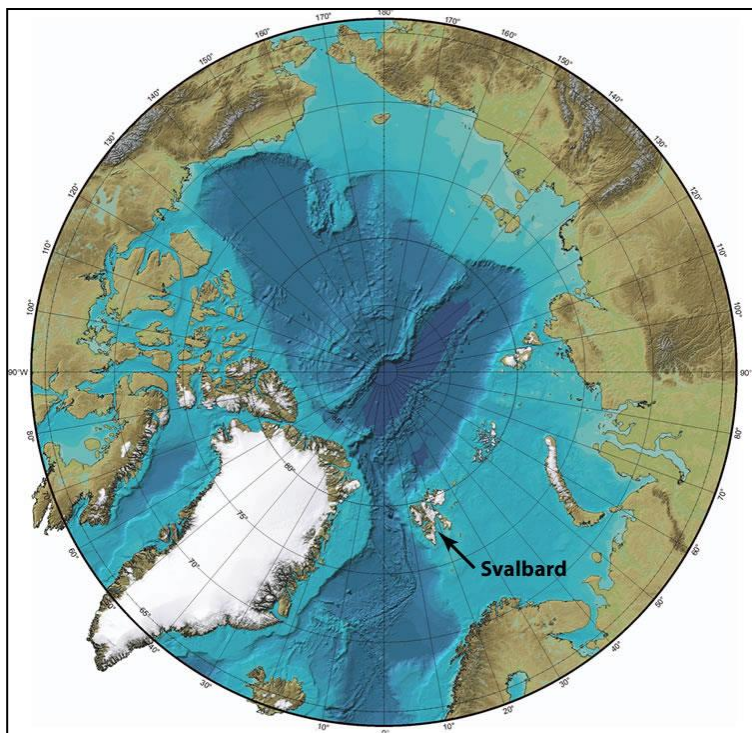


Figure 3.1: Svalbard, located in the Barents Sea. (Figure from <http://www.ngdc.noaa.gov/mgg/bathymetry/arctic/arctic.html>)

3.2. Climate & Meteorology of Svalbard

Svalbard is classified as having an arctic climate, although the West Spitsbergen Current, a branch of the North Atlantic Current reaches Western Spitsbergen, and operates as a climate moderator. Therefore surrounding sea water often remains unfrozen (Ingólfsson, 2011).

Another moderator of temperatures on Svalbard is the Siberian High (Humlum, 2003). This strong anticyclone results in cold temperatures over eastern Siberia and frequent cold outbreaks over eastern Asia during the winter. In the event of exceptionally cold winters, the high extends west into Russia and over parts of Europe. During these cold outbreaks there is an advection of warm air to Svalbard, resulting in heavy precipitation and snow melt even in midwinter. The opposite occurs during warmer periods over Siberia, resulting in cold, dry periods in Svalbard. This is termed a “thermal seesaw” (Humlum, 2003).

The mean annual air temperature in Svalbard is approximately -5°C at sea level, dropping to as low as -15°C in the high mountains (Ingólfsson, 2011). The -10°C isotherm is located at approximately 700m above sea level (asl) (Humlum, 2003). As seen in figure 3.2, recorded mean annual air temperatures from the Longyearbyen airport show that temperature holds steady from year to year in the summer, while fluctuating heavily during winter months. Annual precipitation in Longyearbyen is about 180mm w.e., with a vertical precipitation gradient of 15-20%/100m in coastal regions and 5-10%/100m in central areas. Both the west coast and east coast of Spitsbergen receive approximately 400-600mm w.e. precipitation/year (Ingólfsson, 2011). Longyearbyen is considered one of the driest places on Svalbard (Christiansen, 2005). The decrease in gradient towards central locations is due to enhanced orographic effects (Humlum, 2003).

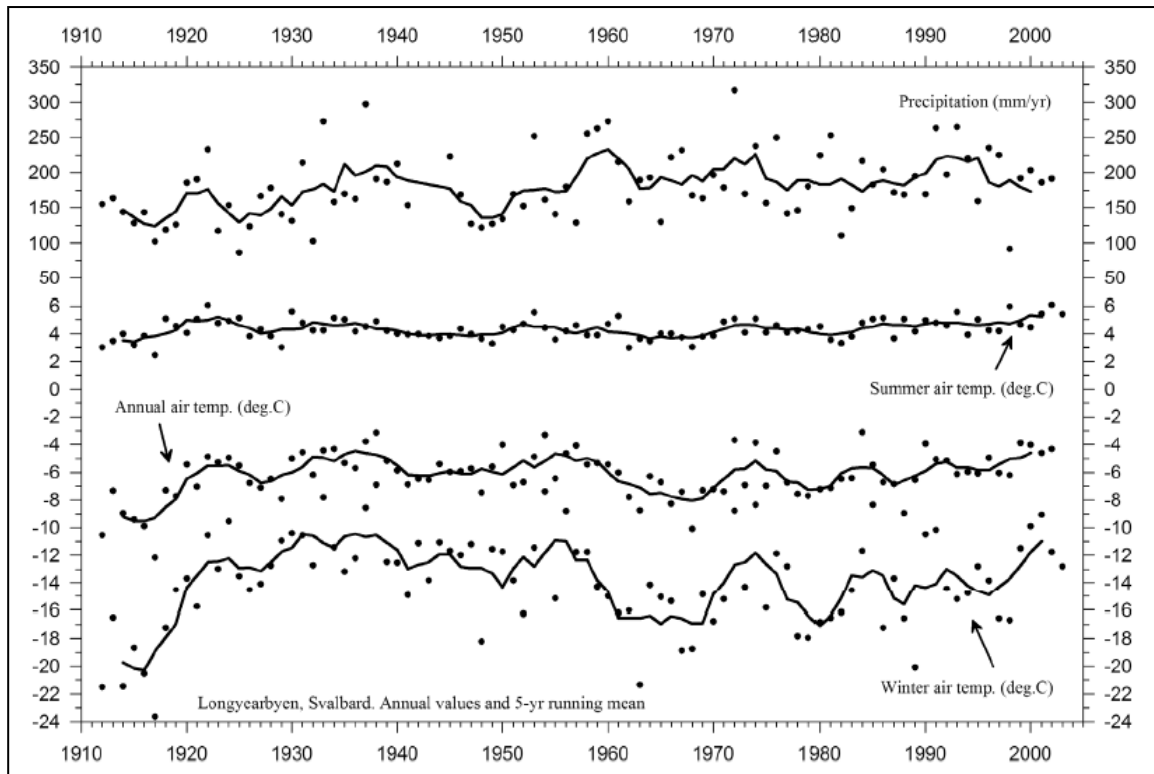


Figure 3.2: Precipitation and Mean Annual Air Temperature (MAAT) beginning in 1911, recorded from Longyearbyen Airport. (Figure from Humlum et al, 2003)

3.3. Geology of Svalbard

The geology of Svalbard is of particular interest to many scientists because the exposed rock ranges in age from the present to the Archean time period (Dallman, 1999, pg 17) (See Figure 3.3). Therefore, it is possible to draw analogues between the exposed geology of Svalbard, and what lies subsurface in the Barents Sea (Steel & Worsley, 1984). Svalbard is the exposed northwestern corner of the Barents Sea Shelf, which was uplifted during the late Mesozoic due to crustal movements (Dallman, pg 17). Several significant tectonic events in Svalbard's history result in the mountainous topography.

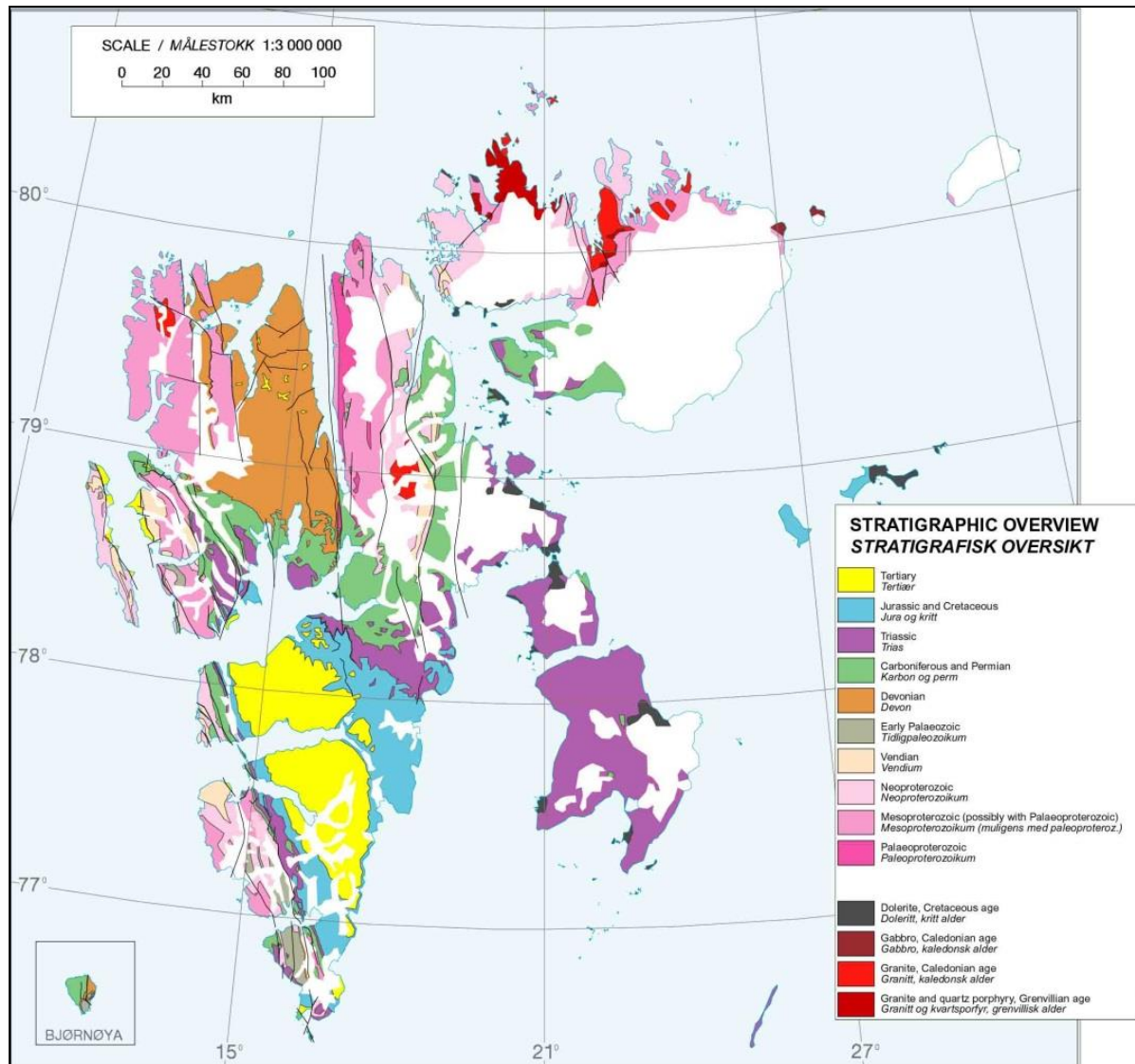


Figure 3.3: Geological map of Svalbard. (Figure from Norsk Polar Institutt)

Beginning in the mid-Devonian approximately 400 million years ago, the material which comprises the modern Svalbard archipelago has migrated north from Equatorial regions to its present 78°N (Figure 3.4). This northward migration is described in differing depositional phases, characterized by differing palaeoclimates as this portion of the Eurasian plate evolved. The sedimentation and depositional history of Svalbard is controlled by a combination of tectonic events and local to regional sea-level changes (Worsley, 2008).

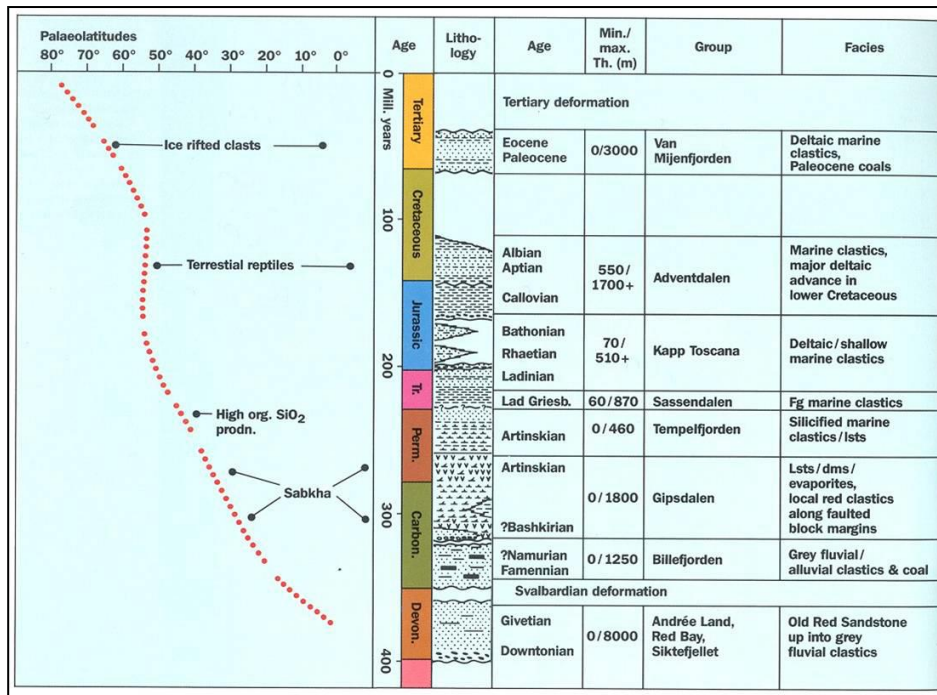


Figure 3.4: Svalbard at palaeolatitudes, showing characteristic lithologies and facies from each time period as Svalbard traveled from the equator to its present location. (Figure from Worsley & Aga, 1986)

Prior to current Svalbard's migration from equatorial latitudes to its present arctic location, basement rock consisting of sediments, metasediments and igneous rocks formed from the Precambrian to the Silurian (Elvevold, 2007). This section of rock is commonly termed "Hecla Hoek" (Worsley, 2008). The Hecla Hoek comprises 20 individual lithostratigraphical groups, and reflects the wide variety and complexity of exposures (Worsley, 2008). This basement rock underwent multiple periods of folding and metamorphism, ending in an important orogenic period; the Caledonian Orogeny, occurring approximately 400 mya during the Silurian (Elvevold, 2007).

A transition from red to grey sediments is observed pointing to a change in the early to mid-Devonian when Svalbard switched from a southern arid climate to the equatorial tropics (Worsley, 2008). Following this northwards movement, the final part of the Caledonian deformation occurred in the late Devonian (Worsley, 2008). The late Devonian rock is dominated by what is referred to as "Old Red Sandstone" (Figure 3.4) (Elvevold, 2007). This is a silt and sandstone conglomerate which alternates with shale and carbonate rocks

(Elvevold, 2007). The red reflects high iron oxide content in the rock which indicates that Svalbard in the Devonian was subject to an arid, desert like climate (Worsley, 2008).

Deposits from the Carboniferous and Permian are observed as plateau shaped mountains encountered predominately in central and northeastern Svalbard (Elvevold, 2007). The horizontal Carboniferous and Permian strata are comprised of fossiliferous beds of limestone and dolostone with white layers of gypsum and anhydrite (Elvevold, 2007). During the late Carboniferous most of the Svalbard and Barents Sea Shelf became a warm-water carbonate platform. Cycles of sea level transgressions and regressions led to alternating shallow sea and sabkha environments (Worsley, 2008).

The Mesozoic (Triassic, Jurassic, and Cretaceous) climate is characterized as being mostly temperate and damp (Elvevold, 2007). During this time period, Svalbard was still primarily inundated, although periods of uplift led to an alternating marine and terrestrial depositional environment (Elvevold, 2007). The exposures from this time period, predominately encountered in southern Spitsbergen, are made up of shale, siltstone, sandstone and limestone. This was also a time of rich plant and animal life on Svalbard, which is realized by the many fossils encountered all over Spitsbergen (Elvevold, 2007). During the end of the Cretaceous period volcanic activity and faulting disrupted Svalbard's fairly stable conditions (Elvevold, 2007).

The plate movements which characterized the end of the Mesozoic reached a high point in the early Tertiary creating a new mountain belt in western Spitsbergen (Elvevold, 2007). This event could possibly be a result of the Greenlandic continental plate pushing towards Svalbard as Svalbard was sliding past northern Greenland. This coincided with the North Atlantic and Arctic Ocean forming by seafloor spreading (Elvevold, 2007). Adjacent to the new mountain range, beginning in Isfjorden and moving southwards, the land began to subside forming what is now known as the Central Tertiary Basin. This basin was deposited with sandstones and shales (Elvevold, 2007). Tertiary age coal seams are now mined from the Central Tertiary Basin. These coal seams are indicative of the vast vegetation present on Svalbard during this time period (Ingólfsson).

Svalbard reached its current latitude during the Quaternary. At this time the earth was entering into an ice age. Due to this, Svalbard experienced several periods of both glacial and interglacial conditions (figure 3.5), resulting in glacial erosion driving landscape dynamics. These intermittent erosions removed much of the sediment deposited by the glaciations (Elvevold, 2007). Since the Quaternary glaciations began on Svalbard, there have been two types of glacial periods; one where Svalbard and the Barents Sea are covered in a large marine-based ice sheet, and one where the glaciers on Svalbard include highland ice fields & ice caps, and valley & cirque glaciers (Ingólfsson, 2011). It is possible to distinguish between these two periods; when Svalbard is fully glaciated it is possible to see pronounced fingerprints on continental shelf margins and slopes, while deglaciation deposits sediments and landforms in the fjords and continental shelf around Svalbard (Ingólfsson, 2011). The first build-up of an ice sheet covering Svalbard and the Barents Sea likely began around the Pliocene-Pleistocene, 3.6-2.4 Ma (Knies, et al., 2009). The number of ice-sheet glaciations of Svalbard and the Barents Sea is unknown, but has been estimated to be up to 16 (Ingólfsson, 2011; Solheim et al., 1996).

The current terrestrial landscape of Svalbard is clearly influenced by these glacial and interglacial periods. Marine records are better at capturing the influence of full-scale Svalbard – Barents Sea ice sheet glaciations due to the erosion which moved large volumes of sediment into the Barents Sea (Ingólfsson, 2011). There are many terrestrial records showing how glaciers have sculpted the land and influenced the pre-glacial fluvial and tectonic landscapes (Ingólfsson, 2011). These include glacially carved out cols, valleys and fjords (Ingólfsson, 2011). It is thought that the erosion of the larger fjords is due to the ice sheets and warm-based outlet glaciers, while the carving out of valleys and high-relief features is due to the smaller cirque and valley glaciers (Svendsen, et al., 1989).

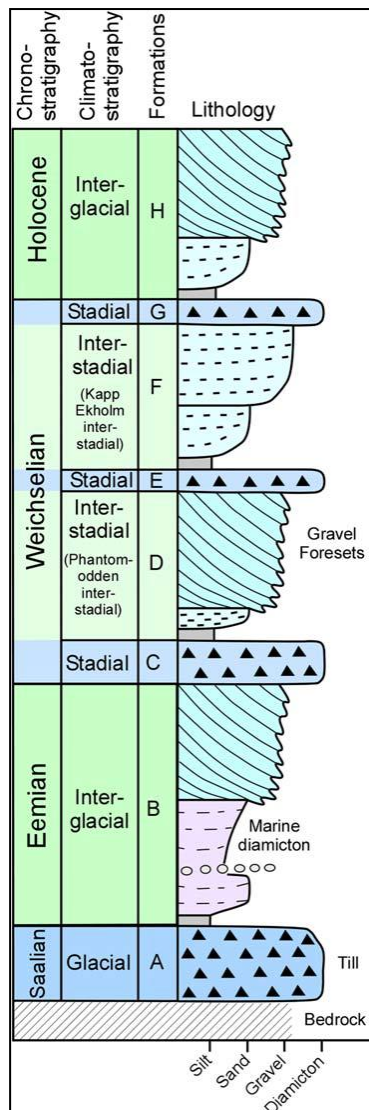


Figure 3.5: Kapp Ekholm stratigraphy reflecting glaciation (till) and deglaciation (marine-to-littoral sediments). (Figure from Ingolfsson, 2011, modified from Mangerud & Svendsen, 1992)

3.4. Geography and Geomorphology of Svalbard

It is difficult to give a simple overall description of the geomorphology of Svalbard, due to the varying temperature and precipitation gradients across the archipelago, as well as the differing topography. However, we can say that two of the most dominating features on Svalbard which dictate current landscape are glaciers and permafrost. Established studies estimate that Svalbard is 60% glaciated, with the remaining 40% considered continuous permafrost (figure 3.6) (Christiansen, et al, 2010, Humlum et al, 2003). Landforms originating from glaciers, weathering, frost processes, mass wasting, fluvial processes, and

aeolian processes are characteristic of the Svalbard landscape (Sørbel et al. 2001; Ingólfsson). The occurrence of glaciers and permafrost on Svalbard result in unique geomorphological phenomena, only encountered in glacial and periglacial environments.



Figure 3.6: Distribution of glaciers and permafrost on Svalbard. Glaciers are indicated by white, permafrost by grey. (Figure from Humlum et al. 2003)

The most dominant ice by area in Svalbard is in the east contained in the large ice masses which are separated into individual ice streams by mountain ridges and nunataks (Hagen, et al, 2003b). In western Svalbard many smaller cirque glaciers are encountered (Hagen, et al, 2003b). Many of the present glaciers on Svalbard are characterized as polythermal, meaning that ice temperatures in the glacier range from below 0°C where the ice may be frozen to the bed, to pressure melting point and above 0°C. This primarily relies on ice thickness which differs in the accumulation and ablation zones of the glacier (Sørbel et al. 2001). Surging glaciers are also widespread on Svalbard (Hagen, et al, 2003b). Glacier surges occur when ice flux is smaller than accumulation (Hagen et al, 2003). The basal shear increases to an

unknown threshold and then a surge can occur (Hagen et al, 2003). Surges result in an ice flux from higher to lower parts of the glacier which may result in a quick advance of the glacier front, as well as increased water and sediment transfer (Hagen et al, 2003). Surging glaciers can result in unique landforms including folded moraines (Sørbel et al. 2001). Other dominant landforms on Svalbard influenced by glaciers include: various moraines, rock glaciers, glacial erratics, kettle ponds, glacial striae, meltwater channels, and flutings (Sørbel et al. 2001).

Permafrost is thought to be present continuously over Svalbard in areas which are not glaciated or underlying large bodies of water (Sørbel et al. 2001; Humlum et al. 2003; Christiansen et al. 2010). Mountain permafrost in Svalbard is thought to be Weichselian age, while the permafrost in valleys and coastal areas is of Holocene age (Humlum et al. 2003; Christiansen et al. 2010). From recent permafrost studies conducted on Svalbard, it is possible to determine that temperatures and active layer depths in Svalbard vary according to factors such as the topography, lithology, altitude and climate conditions of the specific area (Christiansen et al. 2010). Permafrost is a driving geomorphological influence on Svalbard owing to it typically being impermeable to water. This leads to any runoff or meltwater being contained in the active layer or the surface which drives landscape development. Permafrost is responsible for several characteristic landforms encountered in Svalbard including rock glaciers, ice-wedge polygons, pingos and patterned ground (Sørbel et al. 2001).

There are several other processes which act as geomorphological drivers in the Svalbard landscape. Various slope and fluvial processes are also significant contributors to Svalbard landscape dynamics (Sørbel et al. 2001). These include colluvial sediment transport, solifluction, fluvial sediment transport, mass wasting, aeolian transport (Sørbel et al. 2001), and avalanches (Eckerstorfer and Christiansen, 2011; Vogel et al. 2012). A recent report by Farnsworth (2013) also highlights the importance of debris flows in the Svalbard landscape.

3.5. Linnédalen

Linnédalen (figure 3.7) is a valley located at 78°N; 13°E in west central Spitsbergen. Linnédalen is a glacially eroded valley. Previous studies indicate that deglaciation of

Linnédalen was approximately 12300 yr BP. This is indicated by radiocarbon dating marine molluscs above diamict from lake cores (Mangerud and Svendsen, 1990; Snyder et al. 2000). A small glacier, Linnébrean, sits at the southern end of the valley. Water from Linnébrean drains into a braided channel and is the inflow into Linnévatnet. Linnévatnet, at approximately 4.7km length and 1.3km width, is the second largest lake on Svalbard and the most extensively studied (Ingólfsson). The lake, which sits within the Late Weichselian glacial limit (Mangerud, 1987) is contained in a glacially overdeepened basin reaching almost 40m depth (Snyder et al. 2000). Linnévatnet currently sits at approximately 12m asl (Mangerud and Svendsen, 1990). Secondary water sources to Linnévatnet include Kongressvatnet, a karst lake located to the south east of Linnévatnet, as well as drainage from the surrounding mountains Griegaksla to the west and Vardeborgaksla to the east. The outflow from Linnévatnet drains into Linnéelva and then into Isfjord. Secondary drainage into Linnéelva comes from some of the small lakes located on Vardeborgsletta.

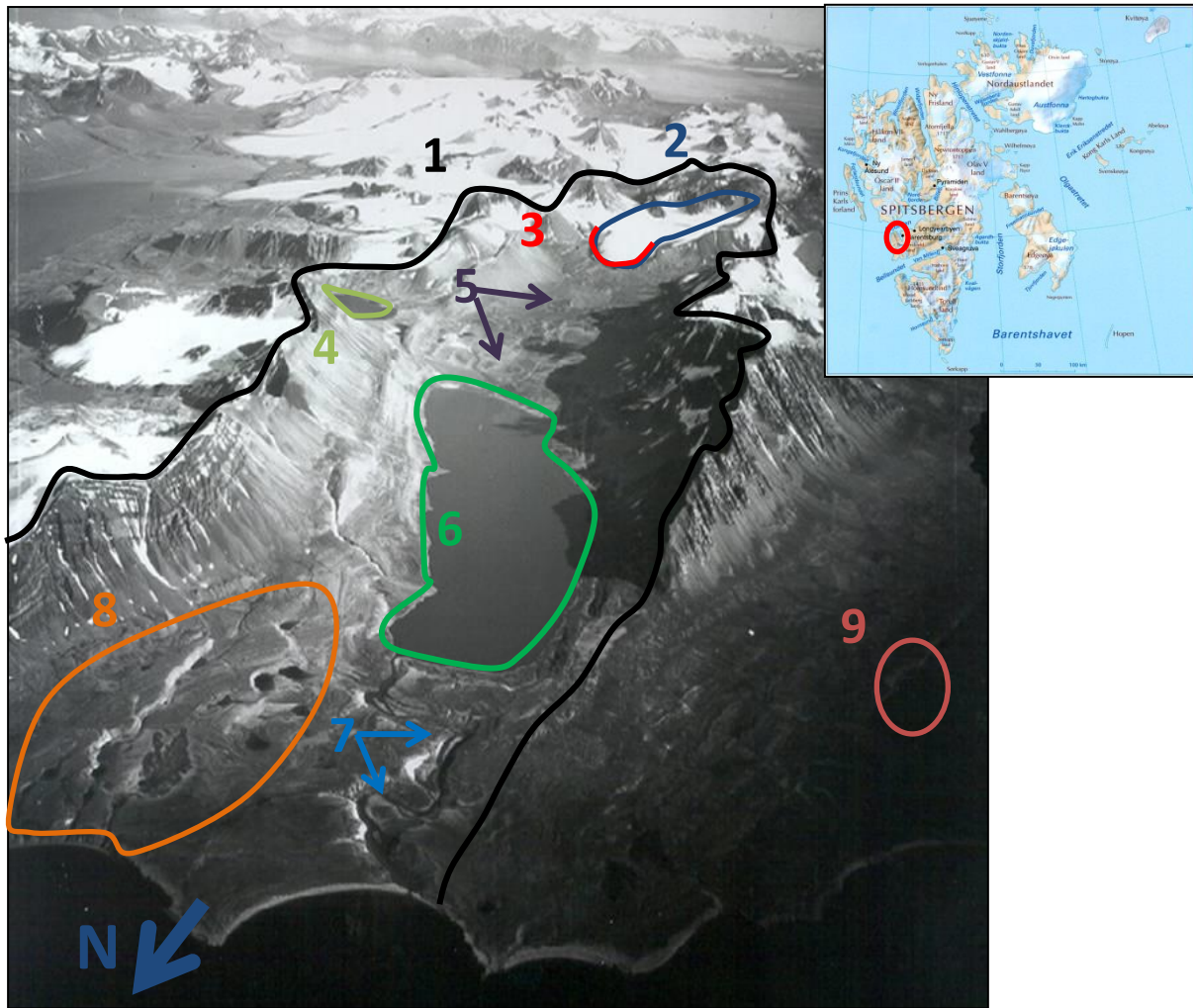


Figure 3.7: Linnédalen, west central Spitsbergen & inset map of Svalbard showing Linnédalen.

1) Linnédalen 2) Linnébreen extent 1936. The glacier front had retreated almost 1.5km from 1936-2008. 3) Little Ice Age Moraine 4) Kongressvatnet 5) Linnéelva inflow from Linnébreen 6) Linnévatnet 7) Outflow from Linnévatnet to Isfjord 8) Vardeborgsletta (beach terraces with karst Lake system). 9) Tunsjøen Lake, located on the strand flat. Background photo from Norsk Polar Institutt, 1936. Inset map from Norsk Polar Institutt. Figure, Cohen, 2013

3.5.1. Linnédalen Climate & Meteorology

Linnédalen's location on the west coast of Spitsbergen puts on the edge of the extreme arctic zone (Åkerman, 2005). However, the maritime location on the North Atlantic Ocean acts as a temperature moderator and brings in more precipitation than at other similar high latitude locations (Åkerman, 2005). The mean annual air temperature from 1912-1975 at Linnédalen, taken from records at Isfjord Radio, situated at Kapp Linné, is -4.8°C (Åkerman 2005). A

recent air temperature time series (appendix d) gives Linnédalen an MAAT of -2.18°C from 2005-2012. Linnédalen fits into French's 1976 definition of a High Arctic Climate, "High arctic climates in Polar latitudes – extremely weak diurnal pattern, strong seasonal pattern, small daily and large annual temperature range," (French, 1976; Åkerman, 1980). Accurate precipitation data is difficult to gather in high arctic climates. This is a factor of extreme weather conditions, lack of infrastructure, high winds, quantifying solid precipitation, and lack of vegetation (Åkerman, 1980; Humlum, 2002). Precipitation estimates from 1912-1975 is 400mm w.e., with little annual variation, (Åkerman, 2005; Åkerman, 1980) but more recent data is unavailable. In Åkerman's 1980 thesis he quantified seasonal variability of precipitation using data from Norsk Meteorologisk Institutt. From 1934-1975 the mean precipitation for December January February (DJF) was 97.7mm, March April May (MAM) was 77.2mm, June July August (JJA) was 101.5mm, and September October November (SON) was 119.4mm.

3.5.2. Linnédalen Geology

The local geology of Linnédalen is suitable for the formation of a karst system. In the eastern side of the valley, at the karst lake location, the observed underlying bedrock is limestone, gypsum, and dolomite (Figure 3.8) from two formations. The Gipshuken formation of the Gipsdalen Group, deposited during the Carboniferous and Permian, ranges from approximately 350-250 million years ago (Svendsen et al. 1989; Dallman, 1999). The Gipsdalen group represents the stratigraphic development of Spitsbergen ranging from the middle Carboniferous clastic graben-related sediments to late Carboniferous/early Permian marine shelf carbonates with evaporate intercalations (Dallman, 1999). The Gipshuken formation has a structural setting from the Late Palaeozoic platform of the Svalbard/Barents Sea Shelf (Dallman, 1999). The main lithologies which comprise the formation are dolomite, limestone, anhydrite/gypsum and carbonate breccias (Dallman, 1999). The Gipshuken formation represents shallow marine and sabkha deposits (Worsley, 2008). The Wordiekammen formation is also described at Vardeborgsletta, (though then termed the Nordenskiöldbreen formation) (Braathen and Bergh, 1995a; 1995b). This formation is of mid-Carboniferous age and represents the late Palaeozoic

platform of Svalbard and the Barents Sea Shelf. The main lithology of this formation is carbonate rock.

At Vardeborgsletta, the bedrock is predominately covered with a thick layer of marine deposits, but outcrops are visible in some locations (Salvigsen and Elgersma, 1985). The west side of Linnédalen and out to the coast is situated on the Hecla Hoek series, consisting of Precambrian-Ordovician rocks (Åkerman, 1984). The series lies predominately parallel to the coast and consists of vertical strata of schists, quartzites, phyllites, tillites, dolomites, limestones and conglomerates (Åkerman, 1984; Åkerman, 1980). To the east of the study area out to Grønfjorden, the steeply dipping rocks become younger where the sandstones of the early Cretaceous Helvetiafjellet formation are dipping vertically (Worsley, 2008).

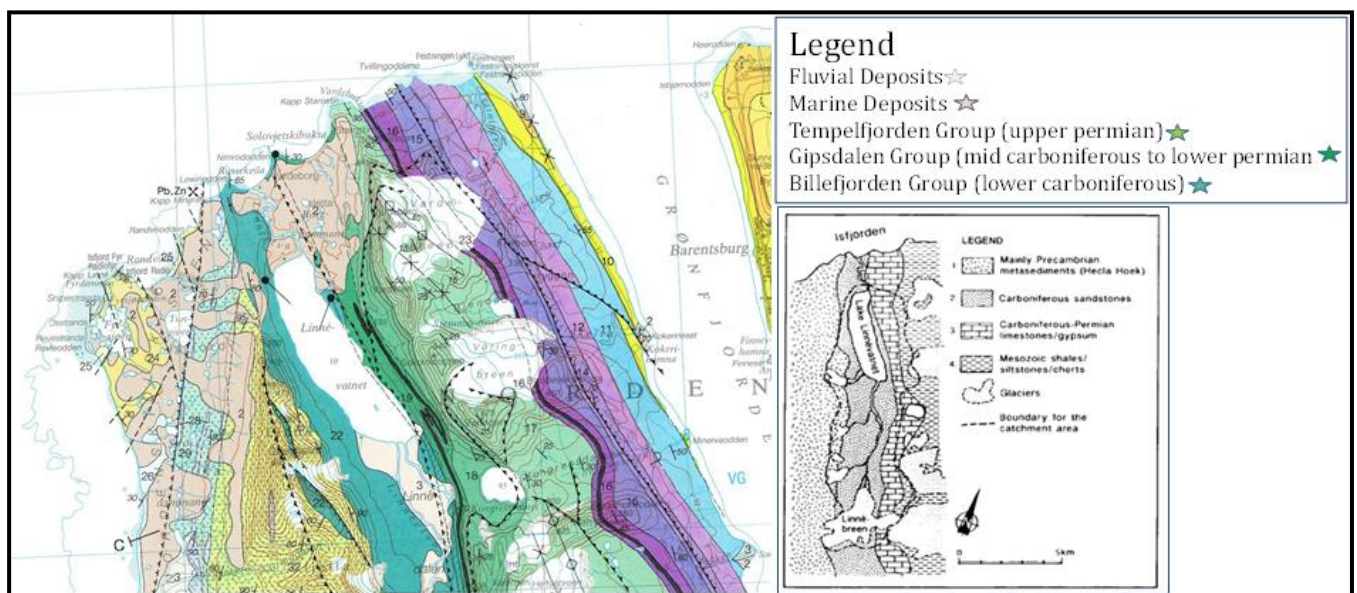


Figure 3.8: Geological Map of Linnédalen and simplified bedrock map. Scale is 1:100,000

(Modified from Norsk Polar Institute & Mangerud and Svendsen, 1990)

3.5.3. Linnédalen Geography & Geomorphology

A study by Mangerud & Svendsen (1990) gives a chronology for the deglaciation of Linnédalen. Sediment cores were taken from the bottom of Linnévatnet which revealed a sequence of lacustrine sediments, marine sediments, basal till and bedrock, from top to bottom. By radiocarbon dating shells at the bottom of the marine sediments, overlying the

basal till, they established that Linnévatnet was deglaciated approximately 12500 BP. Due to rapid isostatic rebound following deglaciation, Linnévatnet became a tributary fjord into Isfjord (Mangerud and Svendsen, 1990). A 30m beach terrace at the northern end of Linnédalen isolated Linnévatnet from the sea approximately 9600 BP. This age was acquired from obtaining radiocarbon dates from the upper part of the marine unit of lake cores (Mangerud and Svendsen, 1990; Svendsen et al, 1989). No younger glacial re-advances extensive enough to reach Linnévatnet have occurred since the deglaciation 12500 BP (Mangerud and Svendsen, 1990).

After deglaciation 12500 BP Svalbard experienced a warm Younger Dryas period in the early Holocene, preventing any further glaciations for the next 6000 years (Svendsen and Mangerud, 1997). 4000-5000 YA Svalbard experienced a cooling period which allowed for the formation of small alpine and cirque glaciers. This led to the formation of the glacier Linnébreen, which currently sits at the head of Linnédalen (Figure 3.7.2). The Holocene glacial maximum occurred during the Little Ice Age on Svalbard, dating to the 13th or 14th century (Svendsen and Mangerud, 1997). This can be seen in Linnédalen at the Little Ice Age moraine (Figure 3.7.3). Linnébreen has been receding to its current location approximately 1.5km southwest of the Little Ice Age moraine (Figure 3.7.2).

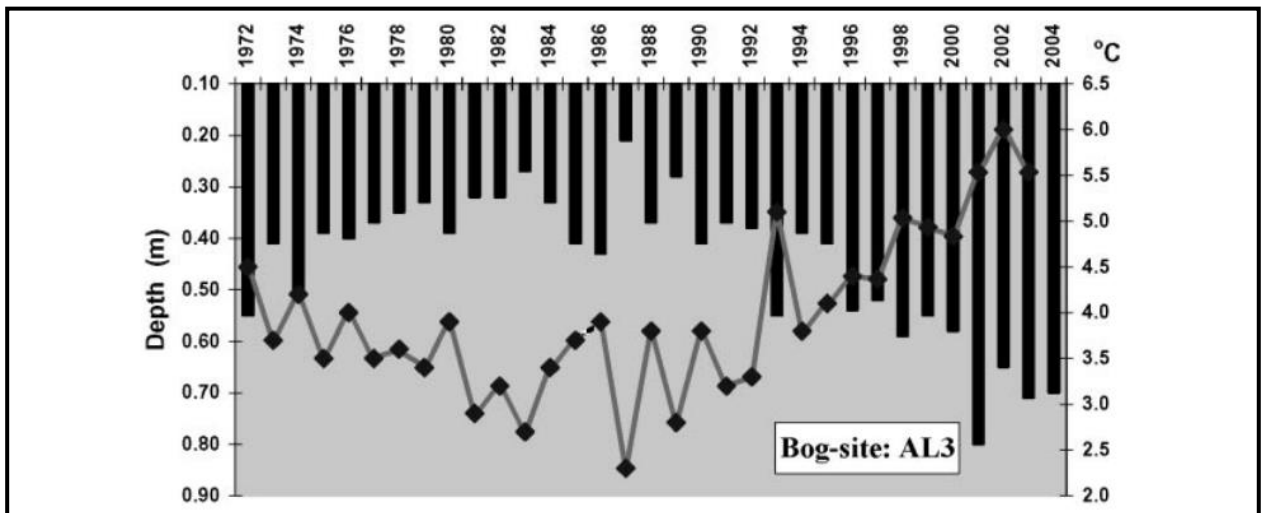


Figure 3.9: Active layer depths from Linnédalen, collected from 1972-2005. (Figure from Åkerman, 2005)

Ground temperature data has been collected in Linnédalen area for various studies since 1972 (Åkerman, 2005; Christiansen et al, 2010). Table 1 shows data compiled from boreholes at Kapp Linné, the closest boreholes to the karst lake system on Vardeborgsletta. The table shows climatic conditions, snow cover, and active layer thickness. Data is obtained from Christiansen et al. 2010.

Table 1: Modified table of permafrost conditions at Kapp Linné

Borehole name/ID	MAGST (°C)	MAGT (°C) at depth of ZAA or lowermost sensor (m)	MAAT (°C)	FDD air (°C days)	TDD air (°C)	Snow max depth (m)	ALT (m)	Time Period
Kapp Linné 1/KL-B-1	-3.2	-3.1 (15m)	-3.4	-1773	549	<0.1	2.5	29.09.2008 - 28.09.2009
Kapp Linné 2/KL-B-2	-3.7	-3.2 (15m)	-3.4	-1773	549	<0.1	1.8	22.09.2008 -
Kapp Linné 3/KL-B-3	-2.7	-3.4 (15m)	-3.4	-1773	549	<0.5	0.8	01.09.2008 - 31.08.2009

Data from the boreholes at Kapp Linné (Table 1 & Figure 3.10) show that ground temperatures can vary spatially over a small area. Factors including thin snow cover from wind redistribution, differences in sediment type and bedrock influence the ground temperatures, and the depth of the active layer. In the case of the boreholes at Kapp Linné, the borehole drilled in bedrock as opposed to sediments and organics has a larger active layer; 2.5m as compared to 1.8m and 0.8m respectively. The bedrock borehole has larger differences in temperature due to the higher thermal diffusivities (Christiansen, et al, 2010). The temperature at the depth of zero annual amplitude ranges from -2.3°C to -3.4°C and are located at depths as shallow as 4m (Christiansen et al, 2010). In general ground temperatures at Kapp Linné can be expected to be warmer due to the coastal, maritime climate. However, due to the thin snow cover at the coast, two of the Kapp Linné boreholes display temperatures of -3.1°C to -3.2°C even at 15m depth (Christiansen, et al, 2010).

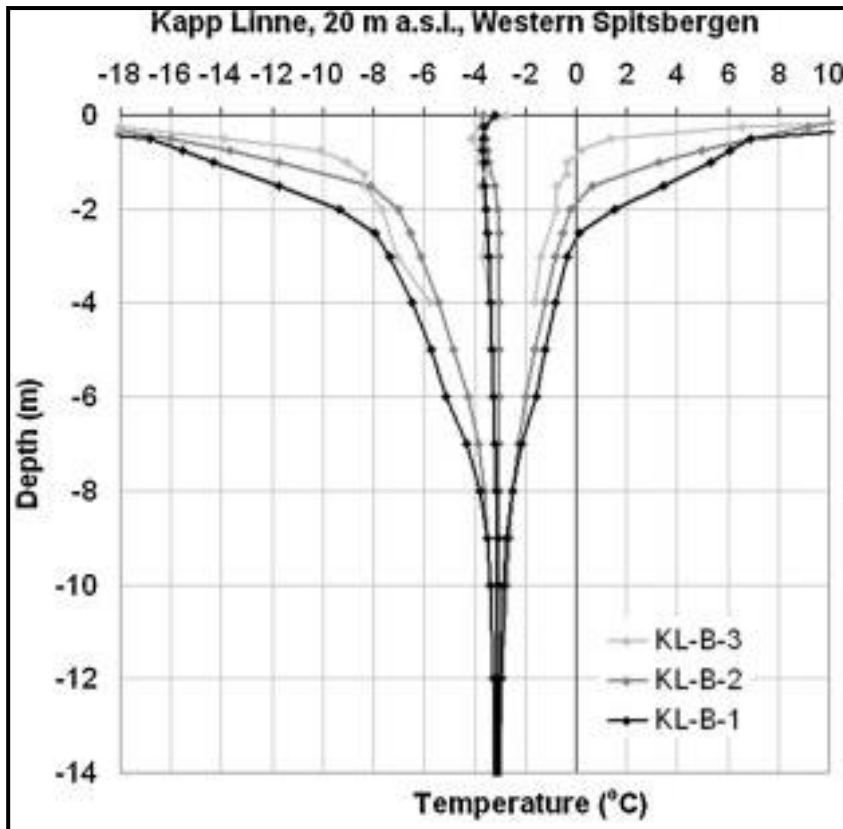


Figure 3.10: Borehole data from three boreholes at Kapp Linné. (Figure from Christiansen et al, 2010)

A study from Åkerman 2005 shows active layer data from 1972-2004 from a borehole near the karst lakes (Figure 3.9). Åkerman's (2005) study measures active layer depth in several geomorphological processes including solifluction sheets, solifluction lobes, non-sorted and sorted steps, non-sorted and sorted stripes, talus creep, and small-scale creep. Åkerman was able to correlate a deeper active layer depth with warmer summer temperatures. Years with deeper active layers correlated with increased slope processes rates (Åkerman, 2005). Figure 3.11 shows increased downslope movement in all monitored geomorphological features at Kapp Linné for a decade long period from 1992-2002, as opposed to a two decade long period from 1972-1992. This corresponded with observed increasing summer temperatures over the study period (Åkerman, 2005).

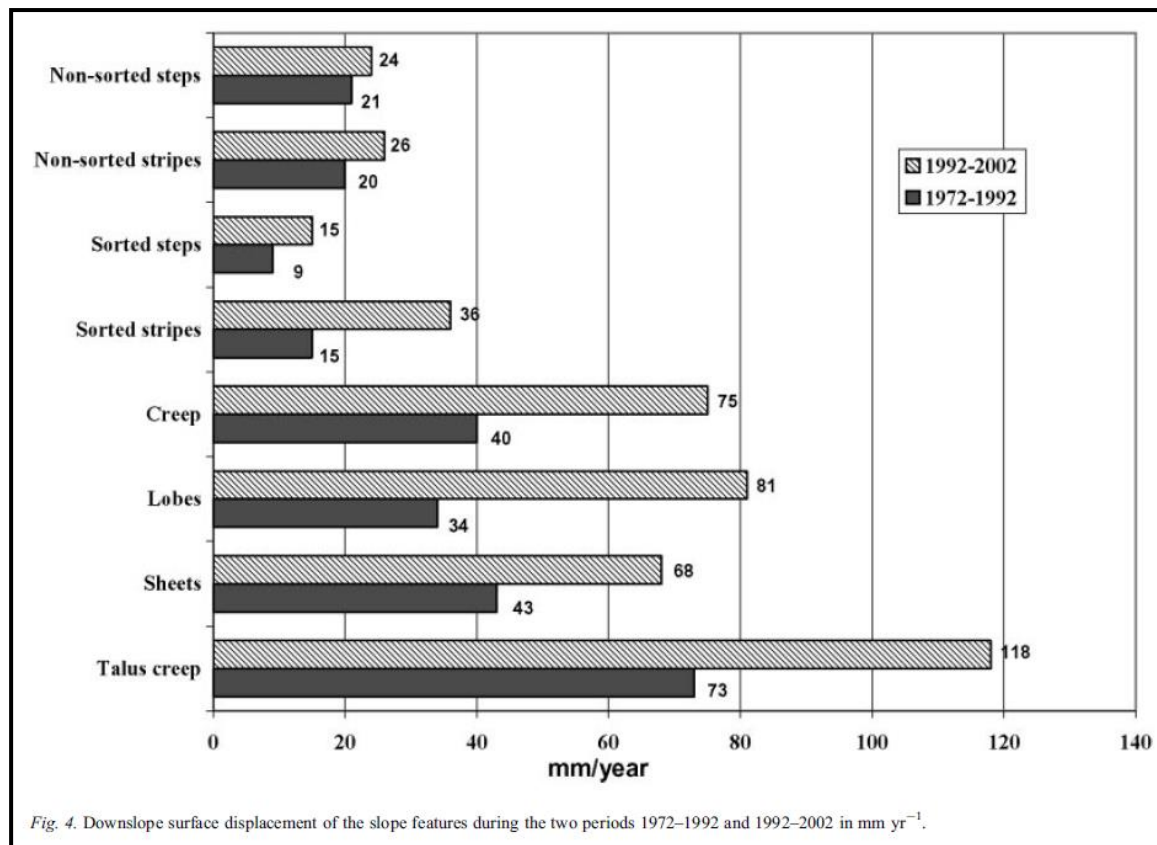


Figure 3.11: Slope movement rates for various geomorphological features at Kapp Linné.
(From Åkerman, 2005)

A 1992 Åkerman study details the influence of lakes and ponds on the periglacial geomorphology of the Linnédalen area. The study inventories 87 lakes and ponds in a 50 km² area around Kapp Linné. Nine shore types are characterized for the area including; rock shores, block shores, bog shores, patterned shores, ridge shores, thermokarst shores, delta shores, talus shores and terrace shores. This area exhibits a particularly concentrated amount of water bodies in one area for Svalbard. This presence influences the geomorphology of the area by feeding water to the active layer during the summer season (Åkerman, 1992). This can lead to heightened activity of ground ice formation, physical and chemical weathering and patterned ground development (Åkerman, 1992).

3.5.4. Linnédalen Measurement Sites

Following are maps which display the locations around Linnédalen which were mapped and monitored during the study period, as well as where the longer-term ground temperature collection points are located. The basemap is a 2m interval contour map from Åkerman, 1980. The scale is 1:14,286. The inset map is from the Norsk Polarinstitut TopoSvalbard (www.toposvalbard.npolar.no). There are three different location maps which display two different areas where the measurements come from. The entire study area is shown in figure 3.7. Figure 3.12 displays lakes 1, 2, 3 and 4, as well as all of the monitoring in the immediate vicinity. It is the northern part of the Vardeborgsletta plain (figure 3.7). Figure 3.13 displays lakes 5, 6, 7, 8 and 9, as well as all of the monitoring locations in the immediate vicinity. It is the southwestern part of the Vardeborgsletta plain (figure 3.7) Figure 3.14 displays Tunsjøen Lake, and all of the monitoring locations in the immediate vicinity. It is located to the west of Vardeborgsletta (figure 3.7).

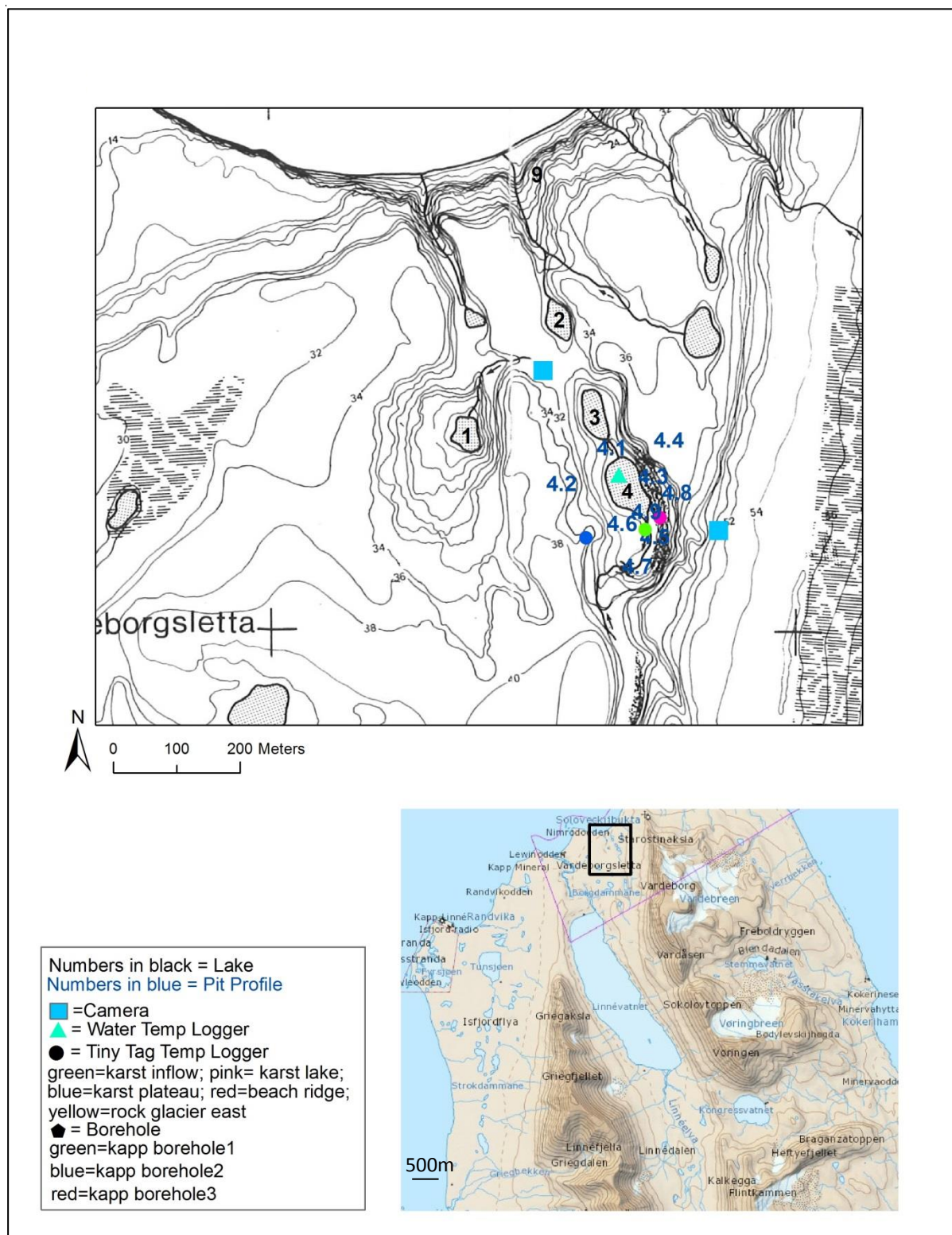


Figure 3.12: Locations map showing all monitoring sites where data was obtained at Vardeborsletta, Lakes 1, 2, 3 and 4. Basemap is from Åkerman, 1980. Inset map is from Norsk Polarinstitutt. (Cohen, 2013)

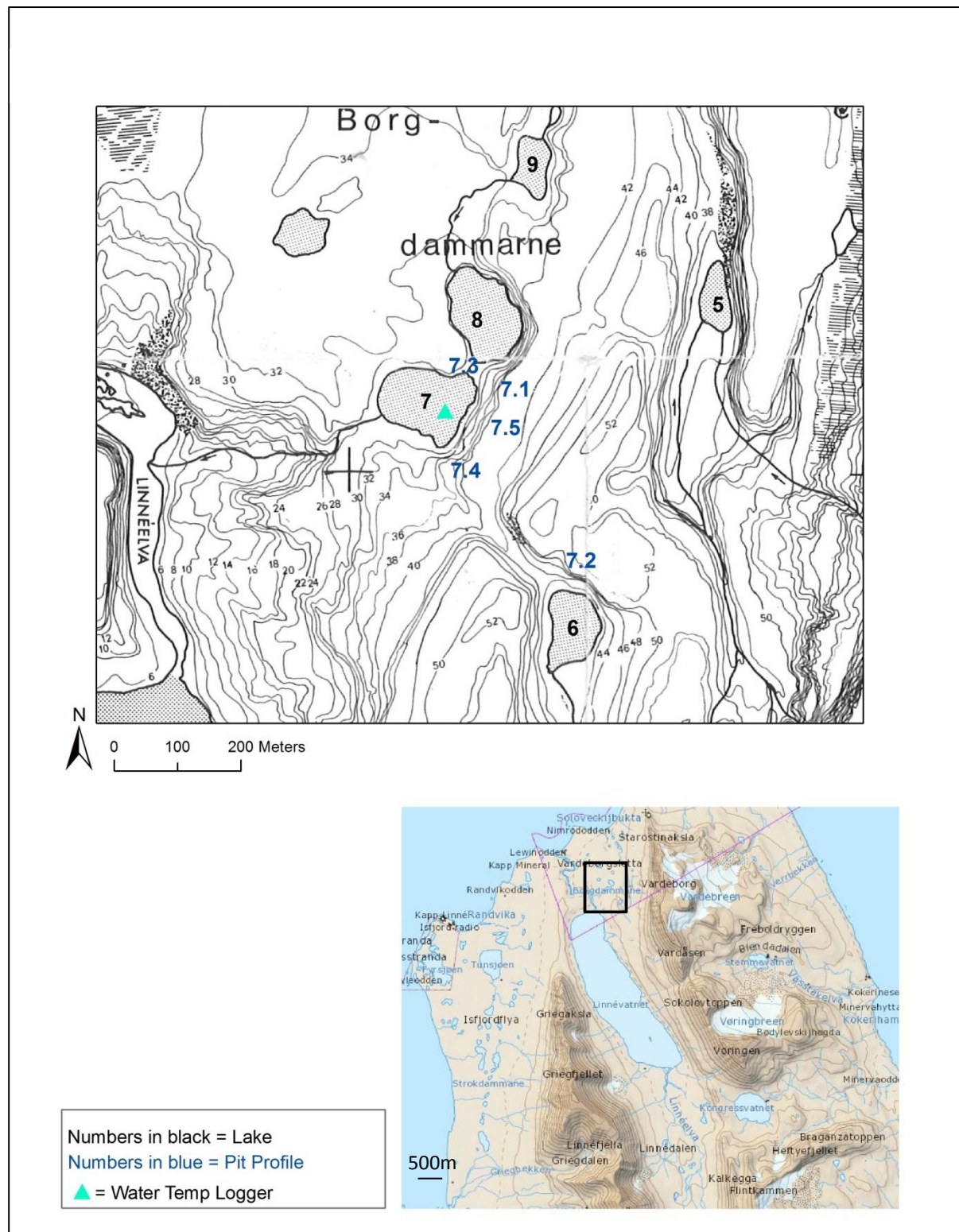


Figure 3.13: Locations map showing all monitoring sites where data was obtained at Vardeborsletta, Lakes 5, 6, 7, 8 and 9. Basemap is from Åkerman, 1980. Inset map is from Norsk Polarinstitutt. (Cohen, 2013)

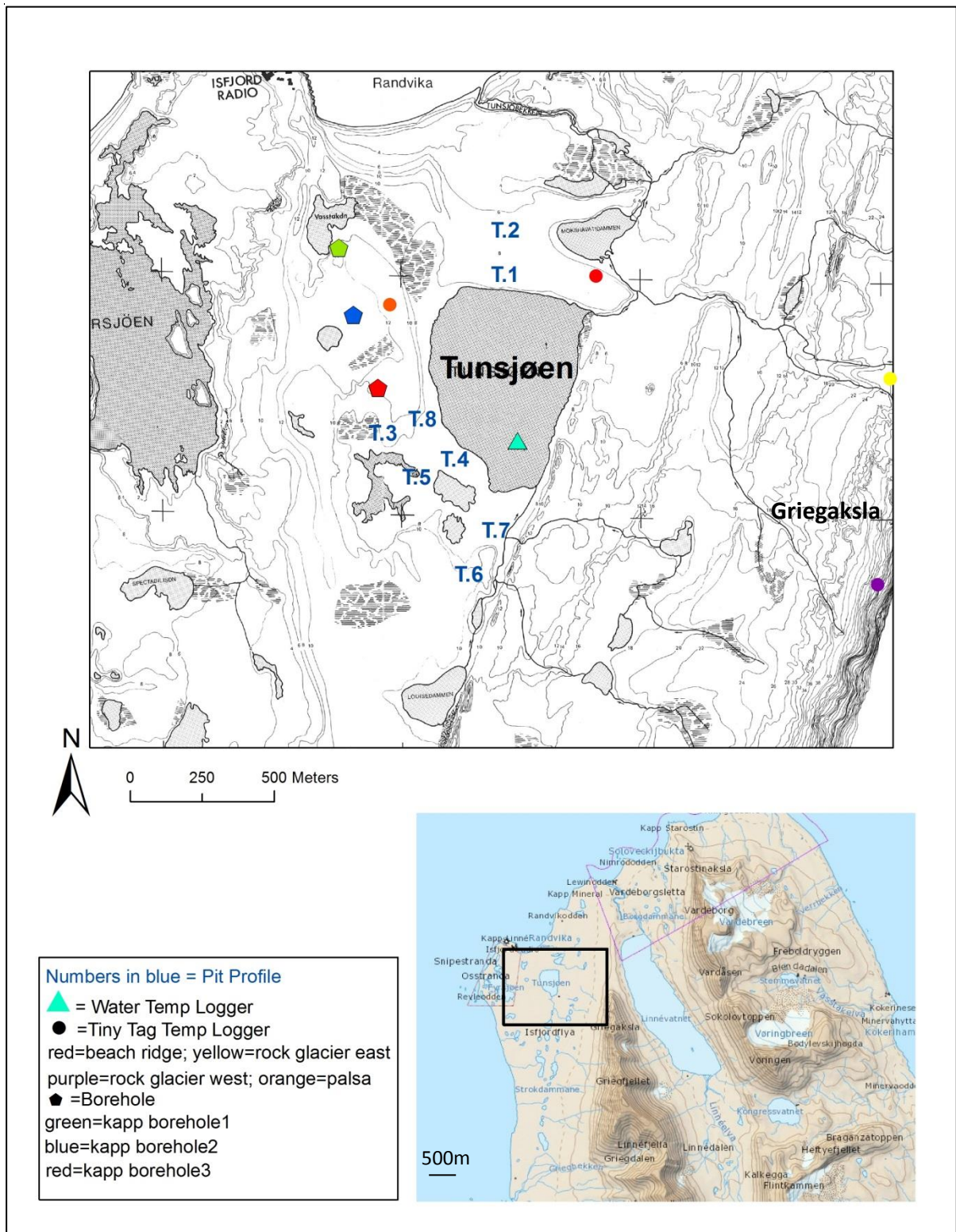


Figure 3.14: Locations map showing all monitoring sites where data was obtained near Tunsjøen Lake, Linnédalen. Temperature profiles created from data at the tiny temp logger locations are located in the appendix. Basemap is from Åkerman, 1980. Inset map is from Norsk Polarinstitutt. (Cohen, 2013)

CHAPTER 4. METHODS

4.1. Geomorphological Mapping

Geomorphological mapping was carried out at the field site at the Vardeborgsletta at Linnédalen, west central Spitsbergen. The majority of the mapping occurred from mid-July to mid-August, 2012. Other field campaigns to complete the mapping took place in the end of August and beginning of September, 2012. Several methods were utilized to accomplish the resulting map (figure 5.1) Mapping in the field involved printing out copies of Åkerman's 1980 (Åkerman, 1980) geomorphological map from his PhD thesis. 1990 Aerial photographs obtained from the Norsk Polarinstitut were also used in the field. The print outs were used to map out the visible surface phenomena over the older maps (Figure 4.1). Many photographs were taken while at the field site in order to have visual references after the field season ended. Other recent aerial photographs were obtained from Norsk Polarinstitut from 2008.

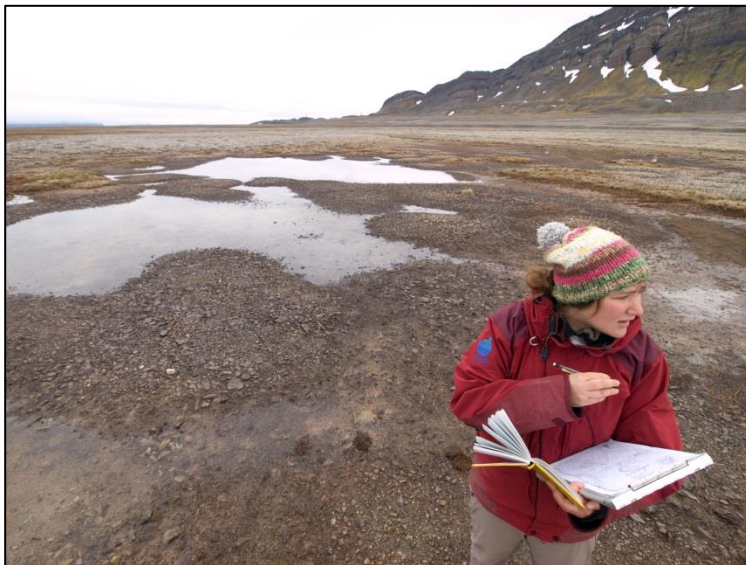


Figure 4.1: Mapping in the field at Vardeborgsletta, summer 2010. (Mertes, 2010)

While out in the field a Garmin® Montana 600 Unit GPS was used to outline the extent of various periglacial features at Vardeborgsletta. The tracks were uploaded into ArcMap 10.0 using DNR GPS software were compared with both the aerial photographs from 1990, 2010, and Åkerman's geomorphological maps from 1980. This gave a perspective into how the

geomorphology of Vardeborgsletta has been changing over the past few decades. The digitizing process of all of the GPS tracks and mapping was completed using ArcMap 10.0.

4.2. Bathymetric Mapping

Over summer 2013 nine bathymetric maps were made of the karst lakes at Vardeborgsletta (figure 7.1). The bathymetry was collected using an instrument consisting of a wooden pole with a Lowrance LC X-17 echo-sounder mounted on one side, and a GPS unit mounted on the other. A small rubber zodiac was used to drag the instrument across the lake in longitudinal and transversal transects (figure 4.2). The GPS recorded locations for each depth measurement acquired by the echo-sounder.



Figure 4.2: Using a zodiac to make bathymetric profiles. (Cohen, 2012).

After sufficient profiles were collected for each of the lakes, the data was downloaded and transformed into UTM coordinates. The data was then uploaded into ArcMap 10.0.

Bathymetric maps were created by using the natural neighbor raster interpolation tool from ArcToolbox. This tool takes the set of xyz points collected by the GPS and echo-sounder, and then interpolates a surface grid by predicting the in-between values, not recorded by the instrument (Childs, 2004). This is determined by the principle of spatial autocorrelation, which measures the degree of relationship between known objects (Childs, 2004). The natural neighbor function uses a deterministic interpolation technique called Inverse

Distance Weight (IDW) to generate values which create the surface grid. IDW is based on the similarity of each cell by using a linear-weighted combination set of sample points (Childs, 2004).

After surface grids were generated for each of the lakes a scale of 0.5m was used for the depth contours. The bathymetric maps were overlaid onto a 1990 aerial photograph of Vardeborgsletta. After completing the bathymetric map, the surface grids were uploaded into Arc Scene, in order to create 3-dimensional profiles. Once in Arc Scene 10, a factor of 10 was used to convert the layer elevation values to scene units. This converts the 1D image to a 3D model of what the lake bathymetry looks like. The scale of the depth contours remained at 0.5m.

4.3. Temperature Profiles

4.3.1. Temperature Loggers

Temperature records have been collected around the Linnédalen area for the past decade. This includes data loggers (figure 4.3) which have been deployed from as early as 2004 by UNIS Professor Hanne H. Christiansen. The United States Research Experience for Undergraduates (REU) sponsored by the National Science Foundation (NSF) has also been collecting data from weather stations in the Linnédalen area since 2003. The data collected from these various loggers include extensive meteorological data, as well as ground and subsurface temperatures. The loggers collecting ground and subsurface temperatures were the Tinytag® Plus and Tinytag® Plus 2 mini temperature data loggers (MTD) from Tinytag®. The loggers are logging external temperatures from several depths at one hour intervals.



Figure 4.3: Tiny tag loggers at Vardeborgsletta. (Cohen, 2012)

During spring & summer temperature loggers were deployed into three of the lakes which are a part of this study. These were Tinytag® Pulse 2 mtds, which take internal temperature readings every hour. On 04.05.2012 one thermistor string was deployed consisting of three data loggers into Tunsjøen. A hole was drilled in the ice through 9cm of snow and 95cm of ice before reaching water. The total water depth under the ice was 95cm. The thermistor string was 65cm long with the first logger at 30cm below the water surface, the second logger at 50cm below water surface, and the third logger at 55cm below the water surface. A thermistor string was also deployed into Lake 7 on 04.05.2012 (figure 4.5). 1.2m of ice had to be drilled through to reach unfrozen water. The total water depth under the ice was 4.6m. The thermistor string was 4.2m long with the first logger at 10cm below water surface, the second logger at 2m below water surface, and the third logger at 4m below water surface. There was an attempt to drill a hole into Lake 4 in order to deploy a third thermistor string, but it was observed that Lake 4 had completely drained at one point during winter 2012 (figure 4.4) making this impossible, as no water was left in the lake.



Figure 4.4: Lake 3 & 4 drained during the winter 2012, observed April 1st, 2012. (Cohen, 2012)

On 13.07.2012 the thermistor string was deployed into Lake 4. Using a fish finder, the maximum depth of the lake was determined to be 3.8m. The thermistor string was deployed with three data loggers, the first logger at 10cm below water level, the second logger at 2m below water level, and the third logger 3m below water level. On 09.08.2012 we redeployed the thermistor string in Tunsjøen. The new thermistor string was 1m with the first logger at 5cm below water surface, the second logger at 50cm below water surface, and the third logger at 90cm below water surface.



Figure 4.5: Tiny tag thermistor string ready to go into Lake 7, spring 2012. (Cohen, 2012)

4.3.2. Pit Profiles

Temperature profiles were made by digging pits (figure 4.6) into strategic areas around the Linnédalen area. The locations of the pits were chosen due to their proximity to the lakes and ground material. The pits were dug until either 1) the permafrost table was reached, 2) the pit filled with water, or 3) the ground material was too coarse to continue digging. After each pit was dug temperature profiles were made. To create the temperature profiles several temperatures were taken. Air temperature, surface temperature, and then at 10cm intervals

until the base of the pit was reached. The thermometers used were the VEE GEE® Digital thermometer with a temperature range of -50°C to +150°C & the PT1000 thermometer Ebro® TFX 410TFX Digital thermometer with a temperature range of -50°C to +300°C. Thermometers were either held in place or inserted fully into the ground material for one minute to acquire temperatures. After the temperatures were acquired, the removed ground material was placed back into the pits.



Figure 4.6: Taking temperature in an excavated pit, summer 2012. (Cohen, 2012)

4.4. Automatic Digital Camera

On 09.05.2013 an Automatic Digital Camera was set up overlooking Lakes 2, 3, & 4. The camera is a Pentax model, set up in a small weather-proof box. The camera was placed in a previously made rock cairn. The camera was set to automatically capture an image four times per day. On 08.08.2012 I moved the camera to a new location. The camera is still overlooking the same chain of Lakes (2, 3, & 4) but now at the south end of the chain facing north. The image captured by the camera also includes a view of the sinkhole. The camera now captures an image once a day at 12:00.

4.5. Surveying with TOPCON Total Station

Surveying for the purpose of creating precise altitudinal profiles of the Vardeborsletta area was carried out several times during field stints in summer and autumn 2012. The instrumentation used was a TOPCON® GTS-226 Electronic Total Station.

4.6. Conductivity Temperature Depth (CTD) Profiles

In order to learn about both the water column, and to compare the water composition between different lakes, several CTD profiles were made for each lake. Two instruments were used to take measurements; a Seabird Electronics Seacat 23 CTD recording conductivity, temperature, and depth, as well as an In-Situ Troll 9500 which collected CTD data as well as dissolved oxygen (in mg/l & saturation in %), pH and turbidity.

4.7. Additional Data Loggers

In addition, two additional data loggers were deployed into Lake 4. On 21.07.2012 a HOBO U20 Water Level Data Logger was attached to a rock and set on the bottom of the lake at a depth of 1.3m. On 25.07.2012 a HOBO Conductivity Data Logger for freshwater was also deployed into Lake 4, attached to the same rock. Both data loggers took measurements at 30 minute intervals and were both recovered on 06.08.2012.

CHAPTER 5. RESULTS: GEOMORPHOLOGICAL MAP

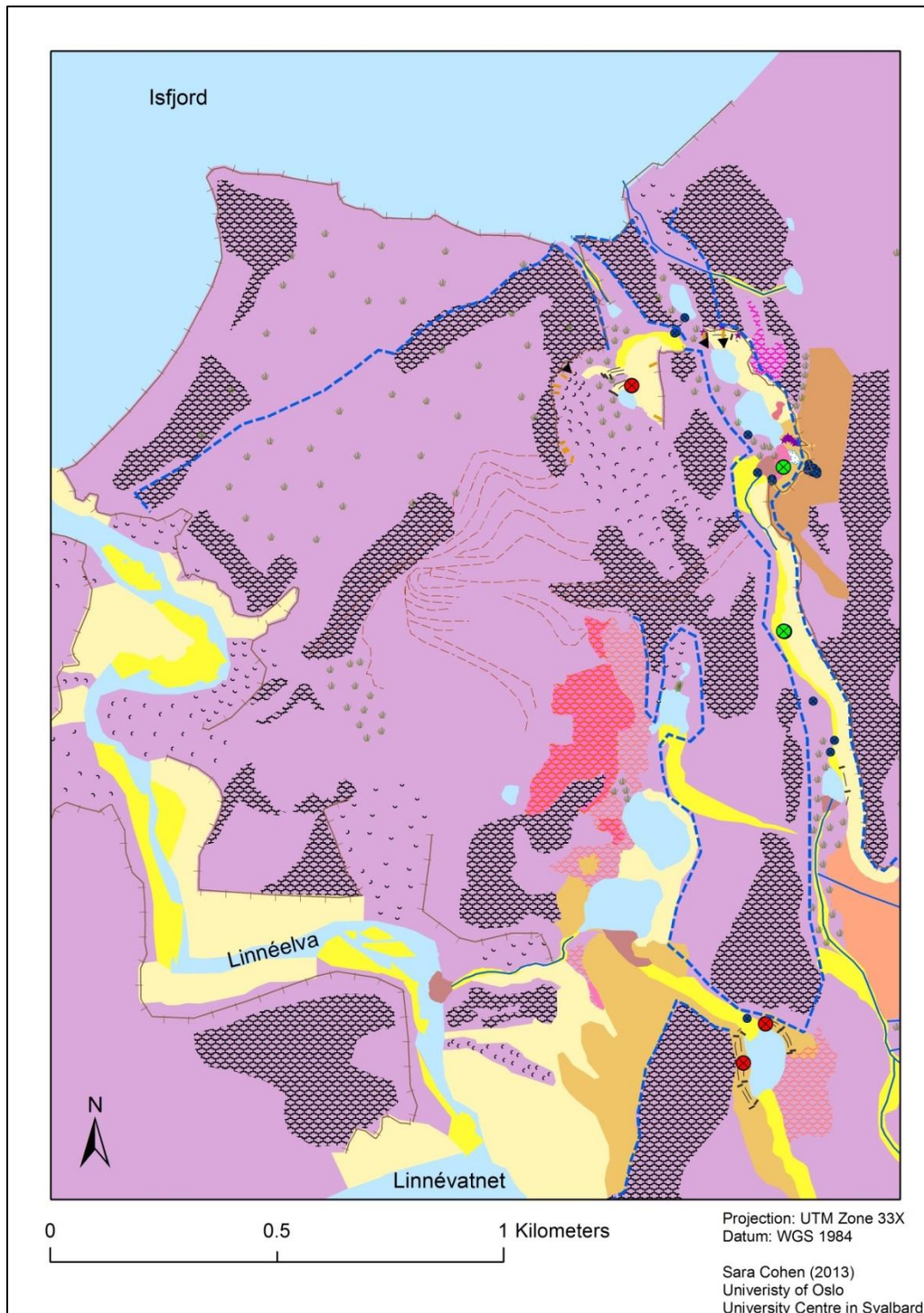


Figure 5.1: Geomorphological map displaying geomorphological processes, periglacial landforms and Quaternary surface cover of the study area at the Vardeborgsletta plain, Linnédalen, Spitsbergen. The inset map is modified from Humlum et al, 2003. (Cohen, 2013)

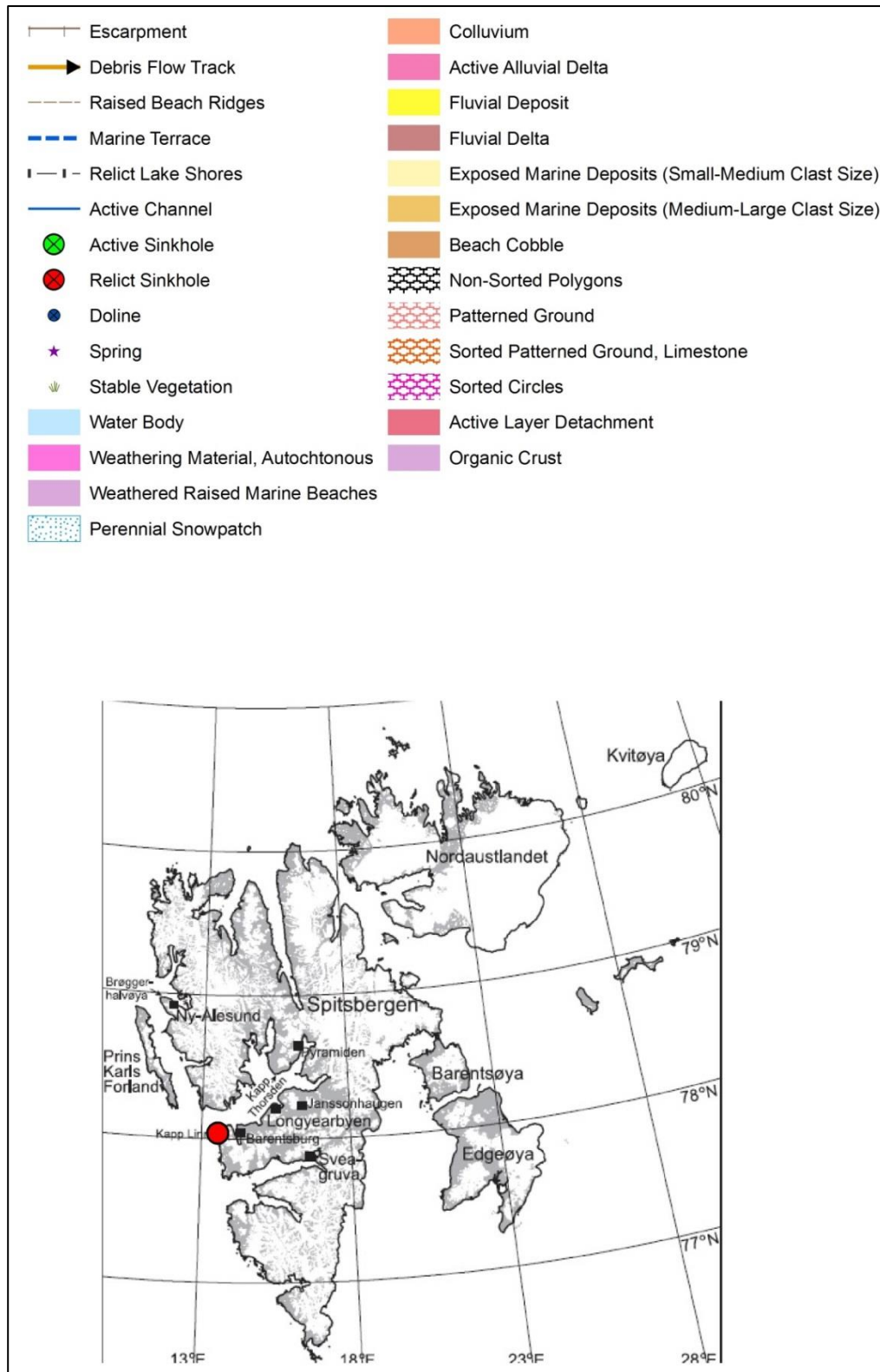


Figure 5.2: Legend and inset map for figure 6.1, the geomorphological map. Inset map is from Humlum et al, 2003. (Cohen, 2013)

A geomorphological map (figure 5.1) was made for the study site at Vardeborsletta where the karst lakes are located. Figure 5.2 shows the key and inset map. The mapped area is delineated by the mountain Vardeborgaksla to the east, Linnéelva River to the west, Isfjorden to the north, and Linnévatnet Lake to the south. The area is situated on top of the Gipshuken formation, which was deposited during the late Carboniferous/early Permian when Svalbard was mostly a shallow marine platform (Dallman, 1999). In the study area there are a few locations where the bedrock penetrates the surface, marked as “Weathering Material, Autochthonous” on the map. The majority of the area is composed of thick marine deposits overlaying the bedrock, measuring up to 20m in depth (Lønne and Mangerud, 1991). Exposed marine deposits are represented different colors depending on clast size. The landform which drapes the marine deposits is labeled as “Weathered Raised Marine Beaches” on the map. This is the landform which covers the surface of the majority of the Vardeborgsletta plain, and is composed mostly of Holocene beach sediments (Salvigsen and Elgersma, 1985). Raised beach ridges are also depicted on the map.

There are several fluvial deposits, depicted in yellow, in the study area cutting deep channels through the raised marine beaches and into the marine deposits. The current channels are dry except for some melt water streams from seasonal snow melt. The fluvial systems which existed at one time at the study site must have been quite powerful, as there are rounded boulders with diameters exceeding 20cm, and may have originated as the raised marine beaches were formed due to sea level regressions and transgressions. The map also includes the river Linnéelva, which is the outlet for Linnévatnet out to Isfjord.

The mapped area displays both inactive and active surfaces. A large portion of the raised marine beaches in the north are covered with an organic crust, showing little to no recent movement of surface materials. These areas display points showing vegetation, to indicate the important presence of stable vegetation. Solifluction is the dominant mass wasting processes in the mapped area. In most areas with a moderate slope solifluction lobes are observed. There are also many periglacial features mapped in the area. Non-sorted polygons are encountered over large portions of the weathered raised marine beaches. These features are often referred to as ice wedge polygons, but in this study there was no proof that ice-wedges do in fact exist subsurface. A study by Wanatabe et al, 2013, labels these features in

the Linnédalen area non-sorted polygons. Sorted frozen ground patterns are also observed in the study area.

There are several classic karst features mapped around the study site. There is one clear active sinkhole at the study site, located to the south of Lake 4 (figure 9.15). Another active sinkhole is located in the relict fluvial channel connecting Lakes 4 and 5 (figure 9.7). There are also three large relict sinkholes at the study site, one located on the eastern side of Lake 1 (figure 9.4) and two located at Lake 6 (figure 9.11). All of the relict sinkholes are located below relict lake shorelines. There are also dozens of smaller dolines located all around Lakes 2, 3, 4 and 5 areas as well as in the relict fluvial channel which connects Lakes 4 and 5.

Palaeo-water levels are clearly observed at the study area in the form of marine terraces, raised marine beaches, raised shore lines, and relict lake levels. These give indication of the development of the study area. The marine terraces, raised marine beached and raised shorelines are remnant from after the last glaciation of the area 12600 yr BP when the sea transgressed the area and then regressed due to isostatic rebound. The old lake levels indicate the development of the karst lake system since the time of deglaciation.

CHAPTER 6. RESULTS: LAKE STATISTICS AND SURVEYING RESULTS

Table 2: Lake Statistics

Lake	Max Depth (m)	Surface Area (m ²)	Volume (m ³)
1	2.09	756	657
2	3.67	2871	3616
3	4.43	4385	7476
4	3.57	8063	11430
5	3.46	4162	3225
6	7.8	10978	22400
7	8.7	17943	40842
8	6.2	17276	30965
9	3.1	5060	2367
Tunnsjøen	1.3	311427	240496

Table two presents maximum depth (m), surface area (m²) and volume (m³) for each of the lakes on Vardeborgsletta and Tunnsjøen. The value for maximum depths was found from the bathymetry mapping on each of the lakes. Values for surface area and volume are derived using ArcGIS.

Table 3: Surveying Altitudes and Locations

Altitude (m.asl)	Description
66.62	Highest Terrace Vardeborgsletta, Marine Limit
43.30	Terrace Directly North Lake 4
35.31	Highest Relict Shoreline Lake 3
36.48	Highest Point, Relict Channel Lake 1-3
36.18	East Side Relict Channel 1-3
31.59	West Side Relict Channel 1-3
31.56	Lowest Point Relict Channel 1-3
32.7	Highest Relict Shoreline Lake 1
30.44	2nd Highest Relict Shoreline Lake 1
29.70	3rd Highest Relict Shoreline Lake 1
29.45	4th Highest Relict Shoreline Lake 1
28.94	5th Highest Relict Shoreline Lake 1
28.49	6th Highest Relict Shoreline Lake 1
27.52	7th Highest Relict Shoreline Lake 1
27.29	8th Highest Relict Shoreline Lake 1
24.02	Highest Water Level 2012 Lake 1
23.95	Current Water Surface Lake 1
38.62	Terrace West Side Lake 1
38.39	Terrace North Lake 1
39.05	Terrace Between Lake 4 & Lake 1
35.78	Current Water Surface Lake 2

Surveying in the northeastern section of Vardeborgsletta was conducted during late summer, 2012. When surveying the point 43.30m on the terrace directly north of Lake 4 was used as the base point and originated from a different survey undertaken earlier in the summer. Data is verified by measuring to the highest marine terrace at Vardeborsletta, which according to this survey is at 66.62m. This terrace is the marine limit, and was measured at 64m from Landvik et al, 1987.

CHAPTER 7. RESULTS: BATHYMETRIC PROFILES

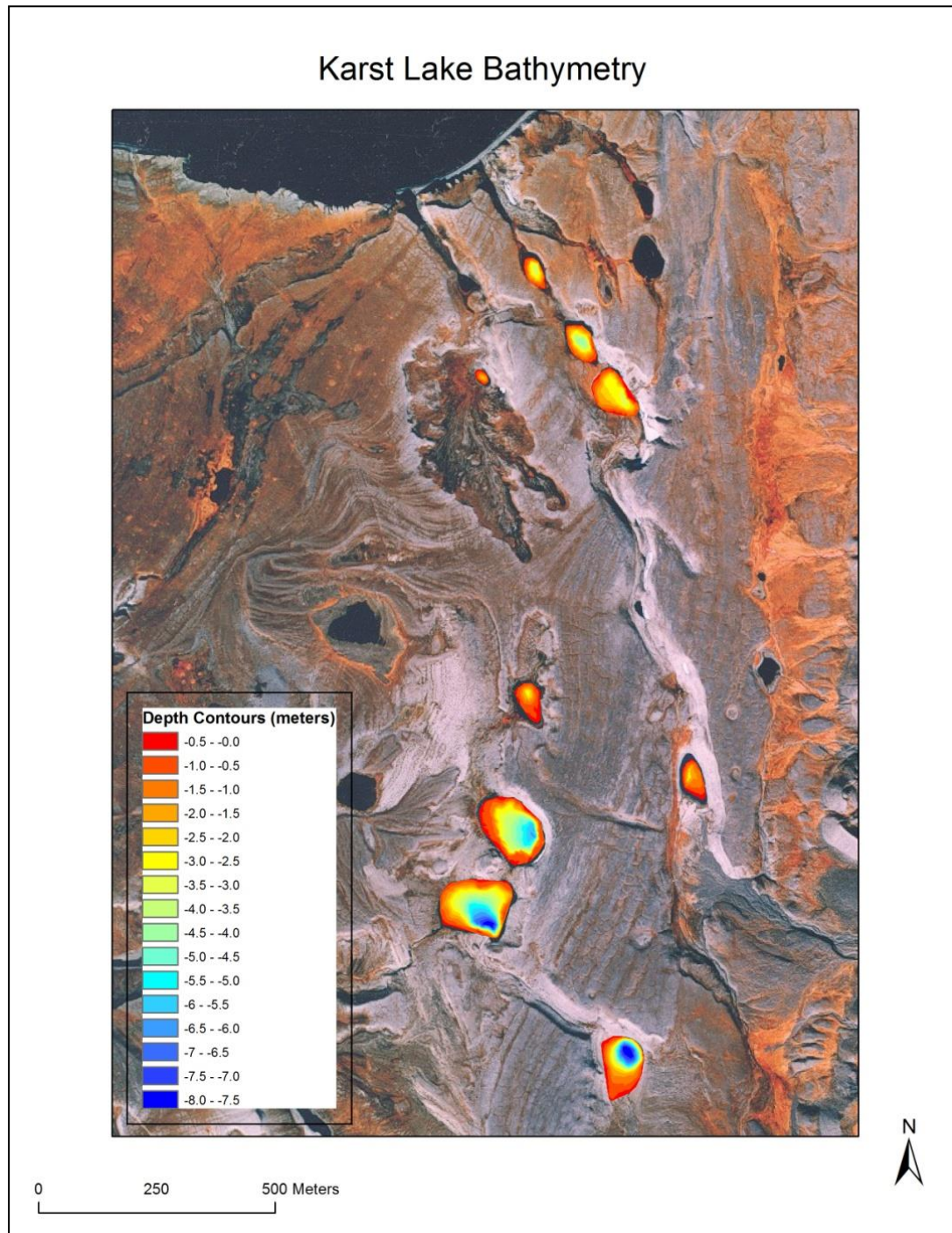


Figure 7.1: Bathymetric map of the karst lakes at Vardeborgsletta. The bathymetric figures are overlaid on a 1990 aerial photograph from Norsk Polarinstitut. (Cohen, 2013)

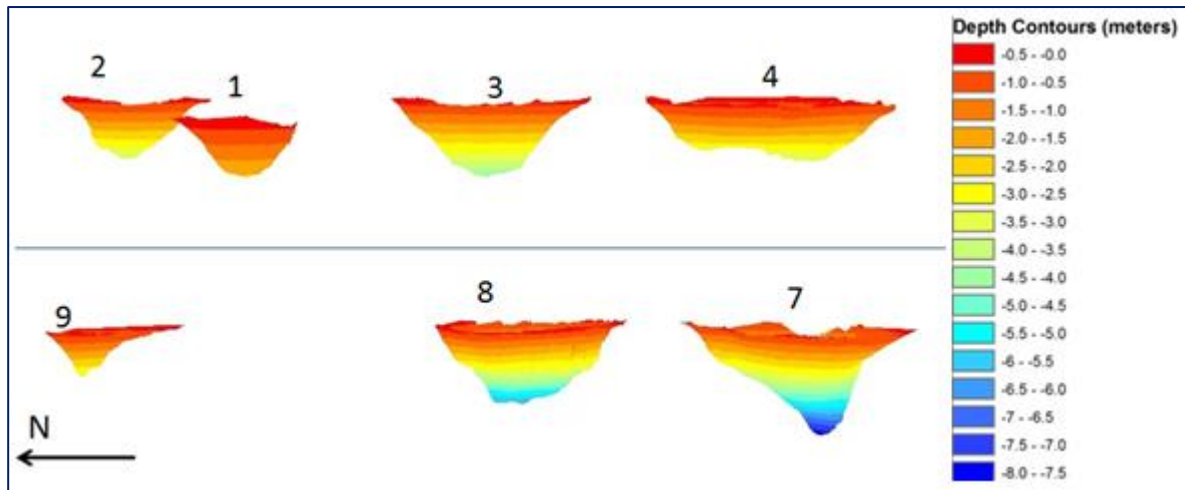


Figure 7.2: Vertical profiles showing the bathymetry of the karst lakes at Linnédalen. (Cohen, 2013)

The bathymetric map and bathymetric vertical profiles show that all lakes with the exception of Lake 4, are shaped like a funnel, characteristic of sinkholes (Ford and Williams, 2007). The points of maximum depth range from 2.09 meters in Lake 1 to 8.7 meters in Lake 7. The lakes in chain 6-7-8 are the biggest and deepest lakes in the system, while the lakes in chain 2-3-4 are smaller and shallower. The bathymetry reveals that generally the maximum depth correlates with the lake volume. Two exceptions to this are Lake 6, which has the second deepest maximum depth, but a smaller volume than Lakes 7 and 8, and Lake 4 which has a larger volume than Lakes 2 and 3, but a shallower maximum depth.

CHAPTER 8. RESULTS: TEMPERATURE AND LAKE LEVEL PROFILES

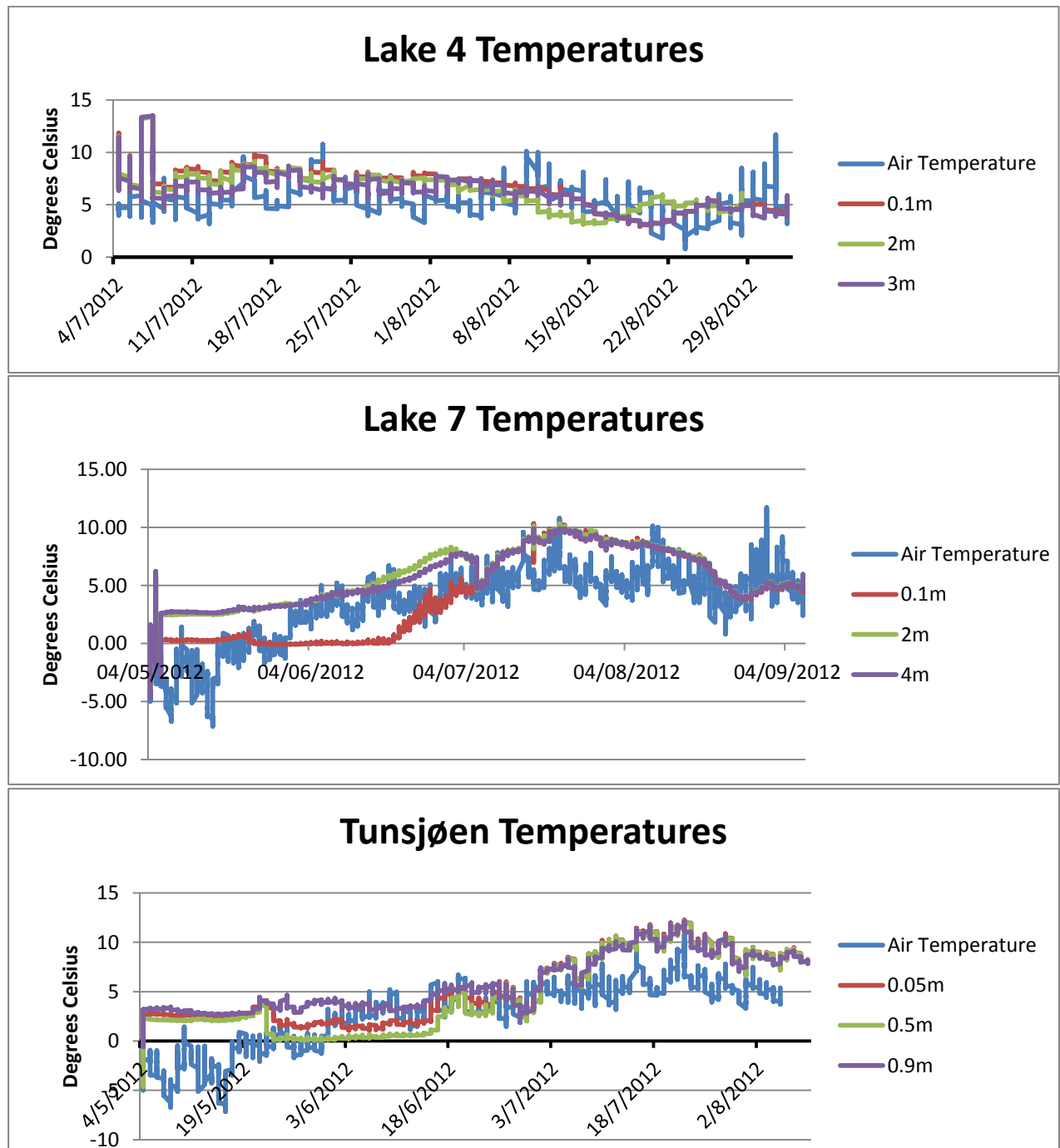


Figure 8.1: Temperature profiles from Lakes 4, 7 and Tunsjøen. Temperature is taken at three different depths in each lake, according to lake depth. Air temperature is from weather station at Isfjord Radio, located approximately 3km west of Vardeborgsletta and 1km north of Tunsjøen. Air temperature from this weather station was available until 05.08.2012. After this date, air temperature is taken from Longyearbyen Airport, located approximately 60km east of the study site, which is the closest weather station available. (Cohen, 2013)

Figure 8.1 represents the changes in lake temperature values over the course of the field season. Temperature loggers in Lake 4 ran from 04.07.2012-01.09.2012. Temperature loggers in Lake 7 ran from 04.05.2012-08.09.2012. Temperature loggers ran in Tunsjøen from 04.05.2012-05.08.2012. The lake temperature profiles reveal that generally the water temperatures do not vary significantly depending upon depth. Air temperatures appear to be mostly colder than water temperatures. Figures 3.12, 3.13 and 3.14 show the location of the temperature loggers.

At Lake 4, temperatures at all depths peaked on the 13th of July to over 11°C, which were by far the highest water temperatures while the loggers were deployed. This does not correspond with a peak in air temperature. After that peak, the loggers at 0.1m and 2m depth stick together tightly, while the logger at 3m lags behind. Air temperature is consistently cooler with a few small peaks which do not appear to have much effect on the lake temperatures.

The 0.1m logger at Lake 7 indicates that the lake ice broke up on 18.06.2012. Before that this logger was frozen, while the loggers at 2m and 4m were nearly identical, also following the highs and lows from air temperature. After ice breakup there was virtually no difference in the three temperature loggers for the remainder of the deployment in the lake. All three loggers follow the air temperature trends.

The top logger at Tunsjøen, at 5cm, indicates that lake ice thawed on 15.06.2012. Prior to this date the bottom logger at 0.9m was the warmest. The top logger was coldest due to its proximity to the lake ice. After ice breakup all three loggers record similar temperatures for the remainder of the logging period, exhibiting warmer temperatures than the air.

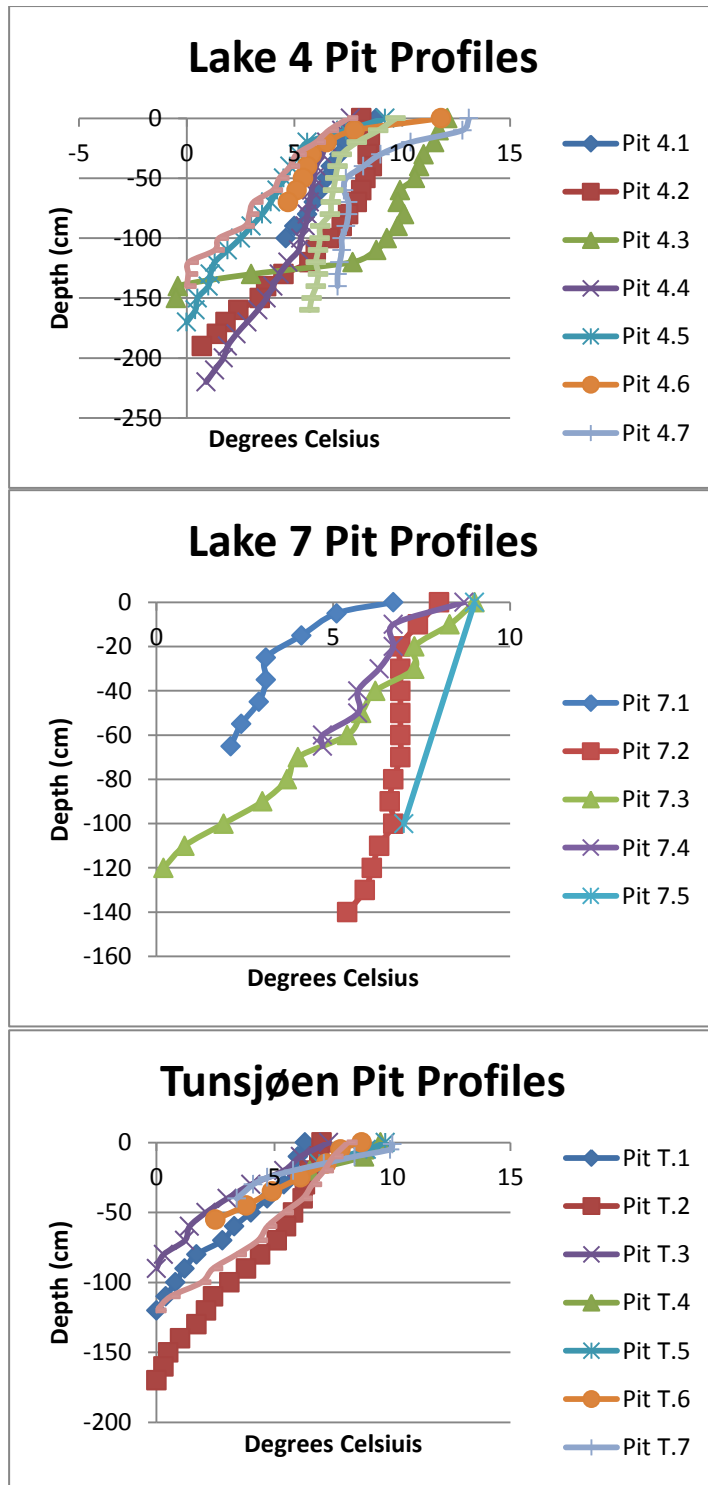


Figure 8.2: Pit profiles from various locations around Lake 4, Lake 7 and Tunsjøen. Excavations were made by students from AG-212 course over summer, 2012. (Cohen, 2013)

Pits were excavated close to the karst lakes and Tunsjøen during the field period in summer 2012 (locations displayed on figures 3.12, 3.13 and 3.14). The pits were dug by students in the UNIS AG-212 Course, Holocene and Modern Climate Change in the High Arctic. Pit profiles displayed varying temperatures over short distances.

Out of the nine pits dug proximal to Lake 4 (figure 3.12), four of the pits reached 0°C, while the other five did not reach lower than 4°C. The pits which reached 0°C were pits 4.2, 4.3, 4.4, 4.5 and 4.8. Pit 4.2, located on the western side of Lake 3 on the stable vegetated plateau, reached 0°C at 190cm depth. Pit 4.3 was dug in the active layer detachment on the eastern slope of Lake 4. It reached 0°C at 140cm depth. Pit 4.4 was dug on the high east plateau above Lake 4. It reached 0°C at 215cm depth. Pit 4.5 was dug near the sinkhole at Lake 4. It reached 0°C at 162cm depth. Pit 4.8 was dug in the delta at Lake 4. It reached 0°C at 140cm depth. The remainder pits did not reach 0°C. Pit 4.1 is located in the land between Lake 3 and Lake 4. At 95cm depth it reached the lowest temperature of 4.6°C. Pit 4.6 was dug in the stable vegetation by the west side of Lake 4 close to pit 4.2. This pit never neared 0°C and at 65cm depth was at 4.7°C. Pit 4.7 was dug in the delta on the northern side of Lake 4. This pit did not reach lower than 7°C at over 130cm in depth. Pit 4.9 was dug in the delta at Lake 4. This pit reached a minimum temperature of 5.7°C at 160cm depth.

Only one of the pits dug proximal to Lake 7 (figure 3.13) reached 0°C. Pit 7.3 was dug between Lakes 7 and 8, and reached 0°C at 120cm depth. All of the other pits didn't reach a temperature colder than 2°C. Pit 7.2, dug near the relict sinkhole on the eastern side of Lake 6 did not reach temperatures colder than 5°C, even at over 140cm depth.

Four of the pits dug proximal to Tunsjøen (figure 3.14) reach 0°C, while four of the pits are positive. The pits which reach 0°C are all located on the north and northwestern part of the lake, while the pits which do not reach negative temperatures are located on the south and southwestern part of the lake. The pits which do not reach 0°C are all shallow compared with the pits which do reach 0°C. These pits only reach a maximum depth of 57cm, which is typical for the active layer to reach on Svalbard, making it not surprising that negative temperatures were not reached.

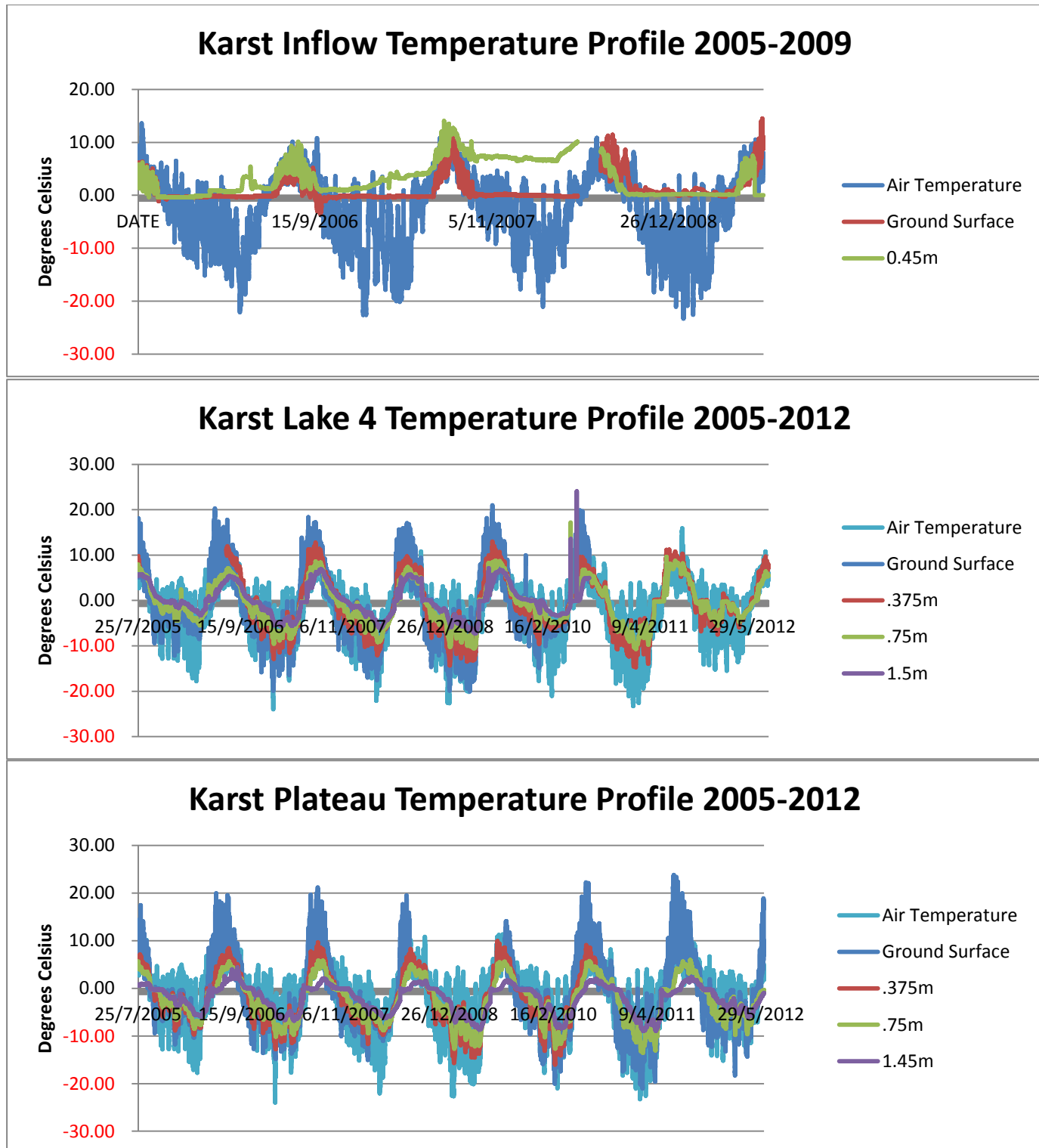


Figure 8.3: Temperature profiles from thermistor strings at locations around the Kapp Linné area. Data available from the TSP (thermal state of permafrost) project from <http://www.tspnorway.com>. (Cohen, 2013)

Temperature profiles were made for the temperature data which has been collected since 2004 in Linnédalen, as part of the TSP (thermal state of permafrost) project. Air temperature is from the weather station at Isfjord Radio, located approximately 3km away from Vardeborgsletta and 1km away from Tunsjøen. Temperature profiles in figure 8.3 are all located close to Lake 4. The temperature profile for the Karst Inflow jumps out as being irregular for a long time series temperature profile in a periglacial environment. This profile is located meters away from the sinkhole at Lake 4, at the bottom of the northern slope. Both temperature loggers barely pass below 0°C during the entire time period. The logger at 0.45m depth is consistently similar or warmer than the logger placed near the ground surface. The Karst 4 temperature profile is located in the relict channel between Lake 5 and 4, close to the shore of Lake 4. The ground temperature and air temperature follow one another quite closely. At this location, the deeper the logger, the less it is affected by the air temperature, with the lowest logger at 1.5m showing the smallest variation. The Karst Plateau temperature profile is located on the stable surface on the western side of Lake 4. The temperature profile here is similar to the Karst Lake 4 temperature profile.

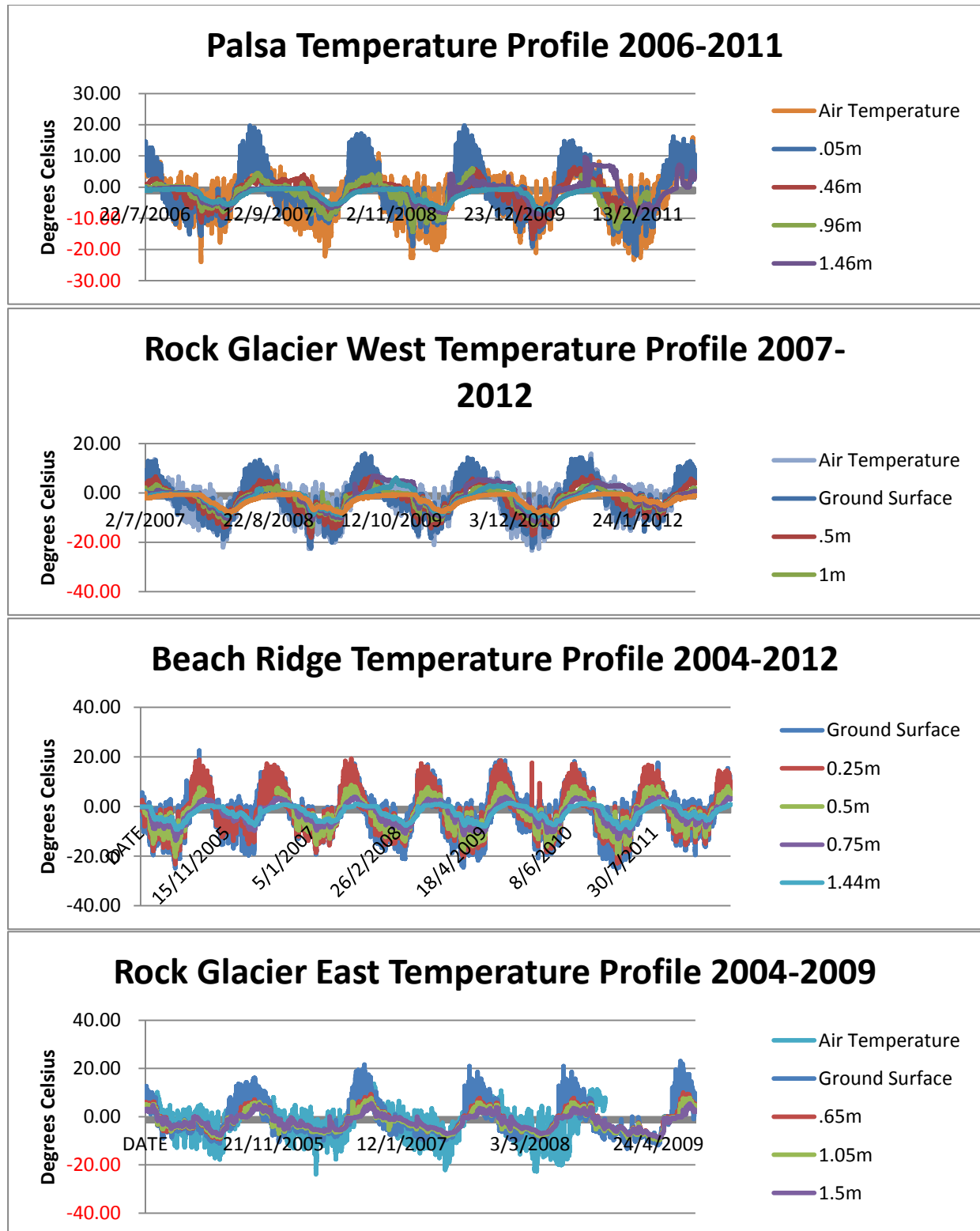


Figure 8.4: Temperature profiles from thermistor strings at locations around the Kapp Linné area. Data available from the TSP (thermal state of permafrost) project from <http://www.tspnorway.com>. (Cohen, 2013)

The temperature profiles in figure 8.4 are from the same project as those in figure 8.3. The air temperature data is the same as well. These temperature profiles are all located west of Vardeborgsletta and the karst lakes. They are located around the strand flat between the mountain Griegaksla and the coast. All four of the temperature profiles in figure 8.4 have ground surface temperatures and air temperatures which follow one another quite closely. There is a clear trend with all of these temperature profiles, where the deepest loggers vary in temperature the least, and the loggers closest to the surface vary the most, closely following ground and air temperatures.

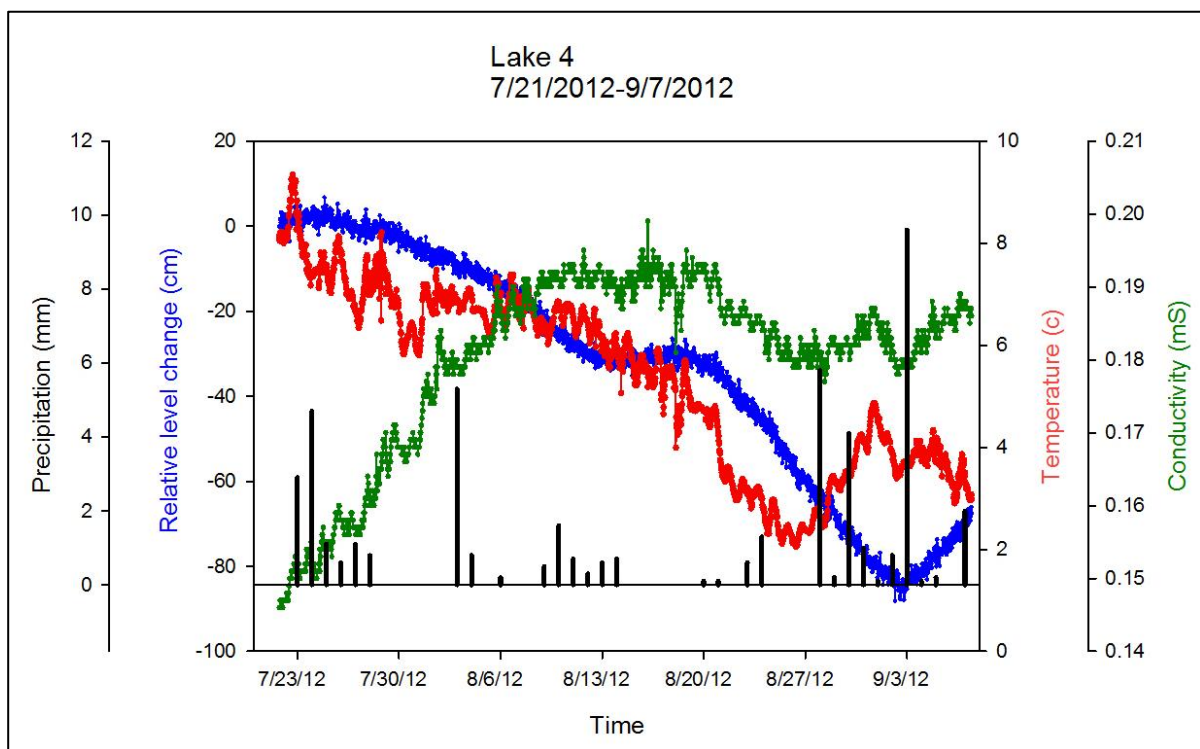


Figure 8.5: Precipitation, level change, temperature, conductivity data for Lake 4, summer 2012. (Figure from Farnsworth & Glaw, 2012)

Figure 8.5 is from an unpublished project resulting from the AG-212 course. This figure displays precipitation (taken from Longyearbyen), lake level change, temperature and conductivity. The figure shows that lake level was mostly declining throughout the study period, with the exception of two times, once on 18.08.2012 and after 03.09.2012.

Conductivity rose quickly at the beginning of the study period, and then followed the air temperature closely after 06.08.2012.

CHAPTER 9. DISCUSSION

9.1. Geomorphological Map Discussion

Geomorphological mapping is an effective tool for understanding landscape development and dynamics. A geomorphological map (figure 5.1) has been created to further understand the active landform processes and how the landscape is affected by the karst system at the Vardeborgsletta plain located in the valley, Linnédalen.

The geomorphological map depicts how this lake system is unique to Svalbard. Lakes and ponds are encountered in Svalbard, but are not typically present due to karst processes. The large lake to the south of the karst lakes, Linnévatnet, is the result of an overdeepened basin from Quaternary glaciations (Ingólfsson, 2011). Arctic lakes are often the result of the damming by moraines (Hambrey, 1984), or the thawing of ice rich permafrost (Yoshikawa and Hinzman, 2003). Figure 5.1 shows that the karst lakes are possibly related features, which were connected by relict fluvial channels. Lakes 2, 3, 4 and 5 are situated on an almost straight line, indicating a connection. Figures 7.1 and 7.2 depict the bathymetry which also suggests the karst origin of these lakes.

9.1.1. Lakes 1, 2, 3, 4 and Relict Fluvial Channel

Figure 9.1 displays the chain of Lakes 2, 3 and 4, with Isfjord to the north. Figure 2.8 displays Lakes 2, 3 and 4 and their heights relative to sea level, showing that the lakes are positioned in a chain, at sequentially lower altitudes heading south, away from the coast. Therefore the lowering water levels observed during the study period are draining into the subsurface at Lake 4 (Figure 9.15) rather than from Lake 2 down to Isfjord. Lake 3 and 4 are situated in basins, with no visible surface outlet.

Lake 2 lies in a shallow basin, closest to Isfjord, with a maximum depth of 3.67m (table 2) and an altitude of 35.78masl (table 3). The shorelines of Lake 2 are not steep and appear stable. Lake 2 is situated in the weathered raised marine beach, with an organic mat covering the western shore and exposed Holocene beach material on the eastern shore. During spring melt, when lake levels were higher, overwash potentially drained surficially to Lake 3. The northern slope of Lake 3 had debris channels which could have initiated with water input

from Lake 2. It was evident that there was some variability in the water height during the study period, as some of the organics proximal to the lake were washed away, revealing beach cobble beneath. There are no higher shorelines visible at the Lake 2 basin, meaning that although some surface drainage to Isfjord or Lake 3 is possible with more water, it is unlikely that Lake 2 was ever connected to any of the other lakes. Due to this, and the stable slopes surrounding Lake 2, it is improbable that Lake 2 was connected by a fluvial system to Lake 1. Lake 2 appears to be the least developed of the karst lakes, both with regards to periglacial and karst processes. The bathymetry shows that (figures 7.1 and 7.2) the Lake 2 basin has one deep point, characteristic of a karst feature.



Figure 9.1: Lakes 2, 3, 4 and Isfjord to the North. Photo taken 04.08.2010. (Cohen, 2010)

Lake 3 has a maximum depth of 4.43m and Lake 4 has a maximum depth of 3.57m (table 2). The bathymetry reveals that Lake 3 has one deep spot (figure 7.2). The shape of Lake 4 is reminiscent of a bathtub, though there is one deep spot located in the southeastern part of the lake (figure 7.2). The active sinkhole is located to the southeast of this deep point (figure

5.1). Throughout the summer field period active slope processes (figure 9.2) occurred on a daily basis, and water levels were variable (figure 8.5 & figure 9.15). On the southeastern slope of Lake 4, it is possible to see the sequence of marine deposits. It is a coarsening upwards sequence, with large beach cobbles on top and subsequently smaller clast sizes to gravel, sand, and marine muds (figure 9.2). The slope directly above the active sinkhole at Lake 4 is a steep scree slope, with beach cobbles actively falling downslope throughout the melt season.

Throughout the study period, there were several mass wasting events observed, such as an active layer detachment slide and debris flows around the Lake 3 and 4 eastern shorelines (figure 9.2). The eastern side of the Lake 3 and 4 basin is active due to the steepness of the slope, the moisture input from snowmelt, and ice content, allowing sediments to detach and flow. Alternatively, the western side of the Lake 3 and 4 basin is very stable with vegetation covering the raised marine beaches. The slopes on the western side are shallow, with an organic crust covering and almost no movement (figure 9.2 & figure 9.1).

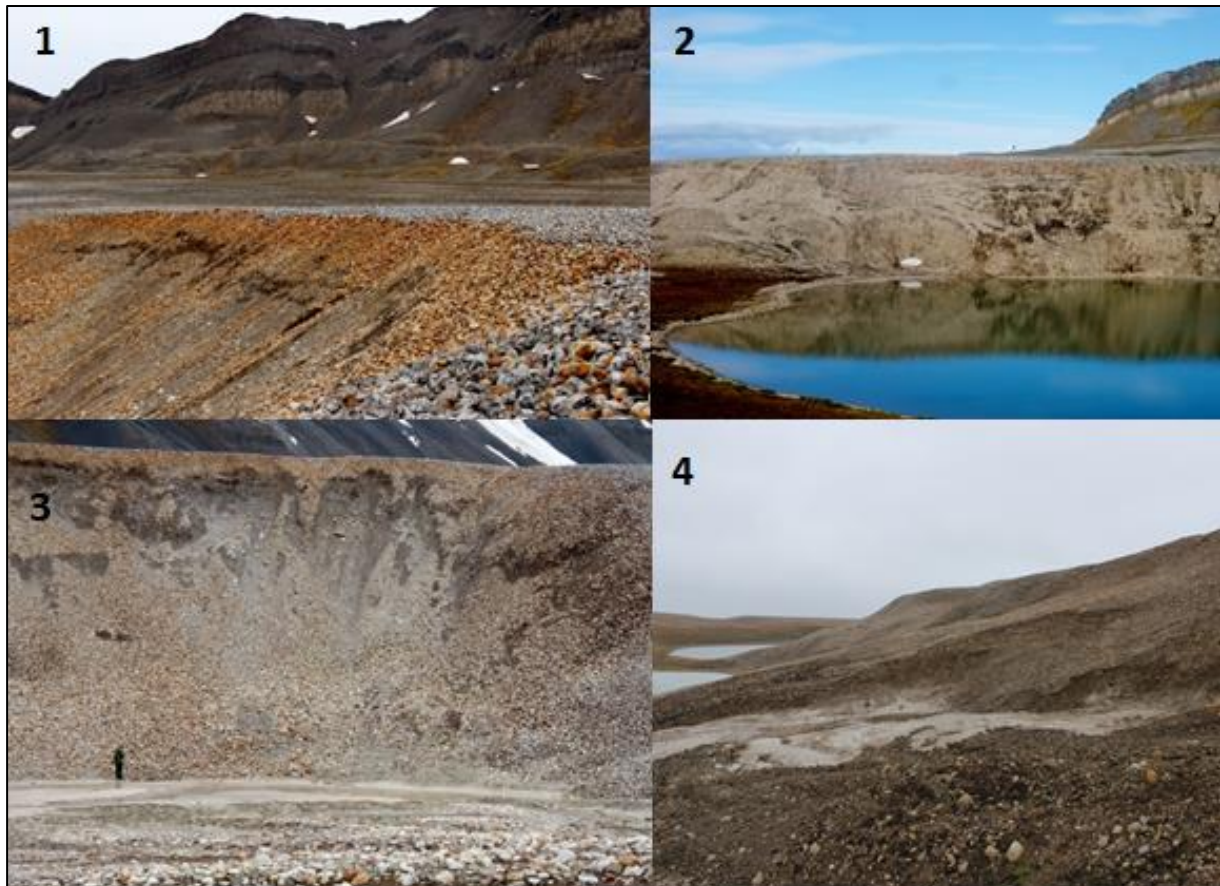


Figure 9.2: Slopes and features at Lakes 3 and 4. 1) Southeastern slope behind Lake 4. This is the escarpment face, showing the marine deposit sequence and the newly exposed face as the top beach cobble falls down slope. 2) The northern shorelines of Lake 3, showing steep slopes composed of marine deposits on the eastern side and shallow slopes covered with organic mat on the western side. 3) Southern slope behind the sinkhole and Lake 4, showing active slope processes. 4) Active layer detachment on the eastern side of Lake 4, occurred 25.07.2012. (Cohen, 2013)

Both the stable terrace above Lake 3 and the presence of a high shoreline at 35.31masl (table 3) indicate the long term development of the Lake 3 basin. The high shoreline signifies that Lake 3 at one time may have been high enough to connect to the relict fluvial channel which is between the terrace at the north end of Lake 3 and Lake 1 (figure 9.5). The highest point of the relict channel is 36.48masl, higher than the relict shoreline at Lake 3, but higher relict shorelines could have been eroded away by periglacial processes. The height difference between the surface of Lake 3 and the relict shoreline lead to two possible conclusions: first, periglacial processes and slope processes have been active, removing an immense amount of material to lower the lake basin; and second, the groundwater system beneath Lake 3 has developed overtime to allow for more efficient water drainage.

The Lake 4 basin continues to actively develop, which is evident in the rich slope activity. The beach cobbles at the tops of the southeastern slopes (figure 9.2) are an active source of sedimentation into the lake and as the cobbles fall down the scree slope, the basin is further eroded. A perennial snow and ice patch (figure 5.1 and figure 9.14) is a constant supply of water to the slope, increasing the potential of mass wasting and debris flows. The small dolines located on the top of the southeastern slope (figure 5.1) act as small basins which fill up with snow which lasts late into the melt season. No relict shorelines are visible for Lake 4, but this could be due to erosion of the steep southeastern slope due to the active slope processes. The lowering water levels, clear sinkhole, and unstable slope surroundings indicate that Lake 4 will continue developing in the future.

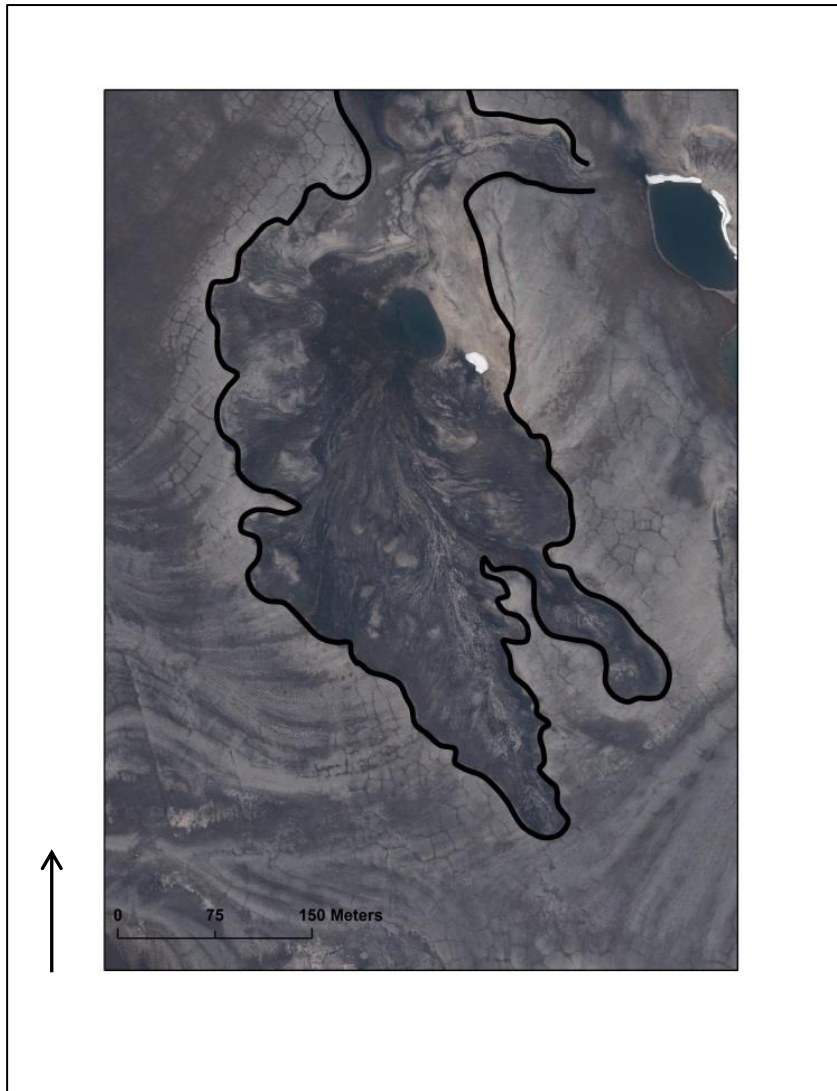


Figure 9.3: Lake 1 basin outlined in black, base aerial photograph is from Norsk Polar Institutt, 2010. (Cohen, 2013)

Lake 1 is at present the shallowest and smallest of the karst lakes (figure 5.1), with a maximum depth of 2.09m and volume of only 657m³ (table 2). Figure 9.3 shows the Lake 1 basin outlined in black, which indicates that Lake 1 was a larger feature in the past. Figure 6.1 emphasizes that solifluction processes have shaped the Lake 1 basin. Solifluction lobes line the western slopes of the lake (figure 9.4). On the northern side of Lake 1, eight relict shorelines remain and were surveyed during late summer, 2012 (table 3).

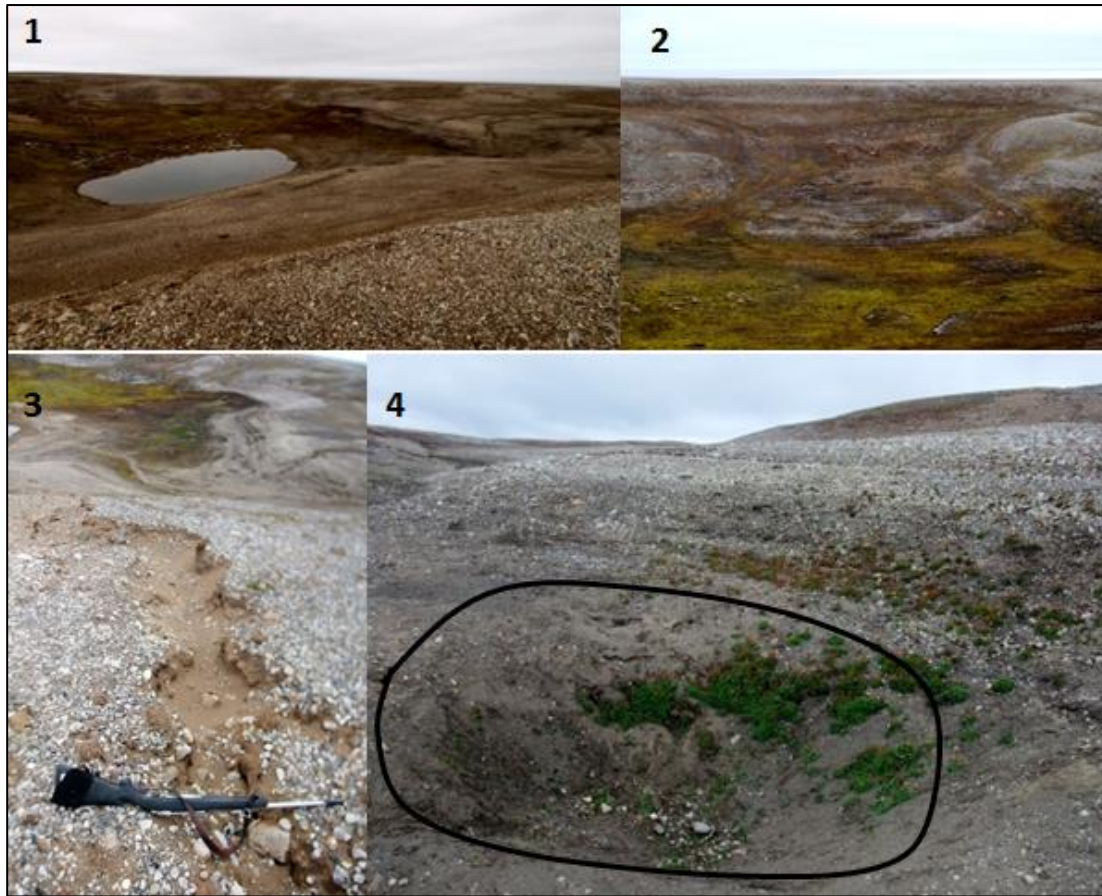


Figure 9.4: Photographs of Lake 1 and surrounding features. 1) The Lake 1 basin. 2) Solifluction lobes at the Lake 1 basin. 3) Debris flows traveling down slope at the Lake 1 basin. 4) Relict sinkhole (circled in black) above the eastern shore of Lake 1. (Cohen, 2013)

At present Lake 1 appears to be relatively stable. The shorelines are shallow, with solifluction being the dominant active process (figure 9.4, figure 9.3). On the western side of the lake there are several small debris flows (figure 9.4) present during the field season. The weathered raised marine beaches on the east and west sides of the Lake 1 basin are stable, with organic crust and non-sorted polygons indicating little movement. The raised marine beaches surrounding the basin are all composed of the same weathering material, and surveying shows that they have almost identical altitudes. On the northeast side of Lake 1 the marine deposits are visible which display the same downslope erosion as the eastern slope of Lake 3. The terrace on the east side is 39.04masl, the terrace on the west side is 38.62masl and the terrace on the north side is 38.38masl. The current level of Lake 1 is 23.95masl (table 3). With a maximum depth of 2.09m, approximately 18m in depth of marine deposits have been removed from the basin, as no bedrock is visible in the Lake 1 area. This

calculation assumes that the surface was relatively flat when basin development began. The surrounding raised marine beach ridges with similar altitudes imply that the Lake 1 basin has been completely eroded out from a flat surface due to karst processes in the northeastern part of the basin, where the lake and relict sinkhole are located, and solifluction processes on the southwestern portion of the basin, where the solifluction lobes are located.

Simple calculations show that the basin has been developing for thousands of years during the Holocene. The calculations only take into consideration the distance from the furthest terrace to the present lake shore, and do not account for elevation change. The rates of solifluction are from an Åkerman 2005 study at the Linnédalen area. The paper gives rates for solifluction lobes for two different time periods. Solifluction = 81mm/year 1992-2002 and 34mm/year 1972-1992. Therefore, using a distance of 390m, measured using GPS tracks, from the outermost part of the basin to the current lake shore at Lake 1, give a minimum of 4875 years and maximum of 11470 years needed to create the basin. It is important to consider that solifluction is not the only process present in the basin, but it can give some idea as to how long the basin has been developing. The highest marine terrace at Vardeborgsletta is a 64masl terrace identified by Landvik et al, in a 1987 study. The altitude from surveying during this study was calculated to 66.62masl (table 3). The Landvik study gives an age of 10900-11000 years BP for the 64m terrace, dated using shells. A 30masl marine terrace, which isolated Lake Linnévatnet, is dated to 9600 years BP (Mangerud and Svendsen, 1990). Permafrost at coastal, low altitude areas in Svalbard is of late Holocene age (Humlum et al, 2003). Given these dates, an age for the beginning of basin development due to periglacial processes can be bracketed to 9600-4875 years BP.

Several features in the Lake 1 basin vicinity suggest karst processes and basin development. A large relict sinkhole is present on the northeastern side of the lake (figure 9.4.4). The sinkhole is approximately 1.5m (figure 9.4) in diameter and displays well developed vegetation, indicating its relict status. The eight relict shorelines which are visible on the northwest side of Lake 1 are parallel features, which are approximately two to half of a meter vertically spaced from one another (table 3). Lake 1, similar to Lake 3, has developed due to a combination of karst and periglacial processes, to develop a large basin and efficient groundwater system.

A relict fluvial channel cuts the terrace between Lake 3 and Lake 1 (figure 9.5). The channel was subject to highly energetic amounts of water at one time, evident by the large rounded boulders deposited in the channel, and the cut it makes through the old raised marine beaches. This may be a result of the sea level transgression 6000 years BP (Landvik et al, 1987). The highest relict shoreline preserved in the Lake 1 basin is on the northern side of the lake, at 32.78masl (table 3). The lowest fluvial deposits in the relict channel on the western side, proximal to the Lake 1 basin, are situated at 31.56masl. This indicates that at one time there was a high energy fluvial system running into the Lake 1 basin. There is a possibility that Lake 3 was also connected to this system, evident from the high relict shorelines on the north side of the Lake 3 basin.



Figure 9.5: The relict fluvial channel which runs between the highest relict shorelines of Lake 3 and the highest relict shorelines of Lake 1 (figure 9.1). The southern side of the channel is heavily vegetated, indicating no recent activity, while the northern side of the channel contains deposits of rounded boulders. (Cohen, 2013)

9.1.2. Lake 5 and Relict Channel Connecting Lake 4 and 5

Lake 5 is situated on the eastern side of Vardeborgsletta, connected to Lake 4 by a relict fluvial channel, extending almost one kilometer (figure 5.1). Lake 5 has a maximum depth of 3.46m (table 2). Similar to Lake 4, the Lake 5 basin is characterized by steep eastern slopes

and shallow western slopes (figure 9.6). The eastern slopes are fairly active, with cobbles occasionally falling downslope. The terrace at the top of the eastern slope is stable, unlike Lake 4, and the weathering surface with non-sorted polygons extends to the escarpment. The immediate shorelines surrounding Lake 5 are vegetated. The lake is at the base of a meltwater channel, originating from snowmelt on the nearby mountain, Vardeborgaksla to the east. During the field season the channel was followed up to the base of the mountain. On the western side of the lake, above the vegetated shorelines, non-sorted polygons are present on the beach ridge surface. There is one relict shoreline visible on the eastern slope, which stands above the current lake level. The vegetated shorelines, below the stable beach ridge surface on the western side of the lake stand approximately three meters above the current lake level. This indicates that Lake 5, similar to Lakes 1 and 3, was at one time a larger feature.



Figure 9.6: Lake 5, Isfjord is seen to the north. (Cohen, 2013)

Beginning with the fluvial system which comes down from Vardeborgaksla to Lake 5 and continuing with the relict fluvial channel which stretches from Lake 5 to Lake 4, there was potentially a powerful fluvial system, with Lake 5 being a larger body of water at the time. The relict fluvial channel connecting Lake 5 and Lake 4 (Figure 9.7) is a well-developed channel, with large boulders, uneven topography, and small ponds which were actively draining into the subsurface during the field period and can be considered sinkholes (figure 9.7). There is an elevation difference between the high eastern side of the relict channel and the low western side. Close to Lake 4, the eastern raised marine beach is measured at 43m

asl, while the raised marine beach on the western side is measured at 39m asl. The sinkholes are all located on the eastern side of the channel, and the eastern slopes contain smaller terraces in several locations. The western slope is a more linear shape. This topography could indicate that the raised marine beaches which the karst lakes and relict channels are situated in developed over several stages throughout the late Holocene. After sea level regressed from 12600 years BP (marine limit) and 9600 years BP (Linnévatnet isolated from Isfjord) a sea level transgression occurred 6000 years BP (Landvik et al, 1987). The fluctuating sea level which created multiple levels of marine beach levels facilitated the water movement through the system which aided in shaping the lake basins and water pathways.



Figure 9.7: Relict fluvial channel connecting Lakes 5 and 4. 1) Closer to Lake 4, the channel contains boulders of differing sizes, lots of vegetation, and some water appears from small springs. 2) Closer to Lake 5 the channel exhibits almost no vegetation. A large pond with its own set of fresh shorelines from the current season is observed, possibly another sinkhole. (Cohen, 2013)

9.1.3. Lakes 6, 7, 8, 9 and Relict Channel

The chain of Lakes 7, 8 and 9 exhibit stable conditions in comparison with the other karst lakes. Lakes 7 and 8 are deep with maximum depths of 8.7m and 6.2m respectively (table 2). Both lakes have one deep point, and the bathymetry is classic for karst lake features (figure 7.1 & 7.2). Although the lake bathymetry reveals the sinkhole shape of the lake basins, the

karst system appears to be inactive at these lakes. During the field period, lake levels of 7, 8 and 9 did not fluctuate significantly. Lake 7 has an outlet stream, which runs into the river Linnéelva. Occasionally water from Lake 8 pours into Lake 7 over the small spit of land separating the two lakes. Similar to the other chain of karst lakes, the eastern slopes of Lake 7 and 8 are steeper than the western slopes (figure 9.8). The same marine deposits which are visible at the Lake 2, 3, 4 and 5 chain are revealed below the terrace capped with the weathering surface. Some sedimentation into the lake from these slopes occurred during the field season.



Figure 9.8: Lakes 8 and 7 facing south. Lake 8 is the proximal lake and Lake 7 is distal. (Cohen, 2013)

There are many examples of classic frozen ground patterns proximal to Lakes 7, 8 and 9 (figure 9.9). The frozen ground patterns include sorted circles, sorted stripes and sorted steps. Non-sorted polygons are also wide spread in the area (figure 9.9). At this lower altitude part of Vardeborgsletta, the bedrock from the Gipshuken formation begins to penetrate the surface through the marine deposits in some areas. A large percentage of the sorted patterned ground in this area is composed of carbonate rocks (figure 9.9). One of the most prominent features in the study area is non-sorted polygons (figure 9.9). They range

from approximately 5 to 20 meters in diameter. It is unknown if these non-sorted polygons have ice-wedges or soil-wedges. A recent study (Wanatabe et al, 2013) from approximately 3 kilometers away from the site used ground penetrating radar (GPR) to reveal that there are both ice-wedge and soil-wedge polygons in the area.



Figure 9.9: Examples of frozen ground features from the Lake 7 and 8 area. 1) Sorted stripes exhibiting many different clast sizes which are sorted. 2) Large non sorted polygons are frequent in the area. 3) Sorted circles near Lake 7 and 8, sorted stones are carbonate bedrock. Figure 4) Sorted netting near Lake 7, sorted limestones. (Cohen, 2013)



Figure 9.10: Lake 6, Isfjord to the north. The relict sinkholes are filled with snow at the time of this picture. (Cohen, 2013)

Lake 6 (figure 9.10) is the second deepest of the karst lakes, with a maximum depth of 7.8m (table 2). This bathymetry of the lake displays a sinkhole, with one prominent deep point in the lake (figure 7.1 and 7.2). The northeastern and western slopes of Lake 6 are similar to eastern slopes of Lake 7 and 8, though the clast size is larger gravel and cobbles. The southeastern shoreline of Lake 6 has patterned ground, while the southwestern side is the end of a meltwater stream, similar to the one which empties into the southern shore of Lake 5. This meltwater stream fluctuated in size throughout the season, sometimes running dry.



Figure 9.11: Relict sinkhole on the northeastern shoreline of Lake 6, located below relict shorelines. (Cohen, 2013)

Features around Lake 6 include large relict sinkholes and relict shorelines (figure 9.11), indicating higher lake levels and extensive basin development, similar to Lakes 3 and 1. It is therefore possible here that extensive periglacial and karst processes have formed a large basin and groundwater system. There is a large sinkhole on the northern side (figure 9.11), and another sinkhole of similar size on the western side (figure 9.8). The sinkholes are both heavily vegetated with moss lining the bottoms. The sinkholes at Lake 6 are of similar size and shape to the relict sinkhole on the northeastern side of Lake 1.



Figure 9.12: Relict fluvial channel between Lake 6 and 7. Large rounded boulders and cobbles are deposited in the middle of the channel. (Cohen, 2013)

A large relict fluvial channel (figure 9.12) connects Lake 6 and Lake 7. The water from Lake 6 would have reached the fluvial channel when the water level was at the highest relict shoreline altitude. The relict channel has large rounded cobbles and boulders in the center, indicating a high energy system. It is possible that at one time, Lake 6 was connected to Lake 7 and 8 by this relict channel and all lakes had at least one large sinkhole, through which water drained to the subsurface. Over the field period water levels in Lake 7 and Lake 8 were stable, and there was no drainage event during the winter. This indicates that Lake 7 and Lake 8 are no longer part of an active karst system. Observations were made of Lake 6 lowering throughout the field season, but there is not quantitative data to accompany this.

9.1.4. Åkerman Map Comparison

A PhD dissertation by Jonas Åkerman (1980) extensively maps the geomorphology of the entire Linnédalen area, including the Vardeborgsletta plain, where the karst lakes are located (figure 9.13). In Åkerman's study, he defines the lakes and sinkholes as thermokarst features, as opposed to true karst features. However, Åkerman does include the sinkhole on the northern side of Lake 4, indicating that it was active over 3 decades ago. The 1985 study by Salvigsen and Elgersma refutes the claim that the lakes are purely thermokarst features, and labels them as true karst features. Åkerman's map is extremely detailed, and comparing the map he made to the map in this study (figure 5.1) shows that much of the area has not changed drastically over the past three decades. The occurrence of frozen ground patterns and non-sorted polygons (Åkerman refers to these as frost fissure polygons) are essentially mapped in the same areas. Åkerman refers to a process called "slope of thermokarst denudation" which in this study is referred to as solifluction. This is particularly evident around the Lake 1 basin.

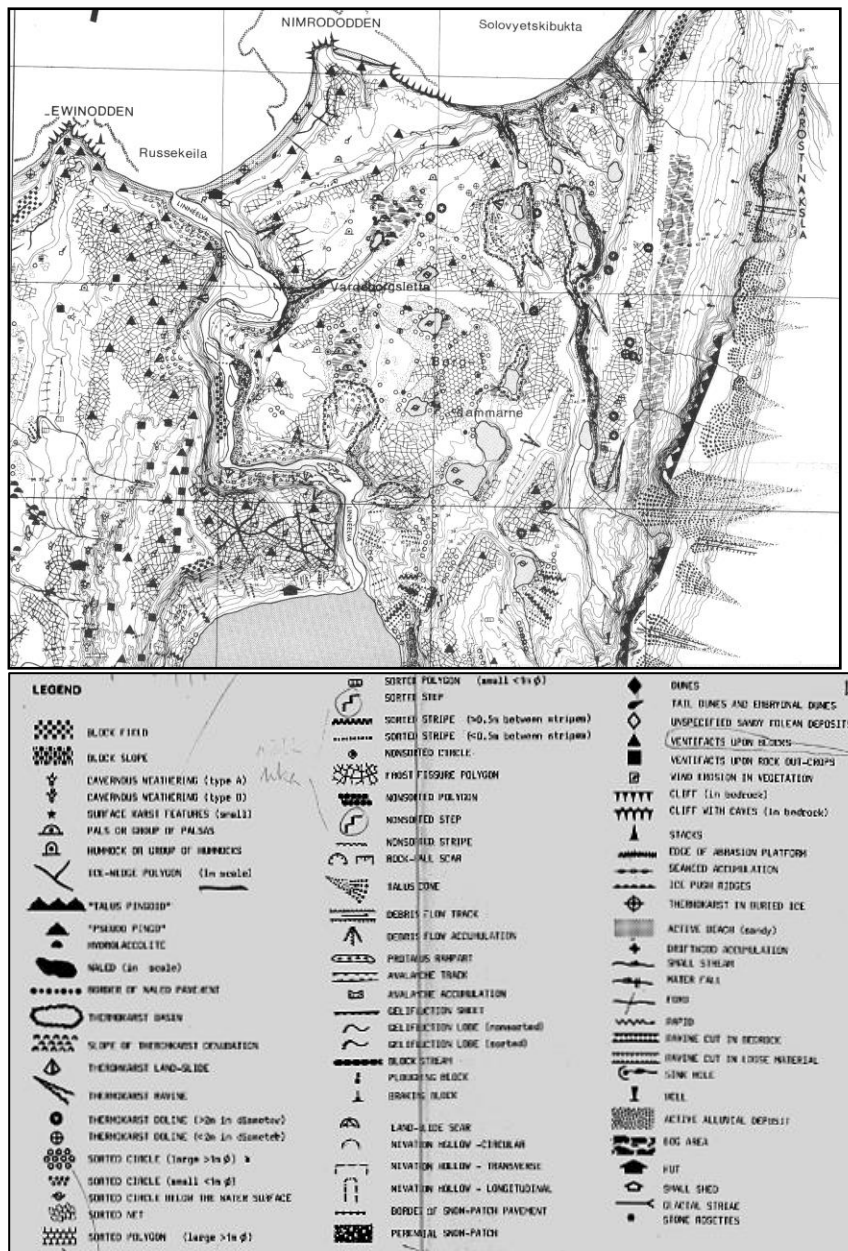


Figure 9.13: Vardeborgsletta portion of Åkerman's 1980 geomorphological map, with legend below. (Figure from Åkerman, 1980)

9.2. Temperature, Thermal Regime Discussion, and Lake Level Discussion

Air, ground and water temperature profiles were made from various locations (figure 3.12, figure 3.13 and figure 3.14) around the study site in Linnédalen, both on the Vardeborgsletta plain and the strand flat near Tunsjøen (figure 3.7). The results of these temperature profiles are presented in Chapter 8. Linnédalen can be considered a unique location in the arctic in terms of the amount of temperature monitoring which has occurred there over the past

decade. Ground temperature loggers are located throughout the area at over a dozen locations at depths ranging from the ground surface to almost 40m in depth. Over twenty pits were excavated throughout summer 2012 to understand how ground temperatures varied spatially at shallow depths in differing landforms and lithologies proximal to the karst lakes. Lake 4, Lake 7 and Tunsjøen had temperature loggers for spring and summer 2012, and in addition Lake 4 had a conductivity and level logger monitoring changes during summer 2012.

9.2.1. Thermal Regime and Temperature Data Lakes 1, 2, 3 and 4

The northeastern part of Vardeborgsletta, where Lakes 1, 2, 3 and 4 are located (figure 3.12) displays a unique thermal regime due to a combination of the presence of water bodies, the presence of permafrost and periglacial features, and the karst lake system.

Lake Temperatures

Due to water's capacity to hold heat, the presence of any water body will affect the surrounding ground thermal regime, but this holds particularly true in permafrost environments, where perennially frozen ground makes contact with water in liquid phase. Lake 4 water temperatures from the summer 2012 study period show water temperatures do not correlate well with air temperatures. Even the surface logger, at 10cm depth closely correlates with the water temperatures at depth, rather than air temperature, which differs from the other lakes (figure 8.1). The main source of water for Lake 4, as well as the other karst lakes, is snow melt, which means that water entering the lakes is near freezing. There is some input from precipitation, though annual values are low at 400mm w.e., though may be higher in recent times with values from 700-900mm w.e. (pers. comm. with O. Humlum). Most of the precipitation on Svalbard falls in solid state, so this is not a huge input during the melt season. There is a perennial snow and ice patch on the eastern shore of Lake 4 (figure 9.14), which supplies meltwater to the lake throughout the entire melt season. Due to this incoming source of cold water to the system, it would be expected that water temperatures would go down after particularly warm periods, which would result in an influx of cold water into the Lake. This is not observed.



Figure 9.14: Perennial snow and ice patch at the eastern side of Lake 4, 07.09.2012. (Cohen, 2013)

Lake Levels

During the summer 2012 field period, the entire Lake 4 basin all the way to the sinkhole and base of the skree slope filled up with water and drained over a period of four days (25.07.2012-29.07.2012). At this time it was possible to see the water actively draining through the sinkhole (Figure 9.15). The lake draining corresponds with lowering water levels, recorded with the level logger deployed in Lake 4 (figure 8.8). This sinkhole has been active since at least 1984, when Salvigsen and Elgersma observed draining water through the same sinkhole (Salvigsen and Elgersma, 1985). They estimated that 100 liters/second of water was draining through the sinkhole into the subsurface. They did not observe any springs in the area, and suggested that the water is draining into a groundwater system which eventually reaches the sea by subsurface outlets. Days before this four day event occurred, on 22.07.2012, Linnédalen experienced a spike in warm temperatures, at 10°C. This could have influenced snowmelt which led to higher levels at Lake 4 making it possible for water to fill up the basin to the sinkhole. Though this spike in temperature may account for some of the Lake 4 drainage, water no longer reached the sinkhole after 29.07.2012, and evident from figure 8.8, water levels continued to lower throughout the rest of the study period until the beginning of September, 2012, with the exception of one rising event on 14.08.2012. Therefore, there must be some subsurface outlet which allows the lake to drain without reaching the surficial sinkhole. It is possible that Lake 4 is still in an active phase as a karst

basin, with the deep point seen in the bathymetric profile functioning as another subsurface outlet (figure 9.0).

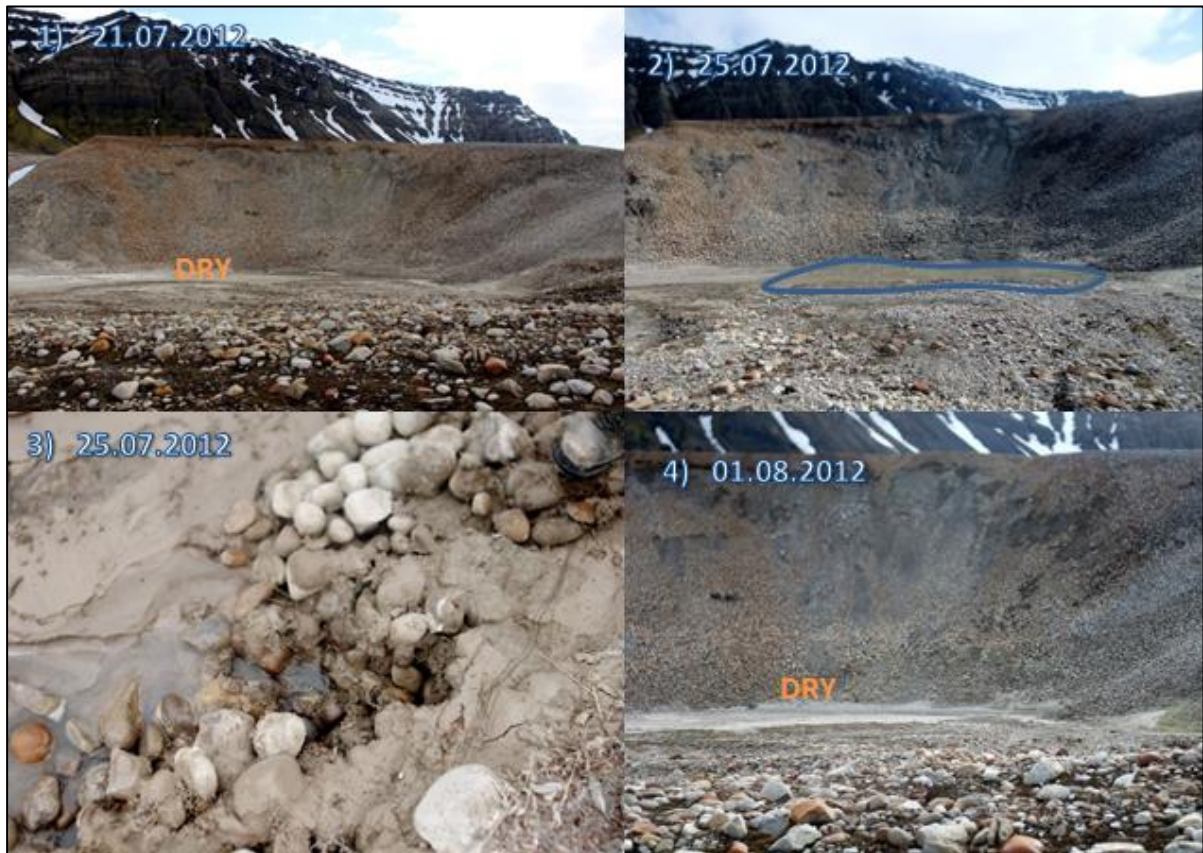


Figure 9.15: Photographs taken at Lake 4. 1) The sinkhole area at Lake 4 shown dry on 21.07.2012. 2) The sinkhole area filled up with water on 25.07.2012. 3) The sinkhole with water draining through on 25.07.2012. 4) Photograph of the sinkhole area dry and drained on 01.08.2012. Area was completely drained by 29.07.2012. (Cohen, 2013)

Field campaigns were also carried out during the spring season at Linnédalen. During spring 2012, a trip to Vardeborgsletta on 01.04.2012 revealed that both Lake 3 and Lake 4 had completely drained (figure 4.4 and 9.16) at some point during the winter or spring. Though the exact date of the drainage is not known, individual chunks of ice had reached 50cm in depth. An attempt was made to drill into Lake 4 in order to deploy the thermistor string, but was unsuccessful as 120cm of ice was drilled through to the lake bottom sediments. While both Lake 3 and Lake 4 drained during this event, only Lake 4 shows a low point which indicates drainage (figure 4.4). Lake 3 had large chunks of ice (figure 9.16), but no obvious drainage. A time lapse camera was set up at the end of the 2012 summer season in order to attempt to catch a lake drainage event during the winter/spring season 2013, but no drainage

visible from the surface occurred during 2013 (figure 9.17). Air temperatures in the winter of 2012 reached values far above freezing (appendix D), which has the potential to influence a mid-winter draining event, but no other lakes in the area experienced such an event, leading to the conclusion that is event was isolated to the karst lake system.



Figure 9.16 Lake 3 and Lake 4 drained during winter 2012. (Retelle, 2012)



Figure 9.17: Lake 4, 3, 2 from automatic digital camera, 19.03.2013 (top) and 18.04,2013 (bottom). No drainage or movement during winter/spring 2013 at Lakes 3 and 4. There is also significantly more snow cover. (Cohen, 2013)

Pit & Temperature Profiles

Nine pit profiles were excavated around Lakes 3 and 4 (figure 8.2). Pit locations (figure 3.12) were chosen according to distance from the lakes, altitude, exposure, surface and subsurface material. Three shallow boreholes are located around Lake 4 (figure 3.12) and temperature profiles were created for the data from these boreholes (figure 8.3). Pit profiles

(pit 4.2 and 4.4) and temperature profiles (Karst Plateau profile) which are distal to the lake show that though the presence of the karst lakes has influence over the proximal ground thermal regime, the distal areas are removed from the influence of the karst lakes. Pit 4.2 and 4.4 are removed from the protected basin of Lake 4, and are located on the exposed marine terraces surrounding the basin. These locations are susceptible to wind and little snow cover, effectively cooling the ground, which is apparent from the pit results. The karst plateau profile is located close to pit 4.2 and is consistent with the 4.2 pit profile, showing that the deepest temperature logger at 1.45m has thawed every summer since the beginning of the series, summer 2005. The shallow borehole would have to be at least a half meter deeper in order to display the frost table.

Pits and temperature profiles located proximal to Lake 3 and 4 exhibit much more variation in temperatures, indicating that the presence of the karst lakes influences the ground thermal regime, creating possible taliks in the permafrost. Pits 4.5, 4.6, 4.7, 4.8 and 4.9, as well as temperature profile Karst Inflow are all located either on the delta on the north side of Lake 4, or close to the sinkhole. Pits 4.5 and 4.8 both reach 0°C and are located on the eastern side of the delta, closer to the perennial ice and snow patch. The snow and ice is deposited in this location due to the topography and is able to persist throughout the year, frozen to the base, indicating permafrost conditions, which these pit excavations support. However, Pit 4.7, 4.6, 4.9 and the Karst Inflow temperature profile, located on the western side near the sinkhole, never approach the 0°C mark. The influence of the karst groundwater system in this area is enough to create a talik, where ground temperatures are warm, and water can actively drain year round into the subsurface. The Karst Inflow temperature profile displays surface and ground temperatures which have almost never reached temperatures below 0°C from 2005-2009, and temperatures which increase with depth.

The Karst 4 temperature profile is located in the relict fluvial channel close to Karst Lake 4. This location is possibly near the boundary of the talik and the typical periglacial environment. The deepest logger is 1.5m which thaws every summer and reached high temperatures in the summer of 2010. The logger at 1.5m at Karst Lake 4 reached 24.06°C on 15.06.2010. The temperature data at this date show that the logger gained 19°C in one hour, stayed in the 20°C range for four hours, and then dropped back down to freezing levels in

two hours. This is an anomaly in the data set, with no other indication of a temperature peak at other depths or from air temperature. This might be a data logger error, although all of the other surrounding data appears reasonable. In the case that it is not an error, warm groundwater circulation may have an influence at this location.

Salvigsen and Elgersma also excavated pits during their 1984 summer field campaign (Salvigsen and Elgersma, 1985). Pit profiles are shown in figure 9.18. Pit A was excavated on the northeastern shore of Lake 1, and at a depth of 3.3m, ground temperatures had not dropped below 10.7°C. This indicates that a talik also exists beneath Lake 1, and though Lake 1 may no longer be an active karst system, local taliks beneath the lake persist. Pits C and D were dug on the eastern shores of Lake 1 in an attempt to find the frost table in the Lake 1 basin. In these two locations, the frost table was penetrated at 1.15 and 1.2m.

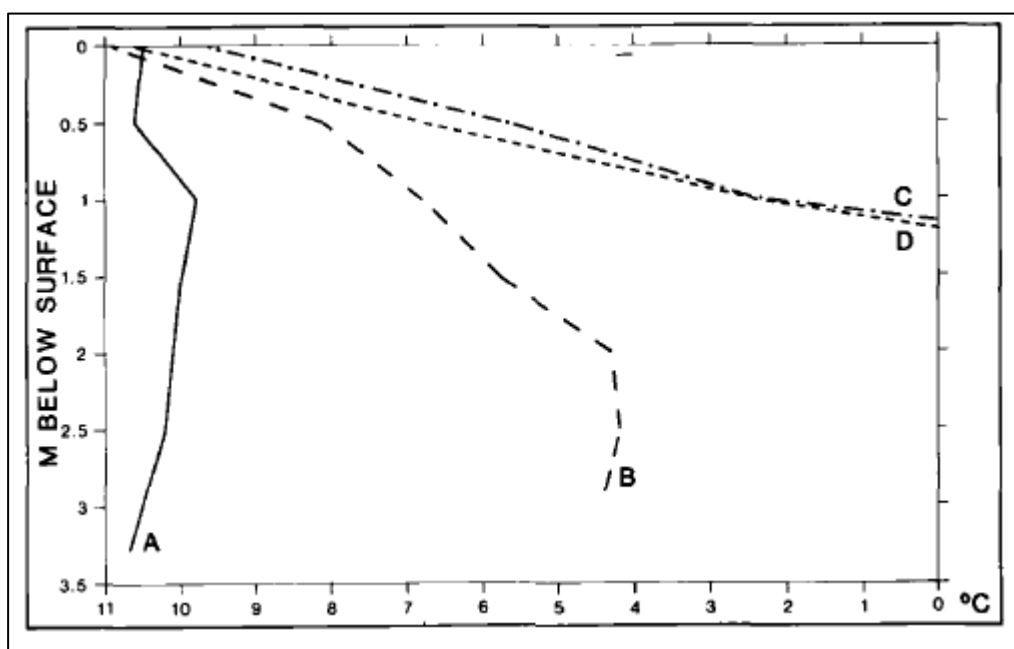


Figure 9.18: Pits dug at Vardeborgsletta by Salvigsen and Elgersma, 1985. Pit A is located at the northeast shore of Lake 1. Pit B is located at Lake 5. Pit C & D are located by the eastern shores of Lake 1. (Figure from Salvigsen and Elgersma, 1985)

9.2.2. Thermal Regime and Temperature Data Lakes 6, 7 and 8

The southwestern area of Vardeborgsletta, where Lakes 6, 7 and 8 are located (figure 3.13) displays a stable lake system with many classic periglacial features surrounding the lakes including frozen ground patterns. 5 pits were excavated (figure 8.2) proximal to Lakes 6, 7 and 8 during the summer 2012 field period. Water temperatures were also recorded from Lake 7 beginning on 04.05.2012 and running for the remainder of the field season (figure 8.1). No temperature profiles are located around this part of Linnédalen.

Lake Temperatures

A thermistor string in Lake 7 logged temperatures at three depths during the spring and summer 2012 field season. Figure 8.1 shows that temperatures in the lake after first deployment in the spring fluctuated quite a bit before the bottom two loggers steadily rose as air temperatures increased, and the top temperature logger remained frozen until the lake ice broke up. This early fluctuation is probably due to the hole drilled in the ice. Temperatures show that Lake 7 is not frozen to the bottom during the winter, and the ice was 1.2m thick when the thermistor string was deployed. The heat capacity from the large volume of water contained in the Lake 7 basin prevents the entire lake from freezing and indicates that a talik exists under the lake. After the lake ice broke up on 18.06.2012, it took two weeks for the lake temperatures to become consistent throughout the entire depth. After this time period, lake temperatures followed air temperatures.

Similar to the other lakes in the area, the main hydrological input to the lake is snowmelt. Due to topography, snow builds up on the eastern shores of the lake and melt completely throughout the summer. Lake 7 temperatures remain cool throughout the summer, never reaching above 10°C. Lake 7 has one surface outlet to the west, which cuts through the marine terraces and penetrates bedrock before emptying out into Linnéelva. Though water consistently leaves the outlet throughout the summer, there are no significant water level changes observed. A talik most likely exists below Lake 7, as well as Lake 8 and Lake 6, but does not prevent frozen ground patterns from forming close to the shorelines of these lakes.

Pit Profiles

Pit profiles were dug in five locations around Lakes 6, 7 and 8 (figure 8.2). Only one of these pits reached 0°C. The other pits never penetrated the frost table, although most were shallow

with the exception of pit 7.2. Pit 7.3, which reaches 0°C at 120cm depth, is located in the land between Lake 7 and Lake 8. This indicates that Lake 7 and Lake 8 are isolated features, which is supported by the bathymetry, displaying a sinkhole in each lake. Pits 7.1 and 7.5 are located on the stable marine terrace above the eastern shoreline of Lake 7. This area is exposed to all elements and does not hold much snow in the winter. It is unknown as to why the frost table was not reached on this plateau, which displays many non-sorted polygons and other periglacial features in other locales. Pit 7.1 shows a cooling trend, with temperatures reaching 2°C at 70cm, and may have reached the frost table if the pit was dug deeper into the terrace. Pit 7.5 however, reaches 8°C at 100cm depth, indicating that there is some kind of local heat source. Pit 7.4 is located in the protected relict fluvial channel, proximal to the shore of Lake 7. This area is a topographic low, and therefore filled with snow during the winter. The pit is shallow, only reaching 70cm. The pit displays a cooling trend with depth and possibly would reach the frost table if it was deeper.

Pit 7.2 was excavated near the relict sinkhole on the eastern shore of Lake 6. This pit is deep reaching 140cm and does not dip below 5°C. The temperature does not vary significantly at depth, and hovers around 7°C for almost 1m. Unfortunately no other pits were excavated around Lake 6, so there is no possibility to understand if this is a very local phenomenon, or characteristic of the entire Lake 6 area. Patterned ground lines the southeastern shores of Lake 6, so it is presumed that this condition does not extend to the remainder of the lake. It is more likely that a ground thermal regime characteristic of a periglacial environment instead is present.

9.2.3. Thermal Regime and Temperature Tunsjøen and Strand flat Area

The strand flat, bordered by Isfjorden to the north and the mountain Griegaksla to the south is where Tunsjøen and several other large, shallow lakes are located (figure 3.14), situated in old beach terraces on top of the old red basement rock, dating to the Precambrian (Landvik et al, 1987). This area is out of the karst lake system, with no karstified bedrock or landforms. Eight pits were excavated around the shores of Tunsjøen and a thermistor string monitored temperatures during the spring and summer 2012 field season. There are both shallow and deep boreholes scattered over the area, all in differing landforms, lithologies and surface covers.

Lake Temperatures

Tunsjøen is wide and shallow, not surpassing 1.3m in depth. Therefore water temperatures are able to get quite high, and follow air temperature closely (figure 8.1). After ice breakup in the middle of June, all three of the temperature loggers correlated well with the air temperature, though always warmer. When the thermistor string was deployed in spring 2012, the top one meter of the lake was frozen, and bottom half liquid. The lake is approximately a half kilometer wide, meaning that even though it is not deep, the water body is large enough to have a talik underneath.

Pit & Temperature Profiles

All of the pits excavated near Tunsjøen (figure 8.2) were located within 20 meters of the shoreline. Half of the pits reached the frost table at depths varying from 90cm to 1.7m. None of the pits which remained above 0°C were dug deeper than 50cm in depth. These pits would not likely have penetrated the active layer. The temperature profiles created from data from shallow boreholes located close to Tunsjøen (figure 8.4) show that active layer depths reach a minimum depth of 1.5m.

The temperature profiles (figure 8.4) created from shallow boreholes around the strand flat and Griegaksla area are all strategically placed in different periglacial landforms, in order to observe near surface ground temperature differences. The strand flat exhibits a wide variety of periglacial landforms, surface and subsurface materials in a relatively small area, designating it a practical area to study ground thermal regime. Three deep boreholes are also located in the area (figure 3.14). Trumpet curves showing maximum, minimum and average temperatures at depth for each of the boreholes, is shown in Appendix C. The temperature profiles in figure 8.4 therefore display ground temperatures for a periglacial environment which is not affected by a karst lake system. The four profiles differ in temperature values from one another, which is mostly a product of the thermal conductivity of the subsurface material and the amount of vegetation and snow covering the ground throughout the year. There are two anomalies in the Beach Ridge temperature profile, at the 25cm depth. On 12.12.2009 the temperature reaches 17.5°C at 25cm depth and on 18.01.2010 the

temperature reaches 9.4°C at 25cm depth. There is no indication of a temperature jump from any of the other sensors, indicating that this is a sensor error.

The temperature profiles in this area all display the ground temperatures at shallow depths not exceeding 2.55m which all thaw in the summer and freeze in the winter. As depth increases the air temperature affect is lessened due to the thermal offset. The palsa temperature profile displays smaller variations in ground temperature due to the thermal conductivity of organic materials. Rock Glacier East and Rock Glacier west display similar variations in ground temperature, as they are located in similar coarse material and both located far from the coast, close to Griegaksla. The Beach Ridge profile displays the greatest amount of variation in ground temperatures. This is due to the exposure of the site, which lies on a high beach terrace, with lots of exposure to wind, preventing much vegetation growth, and flat topography which does not hold snow. This area shows no indication of an active groundwater system and a classic periglacial ground thermal regime.

9.3. Karst System Development Discussion

A specific sequence of geologic conditions in the evolution of Svalbard made it possible for the karst lake system to form on the Vardeborgsletta plain in Linnédalen. Karst landforms and systems are not widespread in Arctic environments compared with the mid- and low-altitudes, meaning that certain circumstances needed to be in place in order for the formation of this system. Figure 9.19 details an interpretation of how the geologic and geomorphologic history of the area resulted in the current system. This interpretation does not account for every period in Svalbard's geologic history but instead it focuses on the steps important for the development of a karst system.

The first stage is deposition. The beginning of this system dates back to the Late Carboniferous- Mid Permian, approximately 320-280 million years ago. During this time, what is now present Svalbard, was located at around 35°N (Worsley & Aga, 1986; figure 3.4). This time period, at the end of the Carboniferous is characterized by regional sea-level rise. The majority of the Barents shelf became a warm-water carbonate platform (Worsley, 2008) (figure 9.19). The two geologic formations associated which make up the bedrock at the karst lakes are the Gipshuken formation and Wordiekammen formation. The

Wordiekammen formation was originally named the Nordenskiöldbreen formation, but due to overlapping definitions was re-named. Both formations belong to the Gipsdalen group (Dallman, 1999). The Gipshuken formation was deposited during the Sakmarian-Artinskian when Svalbard was a shallow stable shelf. The main lithologies are dolomite, limestone, anhydrite/gypsum and carbonate breccias (Dallman, 1999). The Wordiekammen formation has a deposition age of early Moscovian to Sakmarian. It lies under the Gipshuken formation. The main lithology of the Wordiekammen formation is carbonate rock (Dallman, 1999). The pair of these formations adequately lay the framework for karst formation.

The second stage is karstification. After the carbonate and evaporite rocks were formed, karstification of the landscape was possible. During the Permian there sea level transgression and regressions making the stable platform alternate between a shallow warm sea and a sabkha. During time periods of exposure led to dolomitization and karstification with subsequent karst collapse and breccia formation. Further freshwater flushing developed secondary porosity in the karst (Worsley, 2008). By the end of the Permian the karst which will be the future karst lake system at Vardeborgsletta has developed.

The third stage is the tectonic stage. This stage occurs during the beginning of the Tertiary, Svalbard is almost at its present day latitude at approximately 70° (figure 3.4). Svalbard is mostly above the ocean now, and western Spitsbergen is covered with extensive forests, which later evolve into the Tertiary coal deposits which are actively mined on Svalbard (Elvevold et al, 2007). 65 million years ago the North Atlantic Ocean began opening up due to dextral movement of the Barents Shelf past Greenland (Maher et al, 1986; Braathen and Bergh, 1995a; 1995b). This movement resulted in the Spitsbergen Orogenic Belt and Spitsbergen Thrust and Fold Belt. Deformities occurred through the stratigraphy, down to Carboniferous basin structures (Braathen and Bergh, 1995a; 1995b). In the Vardeborgsletta study area several deformities result from this early Tertiary folding and thrusting. These include a Décollement fault, a thrust fault, and faults of exact unknown origin (figure 3.8, geological map of Svalbard). These faults which developed in the karstified rock give structure to the chain of lakes which formed and the beginning of routes for groundwater movement.

Stage four is the Quaternary glaciations. Svalbard is now at its current latitude. Throughout the Quaternary Svalbard has experienced two different modes of glaciations. The full-glacial mode is when the whole of Svalbard and the Barents Sea are covered by a huge ice sheet (Ingólfsson, 2011). Interglacial mode is when Svalbard is characterized by high ice fields, ice caps and smaller valley and cirque glaciers. Svalbard has perhaps experienced full-glacial mode over a dozen times in the past one million years, but it is difficult to determine due to each new glaciation completely wiping out old sediments. It is estimated that 2-3km of rock has been removed from central Spitsbergen since the Eocene (Ingólfsson, 2011). The last time ice reached the outer shelf, by doing so completely filling Linnédalen, was 14800 years BP, during the Late Weichselian glaciation (Svendsen and Mangerud, 1997). The west coast of Spitsbergen was ice free 13000 years BP and the glacier began retreating in Linnédalen 12500 years BP (Mangerud and Svendsen, 1990). After deglaciation the land rose due to isostatic rebound, however sea level also rose, causing marine sediments from long shore drift to infill Vardeborgsletta with 10-30m of marine deposits (Svendsen and Mangerud, 1997). Therefore the lake basins and relict fluvial channels probably do display a high level of glacial influence.

Stage 5 is the Holocene development. Linnédalen is at its current location and has transitioned from a glacial landscape to marine setting and now is transitioning to its current periglacial environment. Linnédalen was a fjord from 12500 BP to 9600 BP. The upper marine limit is a 64m asl marine terrace, dated by Landvik et al, 1987. By 9600 years BP Linnévatnet was isolated from the sea by a 30m asl terrace (Landvik et al, 1987). Sea level then transgressed 6000 years BP (Landvik et al, 1987). This is the time period when Vardeborgsletta and the karst lake system was forming the shape and system observed today. There are several levels of old marine beach terraces at Vardeborgsletta. This indicates that sea level regression and transgression in different stages during the late Holocene shaped the karst lake system with large channels formed by different levels of old raised marine beaches. Evidence from relict fluvial systems, old high lake shorelines and relict sinkholes, all cut through the old raised marine beaches and into the marine sediments gives evidence that the lakes and rivers were larger features during this time period. The karst and initial karst collapse had already occurred and extensive faulting had occurred in the area to allow for further development of the karst lake and groundwater system.

During this time period in the Holocene, marine and then periglacial activity shaped Vardeborgsletta to create the current system. As sea level regressed, permafrost aggraded and periglacial processes began to shape the landscape. As Vardeborgsletta was isolated from the ocean, the karst groundwater system was re-activated and the combination of this and the periglacial activity gives the current lake system observed today. It is possible that the lakes which were connected by relict fluvial systems (Lake 6 – Lake 7, Lake 5 – Lake 4 and Lake 3 – Lake 1) were all developing and active during the same period of time. All of these systems display higher shorelines and relict sinkholes. It appears that the only system which is still active in terms of karst groundwater activity is Lake 4 and Lake 3. The sinkhole at Lake 4 is still actively draining during the melt season (figure 9.15) and both Lake 3 and Lake 4 drained during winter 2012 (figure 9.16 & figure 4.4).

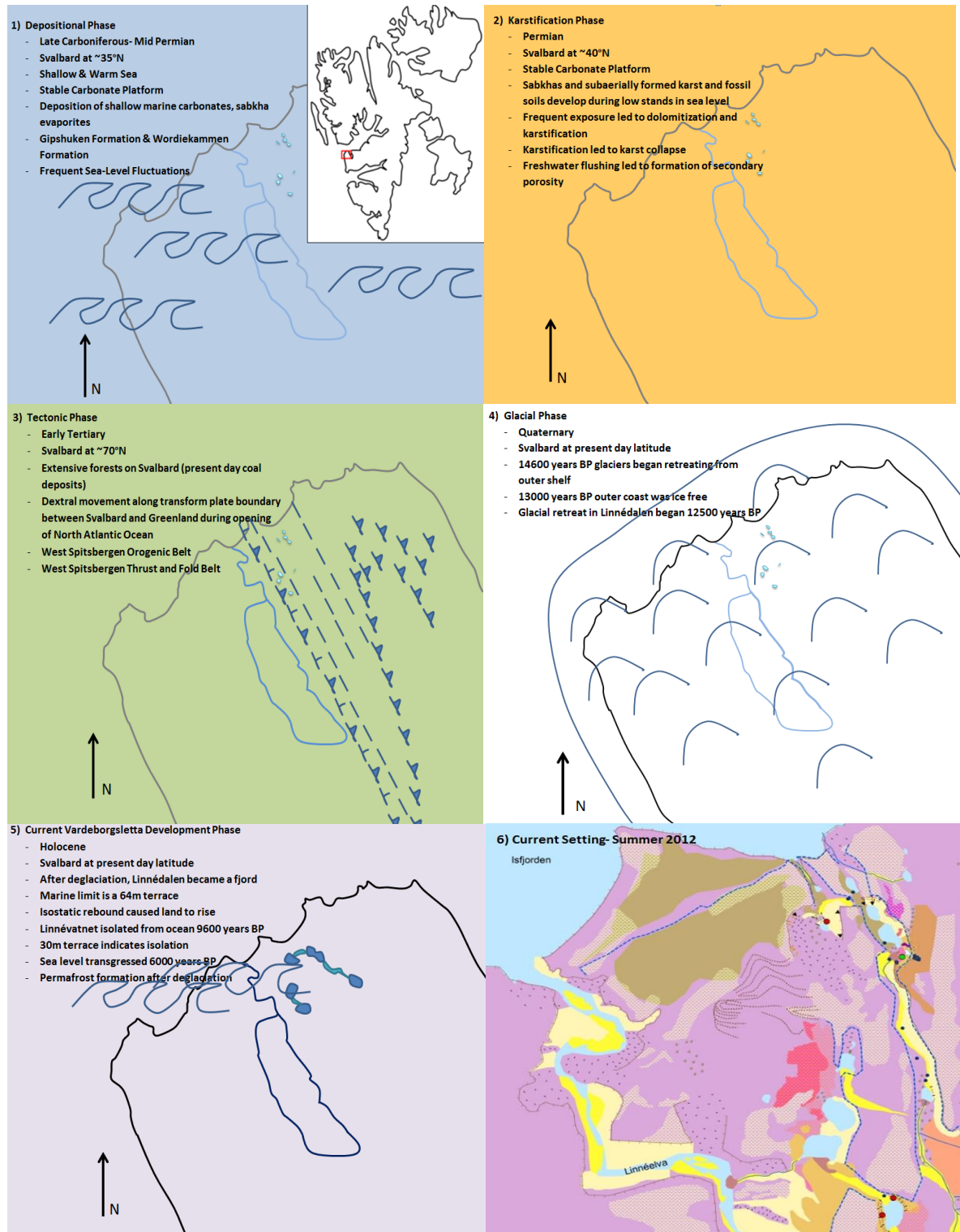


Figure 9.19: Development of the karst system at Vardeborgsletta, Linnédalen. 1) Stage 1 Carboniferous and Permian Development. Inset shows location of Vardeborgsletta in Nordenskiöldland, western Spitsbergen 2) Stage 2 is karstification phase during Permian. 3) Stage 3 is tectonic phase from beginning of the Tertiary. 4) Stage 4 is the glacial stage from the Quaternary. 5) Stage 5 is the current development phase from the mid to late Holocene. 6) Stage 6 is the current stage; geomorphological map from figure 6.1 is used to portray current processes. (Cohen, 2013)

Figure 9.20 is a schematic model showing an interpretation of how the current karst groundwater system might operate at Vardeborgsletta. The figure draws inspiration from figures 2.8 (Salvigsen and Elgersma, 1985) and 2.4 (Clark and Lauriol, 1997). The figure shows Lakes 2, 3 and 4, with the mountain Vardeborgaksla in the background and Isfjord to the North. This interpretation has water actively draining from Lake 4, and the sinkhole near Lake 4 through taliks into the groundwater system, which extends down to the bedrock and eventually reaches Isfjord. The figure shows Lake 3 having a relict drainage, which may have existed when Lake 3 was a larger system. There is reason to believe that Lake 3 and Lake 4 continue to actively drain but are connected, which is evident by the change in lake level observed at Lake 4 over the study period (figure 9.15 and figure 8.8) and because of the event which occurred over winter 2012, when both Lake 3 and 4 drained midwinter (figure 9.16 and figure 4.4). Pit 4.1, which was excavated in the land between Lake 3 and Lake 4, never reaches the permafrost, indicating that the ground between the lakes is not frozen, allowing water to flow through. Because the karst system originates from the karstified bedrock below it is reasonable that the water drains down to the bedrock where the actual karst groundwater system is located. The groundwater system may run along faults originating from the Tertiary faulting episode. At some point the water must drain into the ocean, but there is no direct proof of this, and the dye tracings attempted by Salvigsen and Elgersma, 1985, were not successful in finding an outlet for the water. The question mark below Lake 2 comes from there being no proof that water is draining from Lake 2 through to the subsurface. There is a possibility that Lake 2 is part of the groundwater system, but with no variations in water level and no landforms or features pointing to a connection, it is not reasonable to make that assumption.

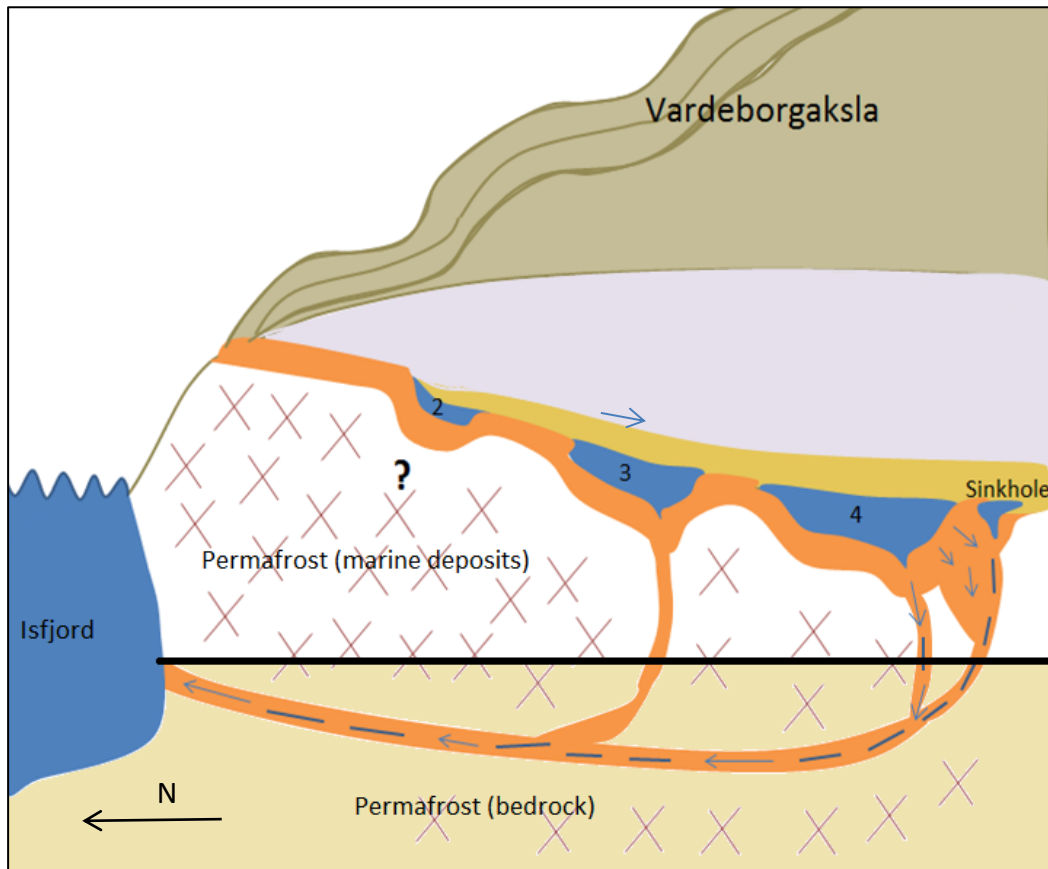


Figure 9.20: Schematic figure showing possible karst groundwater system at Lakes 2-3-4, Vardeborgsletta, Linnédalen, Spitsbergen. (Cohen, 2013)

9.4. Potential Error

The main potential source of error is the temperature loggers which have been logging temperatures in various locations in Linnédalen beginning in 2004. The loggers were purchased and deployed at different times, and all have the potential for error. Obvious anomalies which were observed in the analyzed data were commented on in the text. Another potential for sources of error is the data not collected by the author. The AG-212 course supplied the thesis with some of the data for the pit profiles and the bathymetric profiles. Surveying data also possibly contains errors, due to the original base point being taken from another survey which the author did not have control over.

Chapter 10. CONCLUSION

10.1. Summary and Conclusions

A two year master's thesis concerning the karst lake system at Linnédalen, western Spitsbergen, culminated in a year-long thesis. The purpose of the thesis was to investigate the influence of a karst lake system on the periglacial environment encountered at Vardeborgsletta, Linnédalen. The research questions chosen to investigate this system follow:

- What can geomorphological mapping reveal about the landscape development and current processes at the study site?
- How does the karst lake system affect the thermal and hydrological regime of the study site?
- What geological and geomorphological processes have occurred over time to form the current system?

Data collection from field work campaigns in 2012 and 2013, as well as data analysis pre-existing temperature data from the study site culminated in the following results:

- Depth, surface area and volume statistics for each of the lakes
- Surveying data for the field site proximal to Lakes 1, 2, 3 and 4
- A Geomorphological map of the study area
- Bathymetric profiles for the lakes
- Temperature profiles including:
 - Water temperature profiles
 - Pits profiles
 - Ground temperature profiles
 - Level logger profile

The discussion utilized a combination of the results and past studies to make the following points in conclusion:

- The geomorphological map, bathymetric map and bathymetric profiles reveal the karst origins of the lakes and the karst features located throughout the study area. The geomorphological map shows the current landforms and ongoing processes at the study area. The area is influenced by periglacial and karst processes.
- The map reveals that Vardeborgsletta, the plain where the karst lake system is located, is composed of old raised marine beaches, which have undergone

weathering processes since they emerged from the ocean during the Holocene. In many areas of the study area, particularly on steep slopes, marine deposits are revealed due to the erosion from periglacial and karst processes. The lake basins and relict fluvial channels cut into these old raised marine beaches and were shaped in-situ, as the various levels of marine beaches formed due to Holocene deglaciation, sea level transgressions and regressions, and isostatic rebound.

- The area is full of periglacial and karst influences. Non-sorted polygons, frozen ground patterns, mass wasting from solifluction and active-layer detachments shape the study area and reveal the periglacial influence. Relict sinkholes, dolines, relict lake shorelines and carbonate bedrock reveal the karst influence on the study area.
- The analysis of air, water and ground temperatures from various locations around the study area, as well as level logger data, reveal that the karst lake system influences the thermal regime of the study area.
- In the northeastern part of Vardeborgsletta, where Lakes 2, 3 and 4 are located, ground temperatures vary quite drastically dependent upon proximity to the lake. Lake temperatures are not correlated with air temperatures, and temperature profiles reveal that the ground proximal to the sink hole has rarely reached temperatures below zero degrees Celsius since at least 2005. Changes in lake level which are related to the sinkhole were also observed during the study period, and Lake 3 and Lake 4 drained completely during the winter season, 2012. Here, the thermal regime is influenced by factors such as meteorology, topography, exposure, surface cover, and geology, though the influence of the karst lake system plays an integral role.
- Contrary to Lakes 2, 3, 4 area, temperature profiles reveal that the thermal regime proximal to Lakes 7 and 8, as well as the strand flat where Tunsjøen is located, is influenced by factors such as meteorology, topography, exposure, surface cover and geology. The karst lake system does not influence the current thermal regime in this area.
- An interpretation of the geologic and geomorphologic development of the area was created by combining past studies and field observations. The interpretation determined that the karst system has its first origins from the Carboniferous and Permian, when the present bedrock was deposited and karstified. Tertiary tectonics led to deformation and faulting at the study site. Influences from Quaternary and Holocene glaciations, glacial to marine to periglacial environmental change, isostatic rebound, and marine regressions and transgressions have all shaped the current system.

- The current system at Vardeborgsletta includes lakes which are no longer active within the karst system, as well as lakes which continue to show activity and development. At Lake 4, active water drainage penetrates the subsurface, into a groundwater system.

10.2. Study Implications

The focus of this project, a karst lake system within a periglacial environment, revolves around an occurrence that is not frequently observed. What then, are the implications of this study in the big picture? Geomorphologic mapping, especially at a fine scale, is always a useful addition for future studies at a given area. Linnédalen is frequented by scientists, and hopefully the map can add to future scientific endeavors. The discussion and conclusions regarding how the ground thermal regime is affected by the karst lakes can hopefully add to the discussion on how permafrost and periglacial features are influenced by different variables. Text books (French, 2007) establish how permafrost is affected by factors such as climate, meteorology, geology, surface cover, topography, vegetation, etc. The influencing role of groundwater systems and karst systems on the thermal regime of permafrost and periglacial environments is not as frequently mentioned, and this study can add a perspective to that gap.

10.3. Future Prospects

This thesis by no means closes the door on possible studies to further understand karst lake system at Linnédalen. Other prospects for future studies involving the karst lake system at Linnédalen include:

- Up-scaling the system to extend to the southern part of Linnédalen and include the two lakes Linnévatnet and Kongress vatnet. Kongress is an elevated karst lake (95m asl) located on the southeastern side of Linnédalen. The maximum depth of this lake is 52m asl. A previous study on this lake (Holm et al, 2012) attributes lake changes to climate change as opposed to karst activities. It would be interesting to simultaneously monitor Kongress, Linnévatnet and all of the karst lakes for both changes in level and temperature. A more thorough analysis could be made detailing how connected the entire system is in terms of changing lake levels and if this phenomenon is related to meteorology or karst processes.

-A bachelor's thesis was completed on the karst lakes in 2013 by one of the AG-212 students, Lauren Farnsworth. For her thesis, she extracted two cores from the karst lakes in order to understand the sedimentology of the karst lakes. More coring and analysis could give a better understanding of rates of sedimentation from the slopes into the karst lakes, and how the lake basins have developed in recent times.

-Drilling deep boreholes on Vardeborgsletta and installing thermistor strings could lead to a comparison of permafrost temperatures between Vardeborsletta and the strand flat where three deep boreholes are located (appendix C). This would give a more complete understanding of how the ground thermal regime is affected by the karst lake system.

REFERENCES

- ACGR (Associate Committee on Geotechnical Research) (1988). Glossary of permafrost and related ground ice terms. Permafrost Subcommittee, National Research Council of Canada, Ottawa, technical memorandum, 142, 156 pp.
- Åkerman, HJ, 1980. Studies on periglacial geomorphology in west Spitsbergen. Lund University Geography Institute. pp. 297.
- Åkerman, HJ, 1984. Notes on talus morphology and processes in Spitsbergen. *Geografiska annaler*, 66(a): 267-284.
- Åkerman, HJ, 1992. Hydrographic characteristics of the Strokdammene Plain, West Spitsbergen, Svalbard. *Geografiska Annaler*, 74(2/3): 169-182.
- Åkerman, HJ, 2005. Relations between slow slope processes and active-layer thickness 1972-2002, Kapp Linné, Svalbard. *Norwegian Journal of Geography*, 59 (2): 116-128.
- Axén, H, Roalkvam E, 2012. Holocene and modern climate change in the high Arctic environment: lake 7. Unpublished Report.
- Ballantyne, CK, Harris, C, 1994. *The Periglaciation of Great Britain*. Cambridge University Press, Cambridge. pp. 335.
- Ballantyne, CK, 2002. Paraglacial geomorphology. *Quaternary Science Reviews*, 21: 1935-2017.
- Ballantyne, CK, 2010. A general model of autochthonous blockfield evolution. *Permafrost and Periglacial Processes*, 21: 289-300.
- Barsch, D, 1992. Permafrost creep and rockglaciers. *Permafrost and Periglacial Processes*, 3: 175-188.

- Braathen, A, Bergh, SG, 1995a. Kinematics of Tertiary deformation in the basement-involved fold-thrust complex, western Nordenskiöld Land, Svalbard: tectonic implications based on fault-slip data analysis. *Tectonophysics*, 249: 1-29.
- Braathen, A, Bergh, SG, 1995. Structural outline of a Tertiary basement-cored uplift/inversion structure in western Spitsbergen, Svalbard: kinematics and controlling factors. *Tectonics*, 14(1): 95-119.
- Burn, CR, Smith, MW, 1990. Development of thermokarst Lakes during the Holocene at sites near Mayo, Yukon Territory. *Permafrost and Periglacial Processes*, 1: 161-176.
- Burn, CR, 1997. Cryostratigraphy, paleogeography, and climate change during the early Holocene warm interval, western Arctic coast, Canada. *Canadian Journal of Earth Science*, 24: 912-925.
- Burn, CR, 2011. Permafrost distribution and stability. *Changing Cold Environments: A Canadian Perspective*, First Edition. Edited by Hugh French and Olav Slaymaker. John Wiley & Sons, Ltd.
- Childs, C, 2004. Interpolating surfaces in ArcGIS spatial analyst. *ArcUser*, July-September 2004.
- Christiansen, HH, 2005. Thermal regime of ice-wedge cracking in Adventdalen, Svalbard. *Permafrost and Periglacial Processes*, 16: 87-98.
- Christiansen, HH, Etzel Müller, B, Isaksen, K, Juliussen, H, Farbrøt, H, Humlum, O, Johansson, M, Ingeman-Nielsen, T, Kristensen, L, Hjort, J, Holmlund, P, Sannel, ABK, Sigsgaard, C, Åkerman, HJ, Foged, N, Blikra, LH, Pernosky, MA, Ødegård, RS, 2010. The thermal state of permafrost in the Nordic area during the international polar year 2007-2009. *Permafrost and Periglacial Processes*, 21(2): 156-181.
- Clark, ID, Lauriol, B, 1997. Aufeis of the Firth River Basin, Northern Yukon, Canada: insights into permafrost hydrogeology and karst. *Arctic and Alpine Research*, pp. 240-252.

- Dallmann, W. K. Lithostratigraphic Lexicon of Svalbard: Review and Recommendations for Nomenclature Use : Upper Palaeozoic to Quaternary Bedrock. Tromsø: Norsk Polarinstitut, 1999. pp. 322.
- Eckerstorfer, M, Christiansen, HH, 2011. Topographical and meteorological control on snow avalanching in the Longyearbyen area, central Svalbard 2006-2009. *Geomorphology*, 134: 186-196.
- Eklima.no, 2013. Free access to weather- and climate data from Norwegian Meteorological Institute from historical data to real time observations. <http://www.eklima.no>
- Elvevold, S, Dallman, W, Blomeier, D, 2007. The Geology of Svalbard. Tromsø: Norsk Polar Institute, 2007. pp. 36.
- Farnsworth, WR, 2013. High arctic debris flow literature review: Bjørndalen case study, Norges Geologiske Undersøkelse (NGU).
- Farnsworth, L, Glaw, L, 2012. Investigation of the dynamics of karst lakes at Vardeborgsletta, Western Svalbard. Unpublished Report.
- Ford, D, Williams, P, 2007. Karst Hydrogeology and Geomorphology. West Sussex, England: John Wiley & Sons Ltd. pp. 562.
- Frauenfelder, R, Haeberli, W, Hoelzle, M, 2003. Rockglacier occurrence and related terrain patterns in a study area of the Eastern Swiss Alps. *Permafrost, Phillips, Springman, and Arenson*. pp. 253-258.
- French, HM, 1976. The Periglacial Environment. Longman London 1976. pp. 308.
- French, HM, 2007. The Periglacial Environment. Third Edition. West Sussex, England: John Wiley & Sons Ltd. pp. 458.
- French, HM, Shur, Y, 2010. The principles of cryostratigraphy. *Earth-Science Reviews* 101: 190-206.

- Haeberli, W, Hallet, B, Arenson, L, Elconin, R, Humlum ,O, Kääb, A, Kaufmann, V, Ladanyi, B, Matsuoka, N, Springman, S, Mühll, DV, 2006. Permafrost creep and rock glacier dynamics. *Permafrost and Periglacial Processes*, 17: 189-214.
- Hagen, JO, Liestøl, O, Roland, E, Jørgensen, T, 1993. *Glacier atlas of Svalbard and Jan Mayen*, Norwegian Polar Institute, 129.
- Hagen, JO, Melvold, K, Pinglot, F, Dowdeswell, J, 2003a. On the net mass balance of the glaciers and ice caps in Svalbard, Norwegian Arctic. *Arctic, Antarctic, and Alpine Research*, 35: 264-270.
- Hagen, JO, Kohler, J, Melvold, K, Winther, JG, 2003b. Glaciers in Svalbard: mass balance, runoff and freshwater flux. *Polar Research* 22(2): 145-159.
- Hambrey, MJ, 1984. Sudden draining of ice-dammed lakes in Spitsbergen. *Polar Record* 22: 189-194.
- Harris, SA, 1986. *The Permafrost Environment*. Roman and Littlefield Publishers, Totowa, New Jersey. pp. 276.
- Hinzman, LD, Kane, DL, Woo, M-K, 2006. Permafrost Hydrology in *Encyclopedia of Hydrological Sciences*, vol. 4. M. John Wiley, West Sussex, U.K. pp. 2670-2693.
- Holm, TM, Koinig, KA, Andersen, T, Donali, E, Hormes, A, Klaveness, D, Psenner, R, 2012. Rapid physiochemical changes in the high Arctic lake Kongressvatn caused by recent climate change. *Aquatic Science*, 74: 385-395.
- Humlum, O, 1998. The climatic significance of rock glaciers. *Permafrost and Periglacial Processes*, 9: 375-395.
- Humlum O (2000) The geomorphic significance of rock glaciers: estimates of rock glacier debris volumes and headwall recession rates in west Greenland. *Geomorphology*, 35: 41-67.
- Humlum ,O, 2002. Modelling late 20th-century precipitation in Nordenskiöld Land, Svalbard, by geomorphic means. *Norwegian Journal of Geology*, 56: 93-103.

- Humlum, O, Instanes, A, and Sollid, JL, 2003. Permafrost on Svalbard: a review of research history, climatic background and engineering challenges. *Polar Research*, 22: 191-215.
- Humlum, O, Christiansen, HH, Juliussen H, 2007. Avalanche-derived rock glaciers in Svalbard. *Permafrost and Periglacial Processes*, 18: 75-88.
- Ingólfsson, Ó, 2011. Fingerprints of Quaternary glaciations on Svalbard. Geological Society, London, Special Publications 2011, 354: 15-31.
- Ingólfsson, Ó, Landvik, JY, 2013. The Svalbard-Barents ice-sheet – historical, current and future perspectives. *Quaternary Science Reviews*, 64: 33-60.
- Ingólfsson, O. Outline of the geography and geology of Svalbard. University Centre in Svalbard.
- Kane, DL, Hinzman, LD, Benson, CS, Liston, GE, 1991. Snow hydrology of a headwater arctic basin 1. Physical measurements and process studies. *Water Resources Research*, 27(6): 1099-1109.
- Kessler, MA, Werner, BT, 2003. Self-organization of sorted patterned ground. *Science*, 299: 380-383.
- Knies, J, Matthiessen, J, Vogt, C, Laverg, JS, Hjelstuen, BO, Smelror, M, Larsen, E, Andreassen, K, Eidvin, T, Vorren, TO, 2009. The Plio-Pleistocene glaciation of the Barents Sea-Svalbard region: a new model based on revised chronostratigraphy. *Quaternary Science Reviews*, 28: 812-829.
- Lachenbruch, AH, Cladouhous, TT, Saltus, RW, 1988. Permafrost temperature and changing climate. *Permafrost: Fifth International Conference, Trondheim, Norway, Proceedings, Vol. 3. Tapir Publishers: Trondheim, Norway: 9-17.*
- Landvik, JY, Mangerud, J, Salvigsen, O, 1987. The late Weichselian and Holocene shoreline displacement on the west-central coast of Svalbard. *Polar Research*, 5: 29-44.

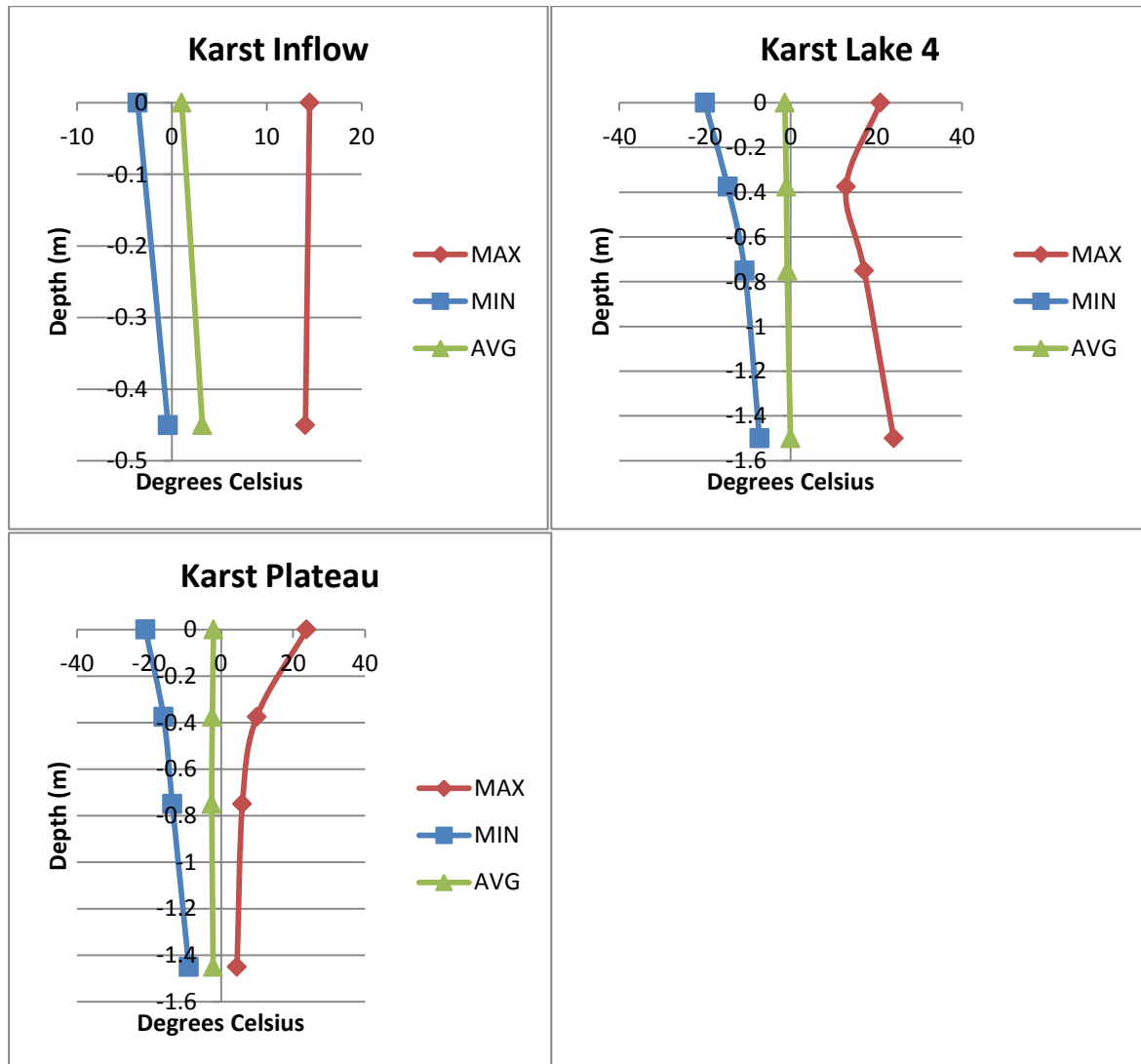
- Liestøl, O, 1975. Pingos, springs, and permafrost in Spitsbergen. *Norsk Polarinstitutt Årbok*, 1975: 7-29.
- Liestøl, O, 1996. Open-system pingos in Spitsbergen. *Norsk Geografisk Tidsskrift*, 50(1): 81-84.
- Lønne, I, Mangerud J, 1991. An early of middle Weichselian sequence of proglacial, shallow marine sediments on western Svalbard. *BOREAS*, 20: 85-104.
- Mackay, JR, 1990. Some observations on the growth and deformation of epigenetic, syngenetic and anti-syngenetic ice-wedges. *Permafrost and Periglacial Processes*, 1: 15-29.
- Mackay, JR, 1995. Ice wedges on hillslopes and landform evolution in the late Quaternary, western Arctic coast, Canada. *Canadian Journal of Earth Sciences*, 32: 1093-1105.
- Mackay, JR, 2000. Thermally induced movements in ice-wedge polygons, western Arctic coast: a long-term study. *Géographie physique et Quaternaire*, 54: 41-68.
- Maher, HD, Craddock, C, Maher K, 1986. Kinematics of Tertiary structures in upper Paleozoic and Mesozoic strata on Midterhuken, west Spitsbergen. *Geological Society of America Bulletin*, 97: 1411-1421.
- Mangerud, J, 1987. The Allerød/Younger Dryas boundary. *Abrupt Climate Change*. D. Reidel Publishing Company, Dordrecht. pp. 163-171.
- Mangerud, J, Svendsen, JI, 1990. Deglaciation chronology inferred from marine sediments in a proglacial Lake basin, western Spitsbergen, Svalbard. *BOREAS*, 19:249-272.
- Mangerud, J, Svendsen, JI, 1992. The last interglacial-glacial period on Spitsbergen, Svalbard. *Quaternary Science Review*, 11: 633-664.
- Matsuoka, N, 2001. Solifluction rates, processes and landforms: a global review. *Earth-Science Reviews*, 55: 107-134.

- Michel, FA, van Everdingen, RO, 1994. Changes in hydrogeologic regimes in permafrost regions due to climate change. *Permafrost and Periglacial Processes*, 5(3): 191-195.
- Michel, FA, van Everdingen, RO, 1988. Karst development in permafrost regions of northern Canada. *Proceedings of the 21st Congress – Karst Hydrogeology and Karst Environment Protection*. pp. 249-254.
- Muller, SW, 2008. *Frozen in Time: Permafrost and Engineering Problems*. American Society of Civil Engineers. pp. 273.
- Osterkamp, TE, Viereck, L, Shur, Y, Jorgenson, MT, Racine, C, Doyle, A, Boone RD, 2000. Observations of thermokarst and its impact on boreal forests in Alaska, USA. *Arctic, Antarctic, and Alpine Research*, 32(3): 303-315.
- Romanovsky, VE, Smith, SL, Christiansen, HH, 2010. Permafrost thermal state in the polar Northern Hemisphere during the International Polar Year 2007-2009: a synthesis. *Permafrost and Periglacial Processes*, 21: 106-116
- Salvigsen, O, Lauritzen, Ø, Mangerud, J, 1983. Karst and karstification in gypsiferous beds in Mathiesondalen, central Spitsbergen, Svalbard. *Polar Research n.s.*:83-88.
- Salvigsen, O, Elgersma, A, 1985. Large-scale karst features and open taliks at Vardeborgsletta, outer Isfjorden, Svalbard. *Polar Research 3 n.s.*: 145-153.
- Schwamborn, GJ, Dix, JK, Bull, JM, Rachold, V, 2002. High-resolution seismic and ground penetrating radar – geophysical profiling of a thermokarst Lake in the Western Lena Delta, Northern Siberia. *Permafrost and Periglacial Processes*, 13: 259-269.
- Shur, Y, Hinkel, KM, Nelson, FE, 2005. The transient layer: implications for geocryology and climate-change science. *Permafrost and Periglacial Processes*, 16: 5-17.
- Smith, MW, Riseborough, DW, 2002. Climate and the limits of permafrost: a zonal analysis. *Permafrost and Periglacial Processes*, 13: 1-15.
- Smith, SL, Romanovsky, VE, Lewkowicz, AG, Burn, CR, Allard, M, Clow, GD, Yoshikawa, K, Throop, J, 2010. Thermal state of permafrost in North America: a

- contribution to the international polar year. *Permafrost and Periglacial Processes*, 21: 117-135.
- Snyder, JA, Werner A, Miller, GH, 1999. Holocene cirque glacier activity in western Spitsbergen, Svalbard: sediment records from proglacial Linnévatnet. *The Holocene*, 10(5): 555-563.
- Solheim, A, Andersen, ES, Elverhøi, A, Fiedler, A, 1996. Late Cenozoic depositional history of the western Svalbard continental shelf, controlled by subsidence and climate. *Global and Planetary Change*, 12: 135-148.
- Sørbel, L, Tolgensbakk, J, 2002. Ice-wedge polygons and solifluction in the Adventdalen area, Spitsbergen, Svalbard. *Norsk Geografisk Tidsskrift*, 56: 62-66.
- Sørbel, L, Tolgensbakk, J, Hagen, JO, Høgvard, K, 2001. Geomorphological and Quaternary geological map of Svalbard 1:100,000 sheet C9Q Adventdalen. Norsk Polar Institute 2001: 57-78.
- Steel, RJ, Worsley D, 1984. Svalbard's post-Caledonian strata- an atlas of sedimentational patterns and palaeogeographic evolution. In A.M. Spencer et al. (eds.): *Habitat of hydrocarbons on the Norwegian continental margin*. Graham & Trotman, London. pp. 109-135.
- Svendsen, JI, Mangerud, J, Miller, GH, 1989. Denudation rates in the Arctic estimated from lake sediments on Spitsbergen, Svalbard. *Palaeogeography, Palaeoclimatology, Palaeoecology*, 76: 153-168.
- Svendsen, JI, Mangerud, J, 1997. Holocene glacial and climatic variations on Spitsbergen, Svalbard. *The Holocene*, 7(1): 45-57.
- TSP Norway: Thermal State of Permafrost in Norway and Svalbard.
<http://www.tspnorway.com>.
- Vogel, S, Eckerstorfer, M, Christiansen, HH, 2012. Cornice dynamics and meteorological control at Gruvefjellet, Central Svalbard. *The Cryosphere*, 6: 151-171.

- Wanatabe T, Matsuoka, N, Christiansen, HH, 2013. Ice- and soil- wedge dynamics in the Kapp Linné area, Svalbard, investigated by two- and three-dimensional GPR and ground thermal and acceleration regimes. *Permafrost and Periglacial Processes*, 24: 39-55.
- Washburn, AL, 1956. Classification of patterned ground and review of suggested origins. *Bulletin of the Geological Society of America*, 67: 823-866.
- White, WB, 1988. *Geomorphology and Hydrology of Karst Terrains*, vol. 464. Oxford University Press, New York.
- Woo, MK, Kane, DL, Carey, SK, Yang, D, 2008. Progress in permafrost hydrology in the new millennium. *Permafrost and Periglacial Processes*, 19: 237-254.
- Worsley, D, 2008. The post-Caledonian development of Svalbard and the western Barents Sea. *Polar Research*, 27: 298-317.
- Worsley, D, Aga, OJ, 1986. Evolution of an arctic archipelago: The geological history of Svalbard. Statoil. pp. 121.
- Yoshikawa K and Hinzman LD (2003) Shrinking thermokarst ponds and groundwater dynamics in discontinuous permafrost near Council, Alaska. *Permafrost and Periglacial Processes*, 14: 151-160.

APPENDIX



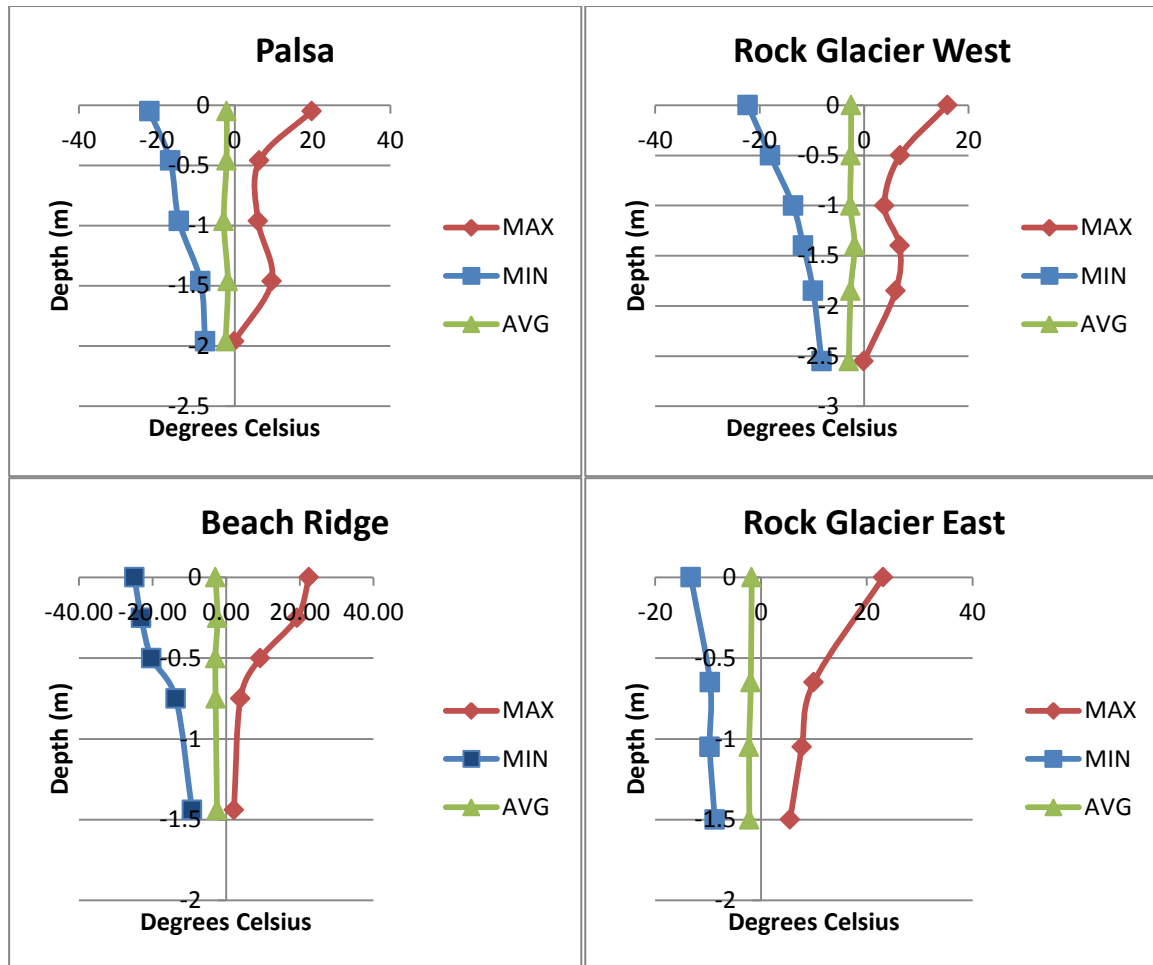
Appendix A: Temperature profiles created from the data from figure 8.3, showing maximum, minimum and average temperatures at depth for each temperature logger. (Cohen, 2013)

A depicts trumpet curves showing maximum, minimum and average temperatures for the temperature profile locations proximal to Lake 4. The largest range of temperatures is at Karst Plateau, where maximum at the ground surface the maximum and minimum temperatures have a difference of over 44°C. At Karst Lake 4 there is a temperature inversion with depth. The maximum temperature at 75cm is 5°C warmer than the maximum temperature at 37.5cm, and the maximum temperature at 1.5m is 7°C warmer than the

maximum temperature at 75cm. The minimum temperatures at Karst Lake 4 show the same inversion, with warmer minimum temperatures at greater depths.

Table A: Summary of maximum, minimum and average temperatures for the temperature profiles proximal to Lake 4

Temp Profile Location & Depth	Max Temperature (°C)	Min Temperature (°C)	Avg Temperature (°C)
Karst Inflow			
0cm	14.5	-3.6	1.03
45cm	14	-0.41	3.21
Karst Lake 4			
0cm	20.98	-20.01	-1.36
37.5cm	12.95	-14.73	-0.99
75cm	17.19	-10.74	-0.81
1.5m	24.06	-7.29	-0.04
Karst Plateau			
0cm	23.77	-21.02	-2.08
37.5cm	9.92	-15.99	-2.43
75cm	5.91	-13.53	-2.58
1.45m	4.42	-8.96	-2.21

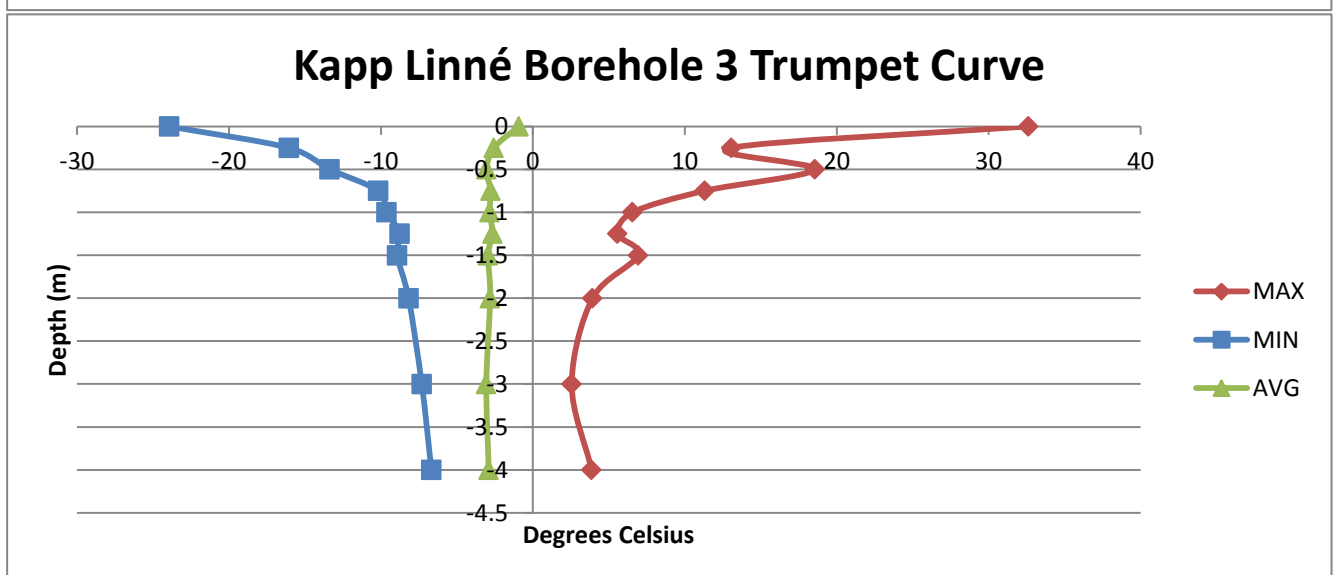
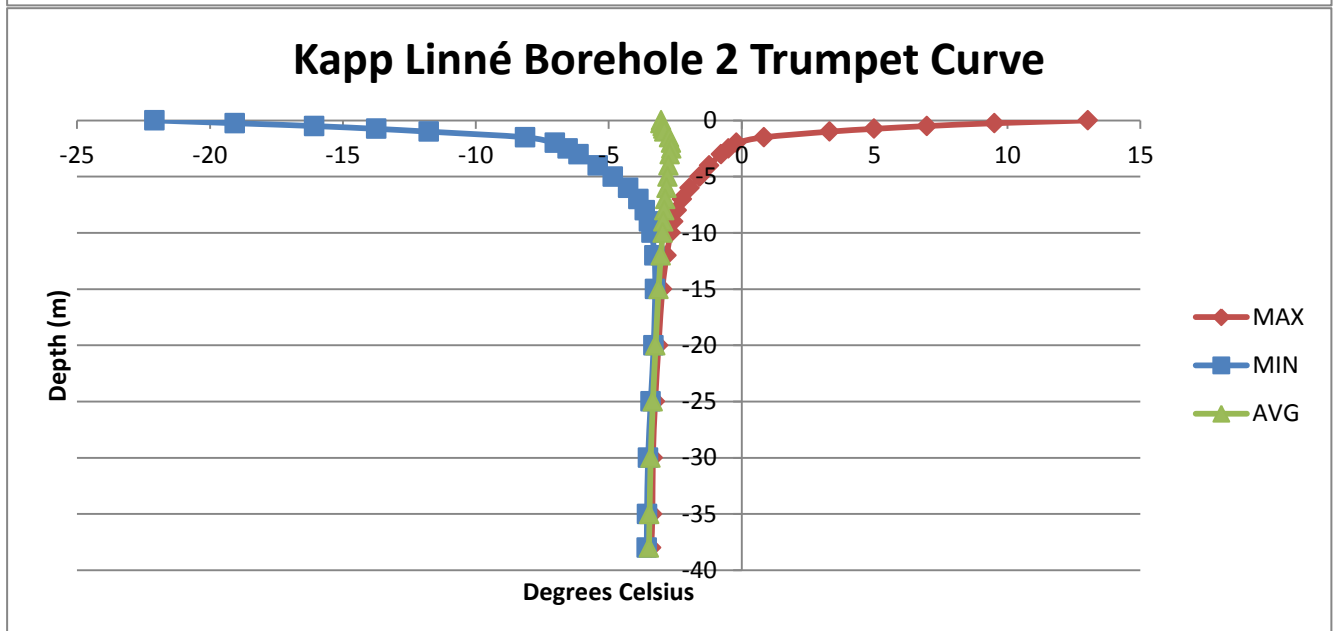
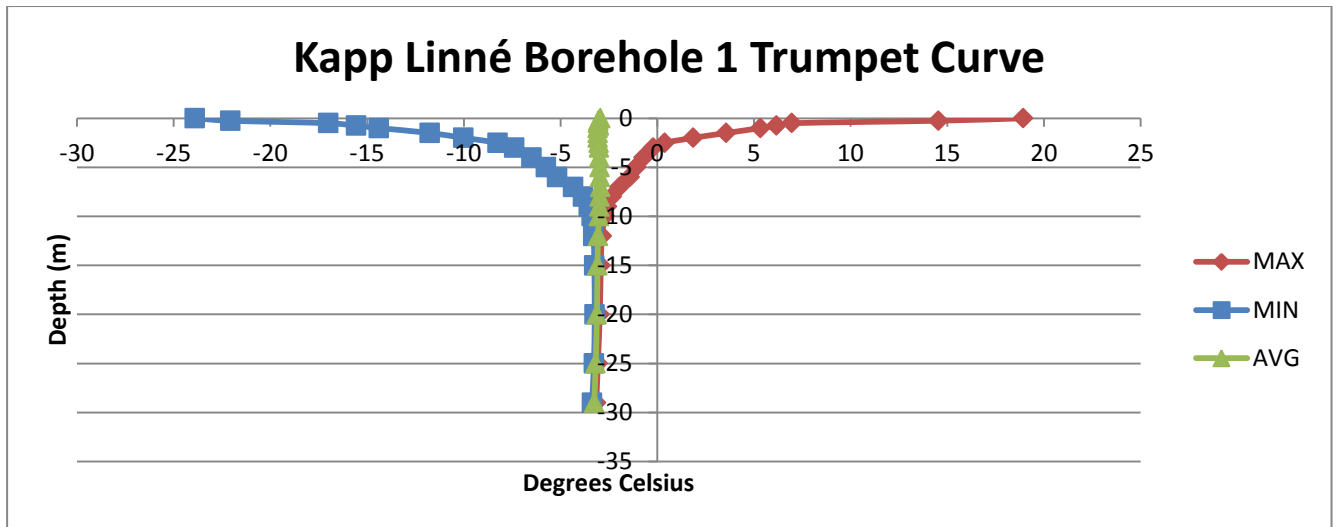


Appendix B: Temperature profiles created from the data from figure 8.4, showing maximum, minimum and average temperatures at depth for each temperature logger. (Cohen, 2013)

B depicts trumpet curves showing maximum, minimum and average temperatures for the temperature profile locations situated on the strand flat and near Tunsjøen (figure 3.14). The largest range of temperatures is at the Palsa site, where maximum at the ground surface the maximum and minimum temperatures have a difference of over 40°C. The Palsa site and Rock Glacier West display temperature inversions, where maximum temperature increases at depth in the middle of the profiles.

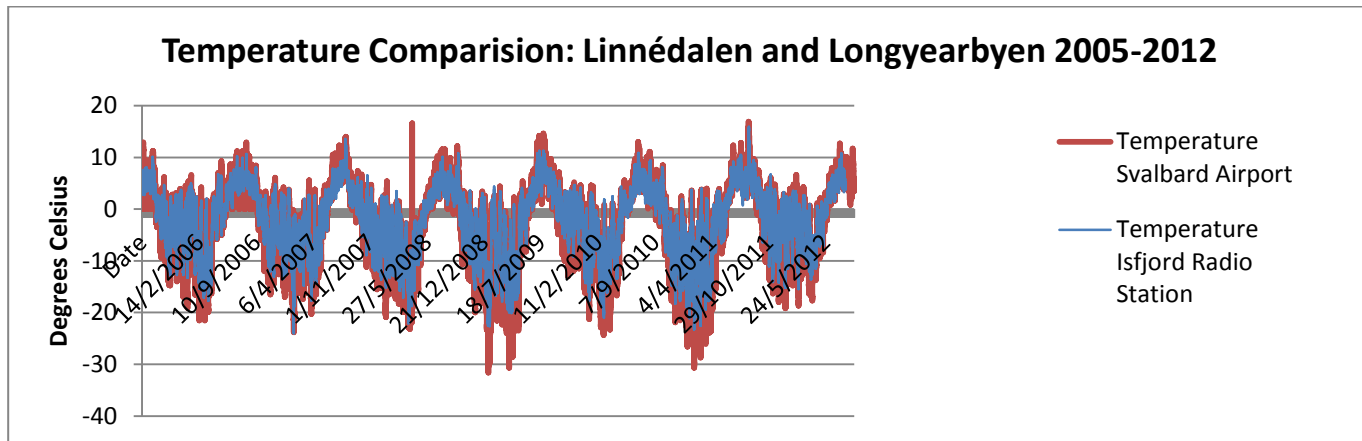
Table B: Summary of maximum, minimum and average temperatures for the temperature profiles from figure 8.4

Temperature Profile Location & Depth	Max Temperature (°C)	Min Temperature (°C)	Avg Temperature (°C)
Palsa			
5cm	19.78	-21.9	-2.06
46cm	6.35	-16.57	-2.09
96cm	5.98	-14.33	-2.81
1.46m	9.544	-8.789	-1.76
1.96m	-0.07	-7.6	-2.33
Rock Glacier West			
0cm	15.95	-22.27	-2.5
5cm	6.89	-17.99	-2.51
1m	3.89	-13.6	-2.62
1.4m	6.82	-11.64	-1.81
1.85m	6.06	-9.75	-2.58
2.55m	-0.07	-8.14	-2.92
Beach Ridge			
0cm	22.5	-24.97	-2.91
25cm	19.26	-23.1	-2.29
50cm	9.24	-20.3	-2.95
75cm	3.85	-13.7	-2.89
1.44m	2.08	-9.3	-2.52
Rock Glacier East			
0cm	23.1	-13.27	-1.76
65cm	9.97	-9.64	-1.93
1.05m	7.71	-9.69	-2.25
1.5m	5.51	-8.74	-2.12

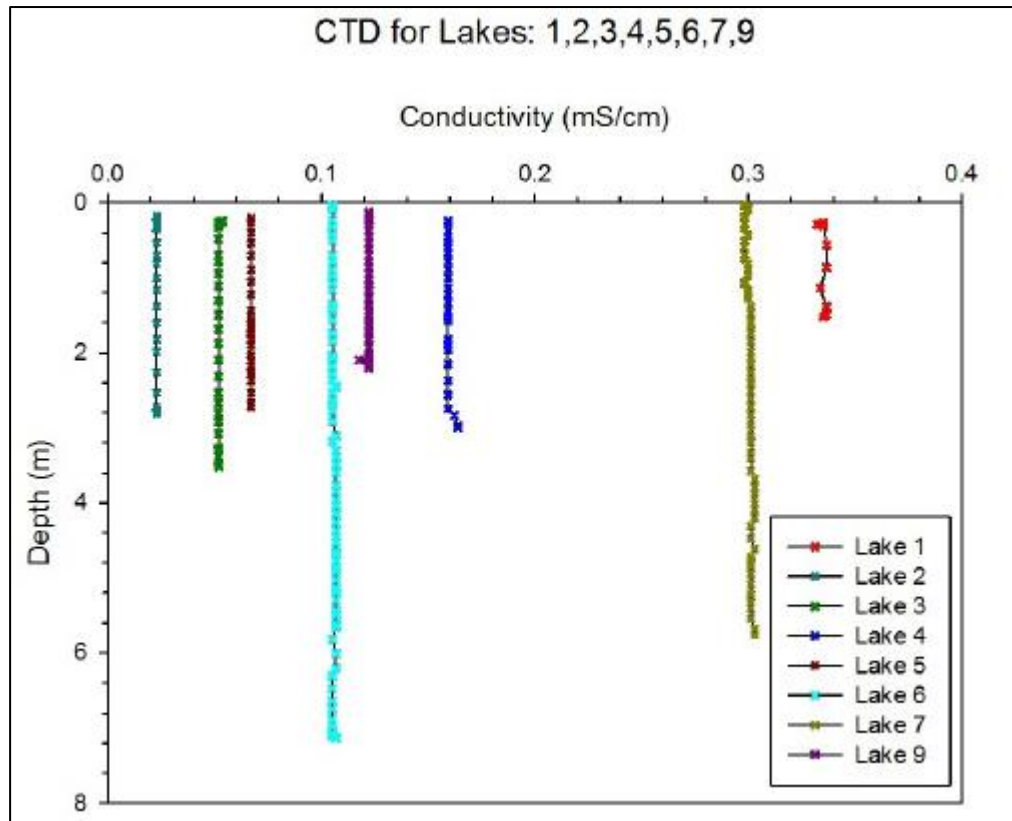


Appendix C: Trumpet curves from borehole data at three boreholes at Kapp Linné, data from the TSP (thermal state of permafrost) project. <http://www.tspnorway.com> (Cohen, 2013)

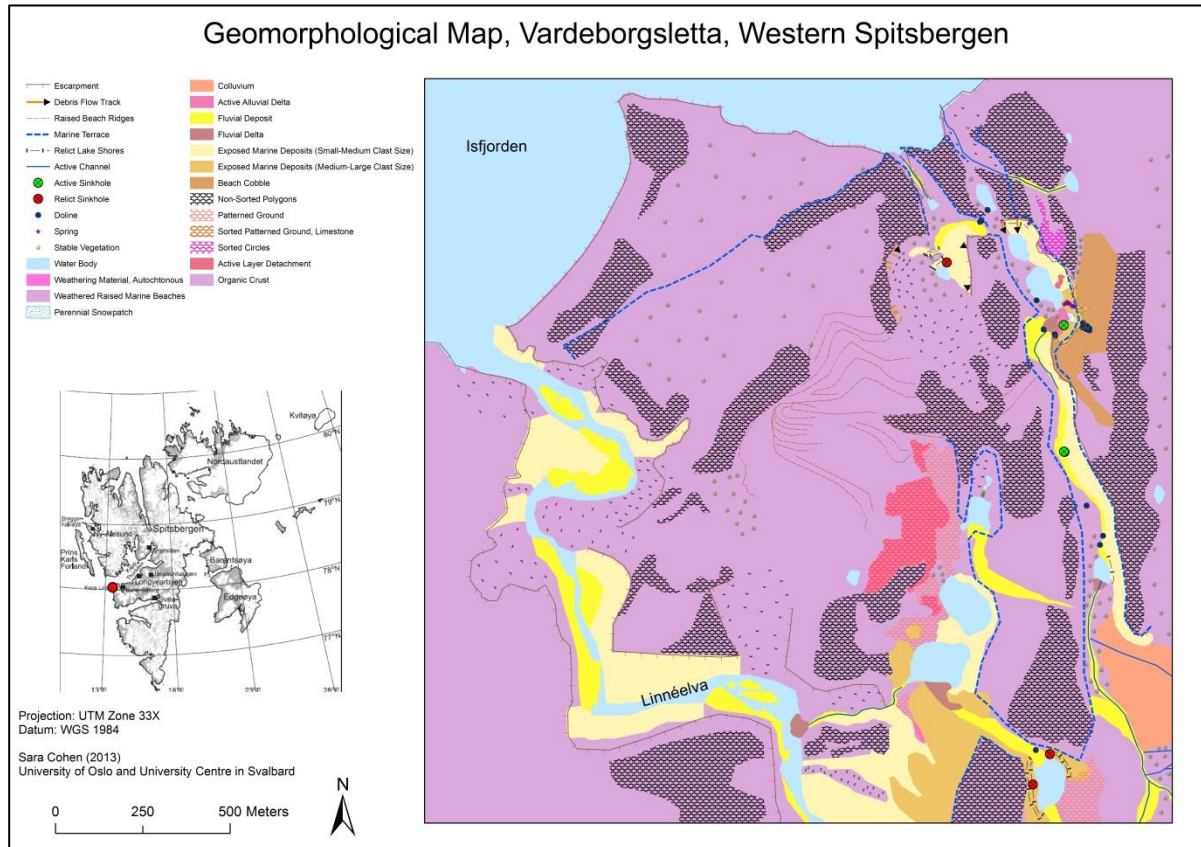
Trumpet curves were made for data from the three boreholes located on the strand flat at Kapp Linné. Kapp Borehole 1 is drilled into a sedimentary beach ridge, Kapp Borehole 2 is drilled into a sedimentary beach ridge and then into the bedrock below, and Kapp Borehole 3 is drilled in organic material overlying beach ridge deposits (Christiansen et al, 2010).



Appendix D: Temperature comparison of hourly air temperatures from Linnédalen (Isfjord Radio Station) and Longyearbyen (Svalbard airport) from 2005-2012. Temperatures are similar, with Linnédalen experiencing slightly less variation. MAAT over the time period for Linnédalen is -2.18°C. MAAT over time period for Longyearbyen is -2.82°C. Temperature from Svalbard airport is provided by eklima.no (Cohen, 2013)



Appendix E: Conductivity at depth for Lakes 1-9. (Figure from Axén and Roalkvam, 2012)



Appendix F: Formatted geomorphological map.